21st Century Soil Carbon Modeling: Evaluating How Management and Climate Impact Future Soil Carbon Storage

A Dissertation

Presented in Partial Fulfillment of the Requirements for the

Degree of Doctor of Philosophy

with a

Major in Natural Resources

in the

College of Graduate Studies

University of Idaho

by

Danielle M. Berardi

Major Professor: Tara W. Hudiburg, Ph.D.

Committee Members: Melannie Hartman, Ph.D.; P. Charles Goebel, Ph.D.;

John Abatzoglu, Ph.D.

Department Administrator: P. Charles Goebel, Ph.D.

May 2023

Abstract

Cellulosic bioenergy crops have potential to meet United States greenhouse gas (GHG) reduction targets and provide energy self-sufficiency. The Renewable Fuel Standard (RFS) calls for increasing the volume of cellulosic biofuel by 16 billion gallons while reducing lifecycle GHG emissions by 60%. Consideration of crop selection, location, and management strategies is critical to meet these goals and prevent environmental and economic costs from outweighing benefits. Depending on the productivity of selected land, 33 to >50 million hectares are required for cellulosic bioenergy production to meet RFS targets. Because a variety of factors are critical to a successful transition to cellulosic bioenergy, biogeochemical modeling is an essential tool to assessing potential scenarios. Models can evaluate potential yield, carbon pools and fluxes, and other GHG and nitrogen fluxes (e.g. nitrous oxide and methane emissions, nitrate leaching) with varying landscapes and management. The first chapter of this dissertation is a review on the current state of biogeochemical modeling and what improvements are necessary to evaluate the sustainability of varying crops, locations, and management to better inform economic models and policy decisions to meet RFS targets.

Representation of soil carbon dynamics in most models is oversimplified with decay constant (i.e. first-order kinetics) driven decomposition and soil carbon pool structures that do not align with measurable pools or current understanding of soil carbon stabilization. Increasing microbial representation in models has shown to reduce uncertainty of predicted soil carbon. This is important not only from a GHG perspective, but also because soil carbon dynamics are intertwined with soil health attributes that increase landscape resiliency (i.e. soil fertility, water holding capacity, and erosion resistance). The second chapter integrates and evaluates microbial explicit mechanisms of decomposition into a new soil sub-model within a version of DayCent that was recently updated to encompass plant traits specific to perennial bioenergy crops. Specifically, the new soil sub-model uses reverse Michaelis-Menten kinetics that incorporate feedbacks between microbial biomass and decomposition rate to simulate soil carbon fluxes. Along with a modified decomposition function the Michaelis-Menten (MM) version of the soil model split the original active soil carbon pool into a live microbial biomass pool and a dead microbial biomass pool with more realistic routing of soil carbon through the pool structure. With these changes, the new MM soil sub-

model improved daily representation of ecosystem carbon fluxes and simulated different ratios of protected to unprotected soil carbon in response to disturbance and climate compared to the original first order soil sub-model.

With improvements to the soil model, DayCent will be better suited to evaluate yield, soil health, and GHG balances across landscapes. Identifying appropriate locations for a particular crop is paramount to meeting GHG atmospheric loading reductions, fulfilling socioeconomic needs, and achieving sustainable land use. In comparison to traditional agricultural crops, some bioenergy crops have physiological attributes (e.g. low N requirements, high belowground biomass, no tillage) that will outweigh the potential negatives if planted strategically. However, there is still much uncertainty and controversy surrounding where cellulosic bioenergy crops will be grown. Conversion of land to cellulosic bioenergy crops that is currently used for food production raises concerns about food-scarcity and sequential conversion of uncultivated land converted for food production (indirect land-use change) resulting in catastrophic losses of sequestered carbon and ecosystem services that will not be recouped through annual row crop production. Conversion of land to bioenergy crops that is not currently used for agricultural production also raises environmental concerns including the effects on GHG balances, biodiversity and ecosystem services, increasing reactive nitrogen through fertilizer, and water use. These potential side effects of conversion are thought to be largely avoided if bioenergy crops are produced on land that has been deemed marginal, or unproductive land that was used for agriculture in the recent past. Chapter three identifies current cropland that is likely to experience increased yield losses as a result of increasing climate variability (aka "marginal land") and analyzes the potential for growing more tolerant bioenergy crops using updated features of the DayCent model. Targeting low-lying, flood susceptible fields for conversion to switchgrass would provide a path to adapt agricultural practices to changing precipitation regimes, mitigate increasing climate variability, and reduce negative environmental impacts of corn production. Documented benefits of perennial grasses in riparian zones include reduced phosphorus and nitrate exports to waterways, decreased nitrous oxide emissions and increased soil carbon sequestration. In comparison to corn-soy production, I found that perennial bioenergy crops in selected flood prone areas will have 1) similar to higher yield, 2) higher soil carbon sequestration, and 3) lower GHG emissions and nitrate exports in flood

prone areas because of lower risk to losses attributed to flooding, higher belowground biomass, decreased erosion, and greater productivity. Lower rates of nitrate leaching and nitrous oxide emissions are expected because switchgrass does not require fertilization.

Acknowledgements

I'm grateful for the support, advice, and mentorship of my major professor, Dr. Tara Hudiburg. Tara advised me through both my Master and Doctoral degree. She has given me a lot of career development and networking opportunities that have shaped who I am as a scientist. Her mentorship style goes beyond the normal expectations and has truly made me feel prepared for the next steps of my career. She has made a lab group of postdocs and graduate students, the 'ITEAM', that is supportive, collaborative, and full of comradery that has helped me through my graduate school career. Tara has always been available to go for a walk, meet at One World or Colter's, or chat over the phone whenever I have needed advice or just to talk through something. Tara has been a stellar advisor and I am glad to have her as a mentor and friend. I have been really lucky to work closely with Dr. Melannie Hartman and Dr. Bill Parton for two of my dissertation chapters. Their guidance and advice taught me so much and shaped my research and my perspective on modeling. Melannie has been a thoughtful and instrumental mentor for my dissertation. I'm also thankful for the mentorship and collaboration from Dr. Eddie Brzostek and Dr. Stephanie Juice. A lot of the work in my dissertation was only possible through collaborations with researchers at the University of Illinois that were willing to share their observational data and expertise: Ilsa Kantola, Elena Blanc-Betes, Adam von Haden, Evan DeLucia, and Mike Masters. All the ITEAM lab members were always there to provide support and comradery along the way: Jeff Stenzel, Kristina Bartowitz, Eric Walsh, Jeff Kent, Justin Matthias, and Kelsey Bryant. Having a network of peers that have been there both to talk about science and enjoy food and drinks with while traveling for conferences and meetings has been a highlight of my graduate school experience. The research in this dissertation was funded in part by a National Institute of Food and Agriculture Predoctoral Fellowship (Award Number: 2021-67034-35046) and a Department of Energy Center of Advanced Bioenergy and Bioproduct Innovation (Award Number DESC0018420).

Dedication

To my partner, Matt Dunkle, and our new baby, Evie.

Your love and support mean the world to me.

Table of Contents

List of Tables

List of Figures

Statement of Contribution

Chapters 1-3 of this dissertation represent collaborative research that have been or will be submitted as multi-authored articles for peer review. All chapters were conceived by D. M. Berardi and T. W. Hudiburg. Chapter 1 was conceived by all coauthors; D. M. Berardi led the writing efforts while some co-authors contributed writing and feedback on their specific areas of expertise. Chapter 2 required model code changes conducted by M. Hartman. All authors have provided feedback and revisions on all chapters.

Chapter 1 : 21st century biogeochemical modeling: Challenges for Century-based models and where do we go from here?

Published in Global Change Biology – Bioenergy as:

Berardi, D., Brzostek, E., Blanc-Betes, E., Davison, B., DeLucia, E. H., Hartman, M. D., ... & Hudiburg, T. W. (2020). 21st-century biogeochemical modeling: challenges for Century-based models and where do we go from here?. *GCB Bioenergy*, *12*(10), 774-788. https://doi.org/10.1111/gcbb.12730

Abstract

21st century modeling of greenhouse gas (GHG) emissions from bioenergy crops is necessary to quantify the extent to which bioenergy production can mitigate climate change. For over 30 years, the Century-based biogeochemical models have provided the preeminent framework for belowground carbon and nitrogen cycling in ecosystem and earth system models. While monthly Century and the daily time-step version of Century (DayCent) have advanced our ability to predict the sustainability of bioenergy crop production, new advances in feedstock generation and our empirical understanding of sources and sinks of GHGs in soils call for a re-visitation of DayCent's core model structures. Here, we evaluate current challenges with modeling soil carbon dynamics, trace gas fluxes, and drought and age-related impacts on bioenergy crop productivity. We propose coupling a microbial process-based soil organic carbon and nitrogen model, with DayCent to improve soil carbon dynamics. We describe recent improvements to DayCent for simulating unique plant structural and physiological attributes of perennial bioenergy grasses. Finally, we propose a method for using machine learning to identify key parameters for simulating N_2O emissions. Our efforts are focused on meeting the needs for modeling bioenergy crops, however, many updates reviewed and suggested to DayCent will be broadly applicable to other systems.

Introduction

Biogeochemical models are used to simulate how abiotic and biotic variables interact through time and across space to determine rates of biogeochemical fluxes. They provide a platform for scientists to evaluate how current and potential changes in climate, land use, disturbance regimes, or vegetation will impact GHG budgets, carbon sequestration and storage, and water quality. As we consider bioenergy crops as alternatives to fossil fuels, it is extremely valuable to use biogeochemical models in tandem with field experiments to make projections that determine which crops will be the most effective and sustainable and in which locations (Whitaker *et al.*, 2018). Challenges we face include the fact that bioenergy crops have unique physiological traits (e.g., dynamic allocation, carbohydrate and nitrogen storage, tolerance for low quality soils), particularly in genetically modified forms (e.g., Energycane, Petro sorghum) that are not currently represented in models. Moreover, N_2O emissions, drought-response, and perennial crop age-related dynamics are poorly simulated by models despite their importance to making future predictions of bioenergy crop GHG balances. With mitigation strategies being developed for decarbonization of the atmosphere, it is becoming increasingly important for biogeochemical models to confidently project GHG emissions in the future for all ecosystem types, land uses, and climatic variability. This is especially true when evaluating the impact of potential bioenergy crops as they are genetically manipulated to maximize biofuel production.

In this review, we discuss the history, current status, and future directions of Century-based biogeochemical modeling in the context of better simulating GHG balances of bioenergy feedstock production, as well as general improvements to soil carbon dynamics that may be used more broadly across all ecosystems. This manuscript covers 1) the history of soil carbon modeling with Century-based biogeochemical models and their relevance in modern ecosystem modeling, 2) future direction of soil carbon modeling, 3) modifications necessary to accurately simulate bioenergy feedstock growth and functions, and 4) how machine learning may be used to refine modeling of N_2O fluxes despite the lack of high resolution spatial and temporal data.

There is a rich history of Century-based models utilizing a simple but powerful framework for predicting soil carbon pools

The Century model was initially used to predict the extent to which abiotic and biotic factors control carbon cycling in temperate grasslands (Parton *et al.*, 1987). Over time, a large number of contemporary earth system models (Table 1.1) have adopted the Century framework as the core prediction of carbon cycling in terrestrial ecosystems. It is difficult to find a study comparing the performance of soil carbon dynamics between models that does not include Century or DayCent, the daily time-step version of Century (Parton *et al.*, 1998), amongst the ranks (Wieder *et al.*, 2013; Walker *et al.*, 2014; Abramoff *et al.*, 2018; Sulman *et al.*, 2018; Ye *et al.*, 2019). Century runs on a monthly time-step and simulates carbon, nitrogen, phosphorous, and sulfur dynamics within soil and vegetation of a specified system. The soil organic matter sub-model uses three major pools to model carbon flow through the soil relying on first-order kinetics (decay constants; k-values value) and soil texture (Figure 1.1a). This system consists of discrete pools to represent soil organic matter (SOM) and litter. SOM is partitioned into active, slow, and passive pools, each with a different intrinsic rate of decomposition which is altered by abiotic factors (i.e. soil temperature and soil moisture; (Parton, 1996)). Most of the models reviewed in Table 1.1 share similar methods of simulating soil carbon dynamics using decay constants to drive decomposition and carbon transfer between pools. While some models, such as DayCent, CASA (Wang *et al.*, 2010), and DNDC (Li *et al.*, 1992; Li *et al.*, 1994), include a microbial biomass pool, they do not use microbial biomass, microbial enzyme production, or microbial carbon use efficiency (CUE; the ratio of carbon assimilated that is converted to biomass vs. that which is respired) to drive decomposition rates. The microbial biomass pool simply serves as another carbon pool with a different rate of carbon loss and transfer.

While Century-like soil carbon dynamics have been the staple for many models over the past three decades (Table 1.1), there is a movement to improve how decomposition is represented in models by progressing beyond k-value driven first-order kinetic equations that lack the complexity necessary to capture smaller scale temporal dynamics that are important for balancing carbon budgets (Wieder *et al.*, 2013). Recent model advances have shown that explicit representation of soil microbial physiology leads to divergent soil carbon flux trajectories not captured by models that rely on first-order kinetics. For example, microbial

models have been successful in capturing ephemeral increases in decomposition due to warming (Allison *et al.*, 2010), re-wetting (Evans *et al.*, 2016), and root-priming (Sulman *et al.*, 2017). Researchers argue that temperature sensitivities are too variable across space to work well with single site observational data and therefore do not allow models of decomposition to be truly mechanistic (Davidson *et al.*, 2006). As such, earth system model development (CLM; Table 1.1) has begun to integrate microbial process-based reverse Michaelis-Menten kinetics (Wieder *et al.*, 2013; Sulman *et al.*, 2019) as well as incorporating vertical connectivity to the Century-based model of decomposition already present in CLM (Koven *et al.*, 2013). However, microbial process-based mechanisms are not being incorporated into the CMIP6 version of CLM. To date, the only CMIP6 model that is incorporating microbial processes (i.e. microbial biomass has an influence on decomposition rates) is IPSL-CM6A-LR which uses the ORCHIDEE-PRIM biogeochemical model.

New empirical evidence is being utilized to improve model mechanisms and constrain model parameters

The ability of models to accurately predict biogeochemical cycling of bioenergy systems ultimately relies on the quantity and quality of data available for parameterization and validation. When initially developed, Century was validated using ecosystem carbon and nitrogen budgets with the goal of accurately simulating biomass yields and equilibrium soil carbon and nitrogen stocks across grassland ecosystems (Parton *et al.*, 1987). Century used these budgets to distill first principle controls (climate, tissue chemistry, etc.) on plant productivity and soil organic matter decomposition into simple yet powerful mechanistic representations of these complex processes. As technology progressed, particularly with the advent of eddy-covariance techniques to quantify ecosystem GHG budgets, these new data streams were used to push the validation of Century and DayCent beyond ecosystem carbon and nitrogen pools to the fluxes that control them. Given the development and maturity of new empirical techniques, there is now the potential to delve even deeper and refine the mechanistic controls on these fluxes. For example, the ability to rapidly measure key leaf and photosynthetic traits (e.g., leaf mass per area, nitrogen content, Vmax, etc.) of bioenergy feedstocks can improve plant functional type parameterizations of such traits in DayCent.

Belowground, the maturity of soil fractionation techniques has led to the development of soil decomposition models (MEMS; (Cotrufo *et al.*, 2013; Robertson *et al.*, 2019) that simulate soil carbon fractions that are measurable in the field; thereby, replacing the conceptual active, slow, and passive fractions used by Century-based models.

Soil/ Ecosystem model	ESM / Land Model	# Litter / Soil / Microbe pools	Temperature Response	Moisture	N	Decomposition Driver
RothC (Harper *et al.*, 2018)	UKESM1 / JULES	0 /4 / 1	Q10	Optimum	No	First-order kinetics
Soil-submodel of CTEM (Arora, 2003)	CanESM5 / CTEM	1/ 1 / 0	Q10	Optimum	No	First-order kinetics
Century + PRIM (Guenet *et al.*, 2016)	IPSL-CM6A-LR / ORCHIDEE-PRIM	2 / 4 / 0	Arrhenius	Optimum	Yes	Optimized first-order kinetics + priming effect
Modified Century or CLM-CN (Lawrence *et al.*, 2018)	CESM2 / CLM5	3 / 3 / 0	Q10	Increasing	Yes	First-order kinetics
CEVSA (Wu *et al.*, 2019)	BCC-CSM2_MR / AVIM2.0	2 / 6 / 0	Optimum	Optimum	Yes	First-order kinetics
ELMv1 (Zhu *et al.*, 2019)	E3SM (previously ACME)	3 / 3 / 3	Q10	Optimum	Yes	First-order kinetics + Equilibrium chemistry approximation
YASSO (Goll *et al.*, 2015)	MPI-ESM1.2-LR / JSBACH3.2	4 / 5 / 0	Optimum	Precipitation	No	First-order kinetics
DNDC (Li *et al.*, 1992)	NA	3 / 3 / 1	Optimum	Optimum	Yes	First-order kinetics
CASA (Wang *et al.*, 2010)	NA	2 / 3 / 0	Q10	Optimum	Yes	First-order kinetics
MIMICS or MIMICS-CN (Wieder *et al.*, 2014)	NA	2 / 3 / 2	Q10	Optimum	Yes	Forward or Reverse Michaelis-Menten kinetics
FUN-CORPSE (Sulman *et al.*, 2017)	NA	3 / 2 / 3	Q10	Optimum	Yes	Reverse Michaelis-Menten kinetics
DayCent (Parton *et al.*, 1998)	NA	2 / 5 / 1	Variable Q10	Optimum	Yes	First-order kinetics

Table 1.1. Selected CMIP6 earth system models (ESM) and their land and biogeochemical/soil sub-models. Models not a part of CMIP6 are designated by "NA." Soil sub-model traits are included. Even though some have microbial pools, microbes do not influence the rate of decomposition, except for ORCHIDEE-PRIM and FUN-CORPSE. "Optimum" describes equations where temperature or moisture increase until a point and then a decrease in decomposition. YASSO uses precipitation events rather than soil moisture to influence decomposition. When N (Nitrogen) is "No" the model is carbon only, otherwise the model includes N dynamics.

New paradigms of soil organic matter formation, stabilization, and loss are not included in ecosystem and earth system models

Despite the success of models that rely on decay constants or "k-values" to control the turnover rates of SOM pools, recognition of new paradigms describing the formation, stabilization, and loss of SOM may improve the ability of these models to predict the environmental impact of bioenergy crops (and other agricultural and native plants) as we transition to novel climatic conditions in the future. At the heart of these new theories is the concept that plant-microbial interactions govern the extent to which plant-derived inputs (i.e., root and leaf litter) form stable SOM (Sokol & Bradford, 2019). For bioenergy crops, there are two key plant traits that feedback on SOM persistence. The first is that there is a strong interaction between feedstock litter chemistry and microbial traits. The second is that differences between feedstocks in belowground carbon allocation to rhizosphere microbes can enhance the formation of stable SOM.

Feedstock litter chemistry drives keystone microbial traits that control the rate and pathway of SOM formation. For example, feedstocks like corn with low C:N ratio litters promote microbes with high carbon use efficiency (CUE- carbon assimilated into biomass per unit carbon taken up) and fast turnover rates (Cotrufo *et al.*, 2013; Zhu *et al.*, 2018). The resulting pool of dead microbial products is thought to be preferentially sorbed to clay minerals in the soil making it physically protected from microbial attack (Schmidt *et al.*, 2011). By contrast, plants with high C:N ratio litters like Miscanthus require greater enzyme investment for microbial decomposition, resulting in lower CUE and turnover rates. As a result, more SOM is chemically stabilized as particulate organic matter because microbial decay is energetically limited (Castellano *et al.*, 2015). Why do these pathways matter for models? SOM that is chemically protected is highly susceptible to loss in a warmer world because rising temperatures lower the activation energy of microbial decay. As such, models that can mechanistically link microbial traits and activity with the distribution of SOM that is physically vs. chemically protected are essential to projecting differences between feedstocks in SOM persistence.

To improve DayCent's ability to better represent plant-microbe interactions and to simulate soil carbon dynamics under future climate scenarios, we plan to integrate microbial

explicit mechanisms of the coupled soil carbon and nitrogen cycling model, FUN-CORPSE (Figure 1.1; (Sulman *et al.*, 2017)) into DayCent. The nitrogen portion of the model, FUN (Fixation and Uptake of Nitrogen), estimates the carbon cost of nitrogen to determine carbon allocation from plants to stimulate N cycling in the rhizosphere (Fisher *et al.*, 2010; Brzostek *et al.*, 2014). The SOC model, CORPSE (Carbon, Organisms, Rhizosphere, and Protection in the Soil Environment), integrates microbial explicit controls of SOC transformations with feedbacks between live microbial biomass and decomposition to drive soil carbon efflux and stabilization (Sulman *et al.*, 2014). We select FUN-CORPSE as a guide to modifying DayCent's SOM cycling processes because, unlike many other microbial explicit SOM models, FUN-CORPSE simulates N and well and C cycling, which are both vital to DayCent's plant growth and trace gas models, and has been evaluated against measurements of rhizosphere fluxes and SOC (Sulman *et al.*, 2017; Sulman *et al.*, 2018). While the mechanisms driving decomposition vary, much of the core structural components of the DayCent SOM cycling serve the similar roles as pools in microbial explicit models, such as FUN-CORPSE. For example, the metabolic litter pools in DayCent serve the same function as the labile carbon pools in FUN-CORPSE. The structural litter and slow SOC pools in DayCent are similar to the recalcitrant or chemically protected pools with varying levels of protection. DayCent's passive pool, defined as microbially-derived inputs sorbed to soil clay particles, is representative of physically protected carbon. DayCent's active pool is its representation of live microbial biomass. While there are similarities between these pools, there is also a fundamental need to redefine and reroute flows between pools so they serve more mechanistic functions that align with microbial frameworks.

While maintaining a similar structure of the DayCent's SOM cycling sub-model (Figure 1.1a), we propose redefining pools to match advances in functional understanding in accordance with the MEMS framework (Cotrufo *et al.*, 2013; Robertson *et al.*, 2019). New pool definitions would align with measurable pools that serve a functional role similar to those described by Lavallee and others (2020) in order to move beyond the conceptual active, slow, and passive framework in Century-based models.

Here, we rename the metabolic surface and rhizosphere litter pools as labile carbon pools to align better with contemporary terminology. They serve the same role as a category of plant residues with simple chemical structure entering the litter or rhizosphere layers.

However, the labile pools will now be routed directly into live microbial pools. Recalcitrant plant material (e.g. lignin, cellulose, etc.) will still enter the litter or rhizosphere through pools categorized as structural carbon. Carbon from this pool will pass through the live microbial carbon pools. After microbial processing of structural carbon this material will be transferred to the chemically protected, recalcitrant carbon pools. Recalcitrant carbon pools can may undergo further microbial decomposition or experience physical transfer of material from the litter recalcitrant pool to the rhizosphere recalcitrant pool. The recalcitrant carbon pools in the litter and rhizosphere will take the place of the slow carbon pools in Century-based models.

Carbon that enters the live microbial biomass pool will either go towards microbial biomass growth or will be lost as CO_2 to the atmosphere based on the CUE of the original pool. The live microbial biomass pool can transfer material to the dead microbial carbon pool as microbial necromass or biproducts. From there, carbon can be transferred abiotically to the Mineral Associated Organic Matter pool (MAOM); this will replace the conceptual passive soil carbon pool in Century-based models. There will be a carbon saturation level of the MAOM pool that will be based on the mineral soil composition (sand, silt, and clay content). Carbon, regardless of the source, must undergo microbial processing before it can be incorporated into the MAOM pool.

We are also integrating mechanisms and parameters from FUN-CORPSE that will incorporate more plant-soil and soil-microbial interactions (Figure 1.1b). We will replace DayCent's decomposition function with the microbial explicit, reverse Michaelis-Menten kinetics functions and add the carbon cost of nitrogen function to determine carbon allocation as root exudates to the rhizosphere carbon pool. The new live microbial biomass pools for each the litter and rhizosphere allow for the feedbacks between decomposition rate and microbial biomass growth and the transfer of microbial necromass to the MAOM pool. While here, we are describing how microbial processes may be incorporated specifically into DayCent, this may be applied similarly to other Century-based soil carbon models.

As microbial processes are incorporated into ecosystem models, the challenge will be to attain parameterization and validation data at larger spatial scales with varying microbial and plant communities. For example, to date, FUN-CORPSE has only been validated in

Eastern USA deciduous forests. Microbial response has been a focus of many warming studies but changes in microbial CUE, microbial biomass, and enzyme activity vary in direction and duration of response (Li *et al.*, 2019; Ye *et al.*, 2019). While studies are addressing the mechanisms driving this variation (Alvarez *et al.*, 2018), more measurements are necessary to validate models across larger spatial scales. Recent studies have found that CUE of microbial communities has a stronger correlation with mean annual temperature (MAT) rather than assay temperature (Sinsabaugh *et al.*, 2017; Takriti *et al.*, 2018). Recently, Ye and colleagues (2019) evaluated using MAT as a driver of CUE and microbial extracellular enzyme kinetics (V_{max}, the maximal activity, and k_m, the half-saturation constant) using three microbial-explicit models compared with an early version of the Century soil model (Parton *et al.*, 1988). They found that there was a strong positive relationship between CUE and MAT and that the microbial models performed better than the first-order kinetics model. In both DayCent and FUN-CORPSE, each SOM pool has its own CUE, and while it can be tuned during model calibration, direct measurements are often not available. Until measurements of microbial traits become more widespread, developing and testing the use of empirical relationships with microbial traits, such as that between CUE and MAT, is a step towards more data driven parameterization. As models progress towards including the more process-based microbial mechanisms of decomposition, it will be vital that we continue to expand on field-based studies that can evaluate microbial model parameterizations and results.

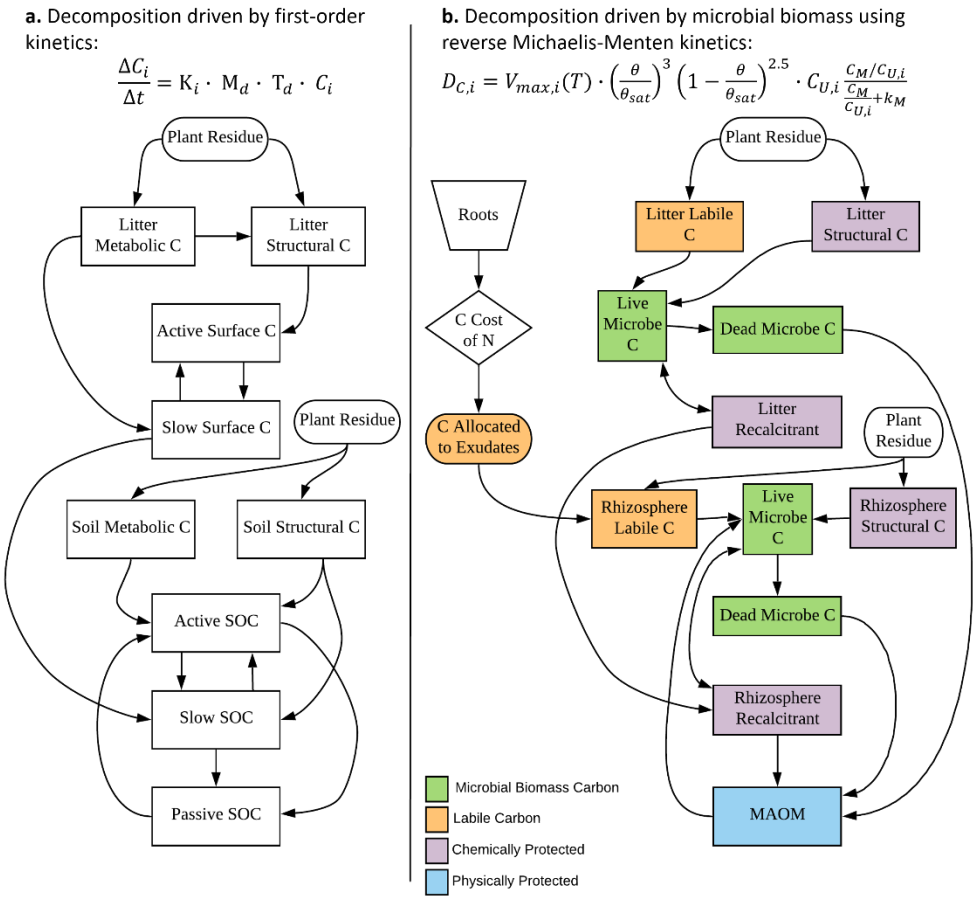

Figure 1.1. DayCent soil sub-model and the proposed FUN-CORPSE integration to Century-based soil submodules. (a) In the current DayCent soil sub-model, each litter and soil pool have empirically derived k-value (Ki) that drives the rate of decomposition along with a temperature (Td) and moisture (Md) effect. Ci represents the size of the carbon pool. (b) Suggested changes to Century-based soil submodules are 1) updating the decomposition function to include microbial biomass pools and use reverse Michaelis-Menten kinetics to drive decomposition in each pool rather than a k-value, and 2) use the carbon cost of nitrogen acquisition by plants described in the FUN model to determine carbon allocation from plants in the form of root exudates to the soil metabolic carbon pool. CO2 is lost as respiration when there is transfer between all soil pools except for the formation of MAOM and live to dead microbes.

Bioenergy crop modeling lacks representation of vegetation dynamics and landscape heterogeneity over time

The perennial growth form of many high-yielding bioenergy crops, including Miscanthus (*Miscanthus x giganteus*), switchgrass (*Panicum virgatum*), and sugarcane (*Saccharum officinarum*) pose a special challenge to modelers as endogenous (i.e. aging) and management factors, in addition to the environment, may affect their yields over long periods of time (Figure 1.2). For several years after planting, perennial bioenergy grasses produce relatively low yields (i.e. establishment effects; Figure 1.2b) and are more vulnerable to nutrient and water deficiencies than established stands. Because of high costs of crop establishment and for the construction of biorefineries, it is desirable that the yield of bioenergy crops remain high and stable over many years, however, this may not be the case. Sugarcane yields decline precipitously after only two or three cycles of vegetative growth – ratoon cycles (Smith *et al.*, 2005) necessitating replanting. Generalizations about the yield stability of Miscanthus and switchgrass are more difficult as few long-term data sets are available. After an initial establishment phase where yields increase for 1-5 years, Arundale et al. (2014) observed a gradual decline in yield for both species thereafter. This study was conducted on rich agricultural soils in the Midwest US without fertilization. After peak yields, reductions also were observed for these species in other regions, however, observed yield reductions are not universal. For Miscanthus it took longer (>15 years) for these reductions to become apparent in the Mediterranean (Alexopoulou *et al.*, 2015).

Predicting age-related declines in yield remains a key challenge for models. Adding to this challenge, the empirical understanding of the mechanisms driving time-dependent yield reductions is limited. Excessive tillage at planting followed by soil compaction contribute to the strong decline in sugarcane yield from one year to the next (Pankhurst *et al.*, 2003). Nutrient management for Miscanthus and switchgrass is not well understood (Heaton *et al.*, 2009). Particularly for Miscanthus, which can yield well in excess of 20 dry Mg ha^{-1} yr^{-1} (Laurent *et al.*, 2015), removal of nitrogen and phosphorus from the soil as plant biomass is harvested can contribute to declining yields. Miscanthus more than switchgrass is sensitive to hard winter freezes which can damage overwintering rhizomes and reduce yields the following summer (Clifton-Brown & Lewandowski, 2000). Physiologically, the extraordinarily dense canopies developed by these crops can reduce photosynthetic efficiency

by shading (Pignon *et al.*, 2017). There is ongoing work that is using a staggered stand age to separate age dynamics from environmental effects on Miscanthus physiology and yield (Tejera *et al.*, 2019). Studies such as this, will provide insight to develop a more comprehensive and integrated understanding of mechanisms driving these changes, including the role of management practices, edaphic and biotic factors and endogenous physiological controls of productivity. It is critical to continue incorporating emerging mechanistic improvements as they are identified in the literature.

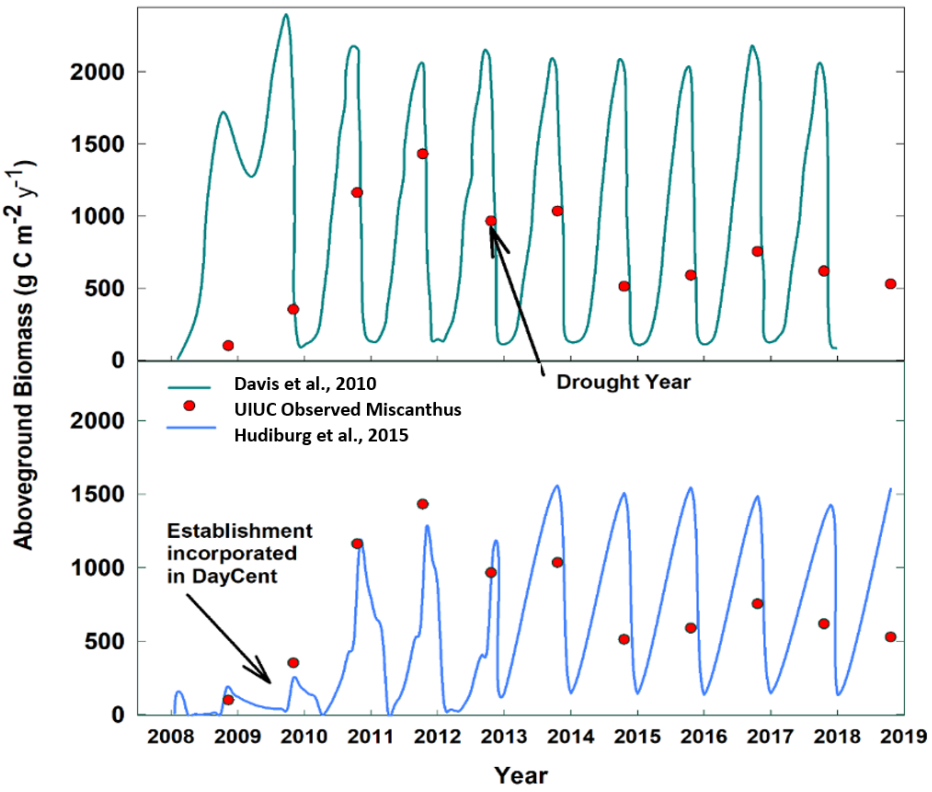

Figure 1.2. Modeled and observed above ground biomass of Miscanthus from two studies at the University of Illinois Urbana Champaign Energy Farm. Davis et al. (2010) did not have any Miscanthus validation data at the time of the study. Hudiburg et al. (2015) had biomass data for validation and used daily site weather data through 2012 when the study was finished. In other words, observations at the time of these studies did not have either a drought or aging-induced decline in yield and in the case of Davis et al. (2010), an establishment phase. DayCent's crop model (primarily used for annual crops) was not designed capture these types of dynamics because annual crops do not have multi-year establisment or multi-year responses to past events. These new observations have led to the development of a new plant sub-model in DayCent that is now being used for the perrenial bioenergy crops.

In addition to an establishment phase for Miscanthus, a decline in yield was observed following the 2012 drought at the University of Illinois Energy Farm (Figure 1.2; red dots); this decline has continued. DayCent model predictions for Miscanthus yield at the Energy Farm prior to planting (Figure 1.2a; (Davis *et al.*, 2010)) neither capture the establishment phase nor a decline in yield (to drought or aging). Model predictions were improved in later modeling studies (Hudiburg *et al.*, 2015) by adding an establishment phase by modifying

DayCent's plant growth potential parameter for Miscanthus. However, representing the establishment phase did not improve the ability of the model to capture the response to drought, or yield declines due to aging. The suggested path to addressing age related decline is described in the following section describing long-term plant dynamics in DayCent.

To improve our ability to model drought effects on yield, we must be able to incorporate the ways in which plants respond to drought which varies between feedstocks. Switchgrass pursues a strategy of drought avoidance by investing in root mass to extract deep soil water, while Miscanthus has been found to have a variety of physiological responses to drought. When established Miscanthus stands were subjected to an extreme drought in 2012, Joo et al. (2017) observed increased ET driven by deep soil water use by Miscanthus compared to switchgrass and prairie plots. In contrast, another study found that Miscanthus had lower evapotranspiration in 2012 than either switchgrass, corn or mixed prairie (Hamilton *et al.*, 2015). Other research has suggested a lack of sensitivity of Miscanthus to moderate drought, with water use and photosynthesis remaining high through early phases of scarcity and stomatal closure only upon onset of severe drought (Ings *et al.*, 2013). DayCent crop parameters currently allow specification of root allocation responses to water scarcity. However, the rate of consumption of available water is dictated by leaf area and climatic factors that are not specific to crop species. If field results establish clear differences in the water use strategies of perennial bioenergy crops it may be necessary to introduce a water consumption algorithm that accounts for species-specific responses to drought.

Recent DayCent developments show improved short and long-term dynamics

To simulate the dynamics of fast-growing, highly productive biofuel plants which have different dynamics and traits than more traditional crops and grasses, we have developed a new bioenergy grass plant functional type (PFT) with additional physiological parameters for the DayCent ecosystem model. Although the new bioenergy grass can represent both annual and perennial crops, it was developed primarily to improve the representation of the long-term dynamics of large perennial biofuel grasses such as sugarcane, switchgrass, and Miscanthus. The grass category differs from the model's traditional crop/grass plant type by representing above-ground biomass as both stems and

leaves instead of as shoots only and representing below-ground root biomass as both rhizomes and fine roots instead of as fine roots only. The stems, which contain a larger percentage of structural material than leaves, have a higher C:N ratio than leaves and the amount of leaves that can grow is dependent on the amount of stem biomass that can support them. Phenology, such as when senescence begins, can be prescribed or can be governed by growing degree days and moisture-related triggers. Shading can cause partial senescence of leaves which can either remain attached to the stems or fall to the ground. During the latter part of the growing season, perennial plants build up carbohydrate storage which will be available for growth in the subsequent growing season. Similarly, during senescence large perennial grasses re-translocate nitrogen from leaves to the rhizomes and this stored nitrogen will be available for growth in the subsequent growing season. Thus, the health of the plant in one growing season may affect yields in the subsequent growing season.

New PFT parameterizations in DayCent-CABBI, a version of DayCent developed by the Center for Advanced Bioenergy and Bioproducts Innovation, have improved the model representation of perennial plant establishment and growth (Figure 1.3; (Moore *et al.*, Unpublished)). Model-data agreement can be tuned with a comparable amount of success for both DayCent-CABBI and DayCent-Photo, the previous version of the model (Straube *et al.*, 2018; Stenzel *et al.*, 2019). However, to simulate lower yields during establishment years for perennials in DayCent-Photo, the model required three consecutive switchgrass PFT parameterizations to be used with varying growth potential (see table in Figure 1.3). In this comparison, DayCent-CABBI captured the effects of establishment in a single parameterization of switchgrass since simulated stem and rhizome growth required several years to achieve peak biomass through additional biomass to LAI and maximum LAI parameters. DayCent-CABBI also differentiates carbon and nitrogen allocation between leaves and stems and root tissues, whereas previous versions of the model only differentiate C:N ratios between above and belowground pools.

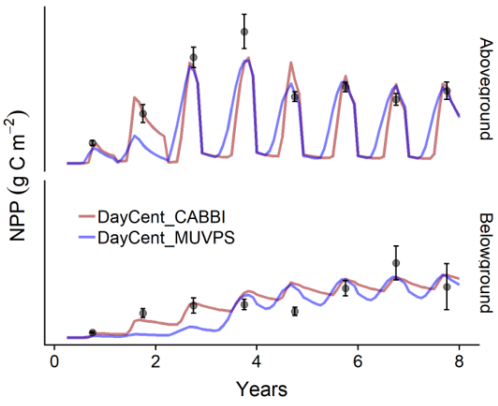

Parameter	DayCent-Photo	DayCent-CABBI
Growth Potential	0.3; 0 .8; 1.0	1.25
Aboveground Min/Max C:N	60 - 220	--
Belowground Min/Max C:N	40 - 60	--
Leaf Min/Max C:N	--	40 - 200
Stem Min/Max C:N	--	100 - 250
Juvenile Fine Root Min/Max C:N	--	20 - 90
Mature Fine Root Min/Max C:N	--	100 - 190
Course Root Min/Max C:N	--	50 - 165
Biomass to LAI Ratio	--	0.02
Max LAI	--	9.0

Figure 1.3. DayCent-CABBI and DayCent-Photo (the previous version of the model) evaluated against measurements of peak above- and belowground peak biomass of switchgrass at the UIUC Energy Farm over eight years following the initial planting. Points represent observed data. Error bars are standard error (n = 5). The table provides differences in major crop parameterizations between the old and the new version of the model. DayCent-Photo adjusting the growth potential coefficient during the first two years to limit growth during switchgrass establishment, whereas DayCent-CABBI achieves this though LAI parameters. The C:N and LAI values were derived from measurements taken at UIEF (Smith et al., 2013; Masters et al., 2016).

To improve long-term dynamics, we are investigating if long-term changes in allocation between above- and below-ground biomass is altered by prolonged drought and plant age. We are also investigating the best way to represent the age-related declines in Miscanthus and switchgrass production that have been observed in field trials in the USA since we are unsure if these yield declines are a result of reduced soil nutrient availability, changing soil conditions or pests and disease. Furthermore, heterogenous conditions within a field may reduce average biomass harvest over time. The model already simulates nutrient uptake and therefore simulated yields will respond to nutrient supply, but other age-related productivity declines are not currently represented (Arundale *et al.*, 2014). These changes to model algorithms will also be useful for woody plants, especially age-related changes to allocation of carbon.

The role of carbon and nitrogen stored belowground is also important to understanding stress response in perennial grasses. Eichelmann et al. (2016) found that water use efficiency (WUE) of mature switchgrass increased in the 2012 drought year relative to

2011 despite lower CO_2 fixation, suggesting the use of belowground stored carbon to "subsidize" drought year biomass production. The new grass category provides for carbon accumulation in rhizomes which will allow for plants to mobilize carbon stored in roots under drought stress for aboveground biomass production. However, algorithms involved with the new grass category will need to be validated against measurements such as these as they become available to enable accurate prediction of yield stability across wet and dry growing seasons.

Current mechanistic understanding about the timing and magnitude of trace gas fluxes (e.g. N_2O) is insufficient for model development

Given the amplified global warming potential of N_2O relative to other GHGs, inaccurate estimates of N_2O fluxes under land use or climate change scenarios represent a large source of uncertainty on terrestrial ecosystems-climate feedbacks, particularly when considering the agricultural sector (Stein & Yung, 2003). Accurate predictions of potential feedbacks are key for evaluating risks and designing mitigation strategies

Because a direct measurement of all factors and interactions integrating the nitrogen (N) cycle is unfeasible and subject to large variability, models of varying complexity have been developed to reproduce the complex processes driving N dynamics and ultimately N_2O emissions. DayCent was developed to link to a daily land surface model to improve estimates of trace gas fluxes by incorporating daily soil hydrological and thermal dynamics in conjunction with modified parameterizations to accommodate a higher temporal resolution of ecosystem processes subject to significant daily variability (Parton et al., 1996, 1998). DayCent simulates N_2O and NO_x emissions from nitrification and denitrification and N_2 emissions from denitrification reproducing the regulation of each process separately. The model assumes that nitrification rates are controlled by the availability in soil of NH_4+, and soil water content, temperature, and pH (Parton et al., 2001). Maximum nitrification rates occur at close to 50% water-filled pore space (WFPS) and are assumed to decreases as temperature and pH decrease. Denitrification is assumed to be a function of soil NO_3^- (e^- acceptor) concentration, labile C (e^- donor) availability, and O_2 (competing e acceptor). Heterotrophic respiration is used as a proxy for labile C availability while O_2 availability is

estimated from WFPS, and soil physical properties related to texture that influence gas diffusivity (Del Grosso et al., 2000).

The DayCent model has been extensively used to generate N_2O flux estimates for regional greenhouse gas inventories, predict N_2O emissions and N_2O emission factors across land uses and management practices, and evaluate the impacts of climate change on agriculture (Adler et al., 2007; Davis et al., 2010, 2012; Del Grosso et al., 2006, 2008; Del Grosso, Mosier, et al., 2005). However, despite yielding more accurate estimates than the IPCC recommended EF methodology (Del Grosso, Mosier, et al., 2005) and a generally better performance relative to alternative process-based models (Abdalla et al., 2010; Yue et al., 2019), DayCent estimates are not devoid of uncertainty, with reported deviations ranging from -57% to 38% (Abdalla et al., 2010; Del Grosso, Mosier, et al., 2005; Gaillard et al., 2018; Yue et al., 2019). The complexity of model predictions of ecosystem N_2O fluxes lies largely on the fact that N_2O fluxes result from multiple processes, whose regulation, drivers and interactions are still not sufficiently understood or even identified.

The lack of mechanistic understanding of N_2O dynamics is largely due to the highly variable nature of these fluxes. In the last few decades, it has become apparent that the majority of N_2O emissions from soil and aquatic systems occurs in hot spots and during hot moments (McClain *et al.*, 2003). Sampling is limited in space and time leading to an uneven representation in the literature (e.g. more accessible vs less accessible areas; growing season vs non-growing season), making it difficult to disentangle the primary variables driving the response of N_2O to changes in the environment.

Predicting ecosystem N_2O fluxes requires integration of multiple processes operating simultaneously (i.e. nitrification and denitrification). These processes have different lag-times and sensitivities to a wide range of biotic factors (e.g. plant-soil interactions, natural inhibitors of the nitrogen metabolism, dominant microbial communities) and environmental conditions which are still not fully understood or even identified. The role of soil pH in denitrification metabolism has only recently been recognized (Liu *et al.*, 2010) and new evidence suggests that the contribution of N_2O emissions induced by freeze-thaw cycles to annual emissions has been underestimated by ~20-30% (Wagner-Riddle *et al.*, 2017).

Neglecting to capture these processes in biogeochemical models likely contributes to strong biases in ecosystem N_2O annual budgets.

Moreover, static model site (or grid cell) parameters such as soil texture, drainage, or pH may not be constant as they can evolve over the course of the development of supported vegetation, buildup of soil organic matter, or particularly following disturbance events. A recent review found that there is frequently high N_2O emissions in the first few years following conversion of annual crops to perennial bioenergy feedstocks (Whitaker *et al.*, 2018). To accurately predict ecosystem N_2O emissions, models need be able to integrate these legacy effects, where the short-term effects of changes in land use and/or climate on the ecosystem physical and biological parameters are foundational to long-term responses.

The complex functional relationships between N_2O and its controlling factors makes it difficult for process-based biogeochemical models to predict spatial and temporal N_2O dynamics. Furthermore, the popular process-based models for N_2O prediction such as DayCent and DNDC are often parameterized based on limited number of observations from controlled laboratory experiments that do not represent the complex variable interactions. The process-based models often fail to accurately predict fine-scale (daily) temporal N_2O predictions (Parton *et al.*, 2001; Jarecki *et al.*, 2008). We propose that data-driven machine learning models could be used to improve predictability as well as understand controlling variable sensitivity and identify their functional relationships with N_2O, which in turn could help to refine the process-based models through improved parameterization (Philibert *et al.*, 2013; Perlman *et al.*, 2014; Reichstein *et al.*, 2019). For example, deep learning models can improve prediction accuracy for poorly understood processes at the expense of interpretability (Brenowitz & Bretherton, 2018; de Bezenac *et al.*, 2019). Whereas, tree-based models such as Random Forest is a non-parametric machine learning technique that learns functional forms between the response and predictor variables from the data (Breiman, 2001). Hence, can provide novel understanding on process controls while improving prediction accuracy. This process can operate in parallel or in fusion with biogeochemical or other process-based models (Walsh & Hudiburg, 2019). Unlike process-based models, the Random Forest algorithm learning is facilitated through an iterative process of recursive data partitioning and constructing hundreds of decision trees to partition the observations into distinct groups characterized by different properties of the predictor variables. Meta-

modeling approach using Random Forest and process-based models has been used in predicting soil N biogeochemistry (Ramanantenasoa *et al.*, 2019; Shahhosseini *et al.*, 2019) however, its use in predicting highly variable temporal soil N_2O fluxes is limited. Saha, Basso, and Robertson (Submitted) developed a Random Forest model based on automated flux chamber data from corn in the upper Midwest that predicted 51% variability in daily N_2O fluxes from an unknown site.

High temporal and spatial resolution input data are critical to facilitate this learning process, hence measured data from diverse soil, climate, and cropping system management practices are critical for model training (Figure 1.4). As more long-term observed flux data from automated flux chamber sites becomes available, the opportunity to use machine learning methods to improve process-based biogeochemical models, like DayCent, is increasing. The predictor variables may include soil properties (texture organic matter, pH), weather variables (precipitation, temperature), management practices (tillage, cover crop, fertilization and land use change), and dynamic soil biogeochemistry (mineral nitrogen availability, soil moisture and temperature). As a way forward, we suggest first identifying the available measured N_2O data sources from diverse soil, climate and production systems. Second, creation of a database of N_2O fluxes and associated predictor variables that are empirically identified as important. Process-based models can be used to fill in the gaps in input data with a certain level of confidence to facilitate an integration of data-driven and physics-based N_2O modeling approach (Figure 1.4). Third, machine learning models should be trained and then tested with separate validation data. Fourth, performance comparisons between the process-based models and Random Forest method in predicting N_2O fluxes can be used as a metric of improved model confidence. This method could extend to other ecosystem fluxes that are also difficult to model under quickly changing environmental conditions such as CO_2 from heterotrophic respiration and CH_4 production and consumption.

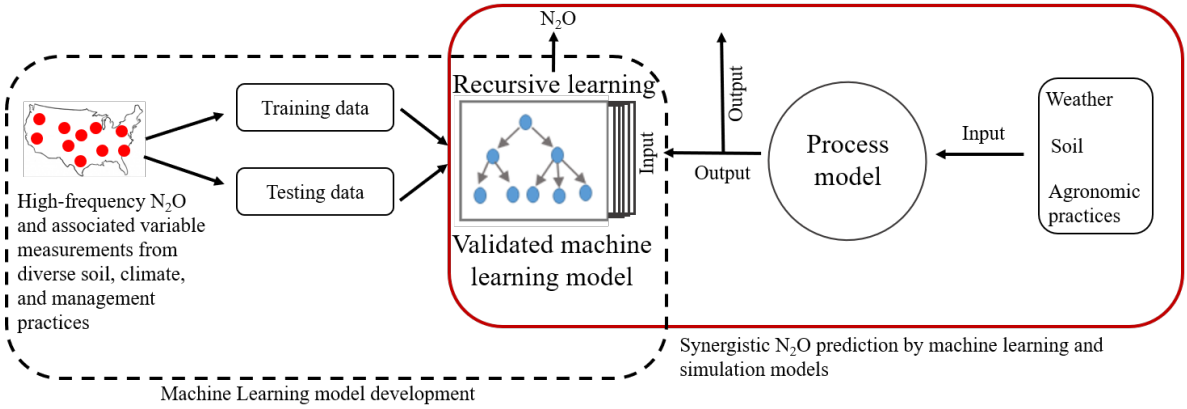

Figure 1.4. A schematic representation of integrating machine learning and biogeochemical simulation models to predict N_2O fluxes. The left broken box represents the development of machine learning model by learning from the data. In order to improve the machine learning model's ability to generalize predictions, the model should be trained and tested on data from diverse environmental and agronomic production systems. The right solid box represents output generation from process-based simulation model. The relevant outputs can serve as input variables for the machine model to predict N_2O fluxes at the same resolution as the simulation model (adapted from Saha, Basso, & Robertson (2021).

Conclusion

Modeling is a powerful tool for generating hypotheses and predictions about how major changes in land use, driven by the expansion of bioenergy crops and other changes in managed landscapes, will affect the land-atmosphere exchange of GHGs. Century-based models have been keystone models representing processes affecting SOC and GHG exchange. Assimilation of new understanding of plant physiology, new paradigms explaining changes in SOC, the ability to quantify feedbacks between the microbial community and decomposition, and the use of machine learning to identify and optimize key parameters when high-resolution data is lacking will improve the predictive power of DayCent when confronted with rapidly changing environmental conditions.

References

Abramoff R, Xu X, Hartman M, O'Brien S, Feng W, Davidson E, Finzi A, Moorhead D, Schimel J, Torn M. 2018. The Millennial model: in search of measurable pools and transformations for modeling soil carbon in the new century. *Biogeochemistry* **137**(1-2): 51-71.

Alexopoulou E, Zanetti F, Scordia D, Zegada-Lizarazu W, Christou M, Testa G, Cosentino SL, Monti A. 2015. Long-term yields of switchgrass, giant reed, and Miscanthus in the Mediterranean basin. *Bioenergy Research* **8**(4): 1492-1499.

Allison SD, Wallenstein MD, Bradford MA. 2010. Soil-carbon response to warming dependent on microbial physiology. *Nature Geoscience* **3**(5): 336-340.

Alvarez G, Shahzad T, Andanson L, Bahn M, Wallenstein MD, Fontaine S. 2018. Catalytic power of enzymes decreases with temperature: New insights for understanding soil C cycling and microbial ecology under warming. *Global change biology* **24**(9): 4238-4250.

Arora VK. 2003. Simulating energy and carbon fluxes over winter wheat using coupled land surface and terrestrial ecosystem models. *Agricultural and Forest Meteorology* **118**(1-2): 21-47.

Arundale RA, Dohleman FG, Heaton EA, Mcgrath JM, Voigt TB, Long SP. 2014. Yields of M iscanthus× giganteus and P anicum virgatum decline with stand age in the Midwestern USA. *Gcb Bioenergy* **6**(1): 1-13.

Breiman L. 2001. Random forests. *Machine learning* **45**(1): 5-32.

Brenowitz ND, Bretherton CS. 2018. Prognostic validation of a neural network unified physics parameterization. *Geophysical Research Letters* **45**(12): 6289-6298.

Brzostek ER, Fisher JB, Phillips RP. 2014. Modeling the carbon cost of plant nitrogen acquisition: Mycorrhizal trade-offs and multipath resistance uptake improve predictions of retranslocation. *Journal of Geophysical Research: Biogeosciences* **119**(8): 1684-1697.

Castellano MJ, Mueller KE, Olk DC, Sawyer JE, Six J. 2015. Integrating plant litter quality, soil organic matter stabilization, and the carbon saturation concept. *Global change biology* **21**(9): 3200-3209.

Clifton-Brown J, Lewandowski I. 2000. Overwintering problems of newly established Miscanthus plantations can be overcome by identifying genotypes with improved rhizome cold tolerance. *The New Phytologist* **148**(2): 287-294.

Cotrufo MF, Wallenstein MD, Boot CM, Denef K, Paul E. 2013. The M icrobial E fficiency-M atrix S tabilization (MEMS) framework integrates plant litter decomposition with soil organic matter stabilization: do labile plant inputs form stable soil organic matter? *Global Change Biology* **19**(4): 988-995.

Davidson EA, Janssens IA, Luo Y. 2006. On the variability of respiration in terrestrial ecosystems: moving beyond Q10. *Global Change Biology* **12**(2): 154-164.

Davis SC, Parton WJ, Dohleman FG, Smith CM, Del Grosso S, Kent AD, DeLucia EH. 2010. Comparative Biogeochemical Cycles of Bioenergy Crops Reveal Nitrogen-Fixation and Low Greenhouse Gas Emissions in a Miscanthus x giganteus Agro-Ecosystem. *Ecosystems* **13**(1): 144-156.

de Bezenac E, Pajot A, Gallinari P. 2019. Deep learning for physical processes: Incorporating prior scientific knowledge. *Journal of Statistical Mechanics: Theory and Experiment* **2019**(12): 124009.

Eichelmann E, Wagner-Riddle C, Warland J, Deen B, Voroney P. 2016. Evapotranspiration, water use efficiency, and energy partitioning of a mature switchgrass stand. *Agricultural and forest meteorology* **217**: 108-119.

Evans S, Dieckmann U, Franklin O, Kaiser C. 2016. Synergistic effects of diffusion and microbial physiology reproduce the Birch effect in a micro-scale model. *Soil Biology and Biochemistry* **93**: 28-37.

Fisher J, Sitch S, Malhi Y, Fisher R, Huntingford C, Tan SY. 2010. Carbon cost of plant nitrogen acquisition: A mechanistic, globally applicable model of plant nitrogen uptake, retranslocation, and fixation. *Global Biogeochemical Cycles* **24**(1).

Goll DS, Brovkin V, Liski J, Raddatz T, Thum T, Todd-Brown KEO. 2015. Strong dependence of CO2 emissions from anthropogenic land cover change on initial land cover and soil carbon parametrization. *Global Biogeochemical Cycles* **29**(9): 1511-1523.

Guenet B, Moyano FE, Peylin P, Ciais P, Janssens IA. 2016. Towards a representation of priming on soil carbon decomposition in the global land biosphere model ORCHIDEE (version 1.9. 5.2). *Geoscientific Model Development* **9**(2): 841-855.

Hamilton S, Hussain M, Bhardwaj A, Basso B, Robertson G. 2015. Comparative water use by maize, perennial crops, restored prairie, and poplar trees in the US Midwest. *Environmental Research Letters* **10**(6): 064015.

Harper AB, Wiltshire AJ, Cox PM, Friedlingstein P, Jones CD, Mercado LM, Sitch S, Williams K, Duran-Rojas C. 2018. Vegetation distribution and terrestrial carbon cycle in a carbon cycle configuration of JULES4.6 with new plant functional types. *Geosci. Model Dev.* **11**(7): 2857-2873.

Heaton EA, Dohleman FG, Long SP. 2009. Seasonal nitrogen dynamics of Miscanthus× giganteus and Panicum virgatum. *GCB Bioenergy* **1**(4): 297-307.

Hudiburg TW, Davis SC, Parton W, Delucia EH. 2015. Bioenergy crop greenhouse gas mitigation potential under a range of management practices. *GCB Bioenergy* **7**(2): 366-374.

Ings J, Mur LA, Robson PR, Bosch M. 2013. Physiological and growth responses to water deficit in the bioenergy crop Miscanthus x giganteus. *Frontiers in Plant Science* **4**: 468.

Jarecki MK, Parkin TB, Chan AS, Hatfield JL, Jones R. 2008. Comparison of DAYCENT-simulated and measured nitrous oxide emissions from a corn field. *Journal of environmental quality* **37**(5): 1685-1690.

Joo E, Zeri M, Hussain MZ, DeLucia EH, Bernacchi CJ. 2017. Enhanced evapotranspiration was observed during extreme drought from Miscanthus, opposite of other crops. *GCB Bioenergy* **9**(8): 1306-1319.

Koven CD, Riley WJ, Subin ZM, Tang JY, Torn MS, Collins WD, Bonan GB, Lawrence DM, Swenson SC. 2013. The effect of vertically resolved soil biogeochemistry and alternate soil C and N models on C dynamics of CLM4. *Biogeosciences* **10**(11): 7109-7131.

Laurent A, Pelzer E, Loyce C, Makowski D. 2015. Ranking yields of energy crops: a meta-analysis using direct and indirect comparisons. *Renewable and sustainable energy reviews* **46**: 41-50.

Lavallee JM, Soong JL, Cotrufo MF. 2020. Conceptualizing soil organic matter into particulate and mineral-associated forms to address global change in the 21st century. *Global Change Biology* **26**(1): 261-273.

Lawrence DM, Fisher RA, Koven CD, Oleson KW, Swenson SC, Bonan G, Collier N, Ghimire B, Kampenhout Lv, Kennedy D, et al. 2018. Technical Note: CLM5 Documentation. *NCAR Technical Note*: National Center for Atmospheric Research.

Li C, Frolking S, Frolking TA. 1992. A model of nitrous oxide evolution from soil driven by rainfall events: 1. Model structure and sensitivity. *Journal of Geophysical Research: Atmospheres* **97**(D9): 9759-9776.

Li C, Frolking S, Harriss R. 1994. Modeling carbon biogeochemistry in agricultural soils. *Global biogeochemical cycles* **8**(3): 237-254.

Li J, Wang G, Mayes MA, Allison SD, Frey SD, Shi Z, Hu XM, Luo Y, Melillo JM. 2019. Reduced carbon use efficiency and increased microbial turnover with soil warming. *Global change biology* **25**(3): 900-910.

Liu B, Mørkved PT, Frostegård Å, Bakken LR. 2010. Denitrification gene pools, transcription and kinetics of NO, N2O and N2 production as affected by soil pH. *FEMS microbiology ecology* **72**(3): 407-417.

Masters MD, Black CK, Kantola IB, Woli KP, Voigt T, David MB, DeLucia EH. 2016. Soil nutrient removal by four potential bioenergy crops: Zea mays, Panicum virgatum, Miscanthus× giganteus, and prairie. *Agriculture, ecosystems & environment* **216**: 51-60.

McClain ME, Boyer EW, Dent CL, Gergel SE, Grimm NB, Groffman PM, Hart SC, Harvey JW, Johnston CA, Mayorga E. 2003. Biogeochemical hot spots and hot moments at the interface of terrestrial and aquatic ecosystems. *Ecosystems* **6**(4): 301-312.

Moore C, Berardi D, Betes-Blanc E, DeLucia EH, Dracup EC, Egenriether S, Gomez-Casanovas N, Hartman MD, Hudiburg TW, Kantola I, et al. Unpublished. The carbon and nitrogen cycle impacts of converting perennial switchgrass to an annual maize crop rotation: PNAS

Pankhurst C, Magarey R, Stirling G, Blair B, Bell M, Garside A, Venture SYDJ. 2003. Management practices to improve soil health and reduce the effects of detrimental soil biota

associated with yield decline of sugarcane in Queensland, Australia. *Soil and Tillage Research* **72**(2): 125-137.

Parton W 1996. The CENTURY model. *Evaluation of soil organic matter models*: Springer, 283-291.

Parton W, Holland E, Del Grosso S, Hartman M, Martin R, Mosier A, Ojima D, Schimel D. 2001. Generalized model for NO x and N2O emissions from soils. *Journal of Geophysical Research: Atmospheres* **106**(D15): 17403-17419.

Parton W, Schimel DS, Cole C, Ojima D. 1987. Analysis of factors controlling soil organic matter levels in Great Plains Grasslands 1. *Soil Science Society of America Journal* **51**(5): 1173-1179.

Parton WJ, Hartman M, Ojima D, Schimel D. 1998. DAYCENT and its land surface submodel: description and testing. *Global and planetary Change* **19**(1-4): 35-48.

Parton WJ, Stewart JW, Cole CV. 1988. Dynamics of C, N, P and S in grassland soils: a model. *Biogeochemistry* **5**(1): 109-131.

Perlman J, Hijmans RJ, Horwath WR. 2014. A metamodelling approach to estimate global N2O emissions from agricultural soils. *Global ecology and biogeography* **23**(8): 912-924.

Philibert A, Loyce C, Makowski D. 2013. Prediction of N2O emission from local information with Random Forest. *Environmental pollution* **177**: 156-163.

Pignon CP, Jaiswal D, McGrath JM, Long SP. 2017. Loss of photosynthetic efficiency in the shade. An Achilles heel for the dense modern stands of our most productive C4 crops? *Journal of experimental botany* **68**(2): 335-345.

Ramanantenasoa MMJ, Génermont S, Gilliot J-M, Bedos C, Makowski D. 2019. Meta-modeling methods for estimating ammonia volatilization from nitrogen fertilizer and manure applications. *Journal of environmental management* **236**: 195-205.

Reichstein M, Camps-Valls G, Stevens B, Jung M, Denzler J, Carvalhais N. 2019. Deep learning and process understanding for data-driven Earth system science. *Nature* **566**(7743): 195-204.

Robertson AD, Paustian K, Ogle S, Wallenstein MD, Lugato E, Cotrufo MF. 2019. Unifying soil organic matter formation and persistence frameworks: the MEMS model. *Biogeosciences* **16**(6): 1225-1248.

Saha D, Basso B, Robertson GP Submitted. Machine learning reveals simplified path for predicting N2O fluxes from agriculture.

Schmidt MW, Torn MS, Abiven S, Dittmar T, Guggenberger G, Janssens IA, Kleber M, Kögel-Knabner I, Lehmann J, Manning DA. 2011. Persistence of soil organic matter as an ecosystem property. *Nature* **478**(7367): 49.

Shahhosseini M, Martinez-Feria RA, Hu G, Archontoulis SV. 2019. Maize yield and nitrate loss prediction with machine learning algorithms. *Environmental Research Letters* **14**(12): 124026.

Sinsabaugh RL, Moorhead DL, Xu X, Litvak ME. 2017. Plant, microbial and ecosystem carbon use efficiencies interact to stabilize microbial growth as a fraction of gross primary production. *New Phytologist* **214**(4): 1518-1526.

Smith CM, David MB, Mitchell CA, Masters MD, Anderson-Teixeira KJ, Bernacchi CJ, DeLucia EH. 2013. Reduced nitrogen losses after conversion of row crop agriculture to perennial biofuel crops. *Journal of environmental quality* **42**(1): 219-228.

Smith D, Inman-Bamber N, Thorburn P. 2005. Growth and function of the sugarcane root system. *Field Crops Research* **92**(2-3): 169-183.

Sokol NW, Bradford MA. 2019. Microbial formation of stable soil carbon is more efficient from belowground than aboveground input. *Nature Geoscience* **12**(1): 46.

Stein LY, Yung YL. 2003. Production, isotopic composition, and atmospheric fate of biologically produced nitrous oxide. *Annual Review of Earth and Planetary Sciences* **31**(1): 329-356.

Stenzel JE, Bartowitz KJ, Hartman MD, Lutz JA, Kolden CA, Smith AM, Law BE, Swanson ME, Larson AJ, Parton WJ. 2019. Fixing a snag in carbon emissions estimates from wildfires. *Global change biology* **25**(11): 3985-3994.

Straube JR, Chen M, Parton WJ, Asso S, Liu Y-A, Ojima DS, Gao W. 2018. Development of the DayCent-Photo model and integration of variable photosynthetic capacity. *Frontiers of Earth Science* **12**(4): 765-778.

Sulman BN, Brzostek ER, Medici C, Shevliakova E, Menge DN, Phillips RP. 2017. Feedbacks between plant N demand and rhizosphere priming depend on type of mycorrhizal association. *Ecology letters* **20**(8): 1043-1053.

Sulman BN, Moore JA, Abramoff R, Averill C, Kivlin S, Georgiou K, Sridhar B, Hartman MD, Wang G, Wieder WR. 2018. Multiple models and experiments underscore large uncertainty in soil carbon dynamics. *Biogeochemistry* **141**(2): 109-123.

Sulman BN, Phillips RP, Oishi AC, Shevliakova E, Pacala SW. 2014. Microbe-driven turnover offsets mineral-mediated storage of soil carbon under elevated CO 2. *Nature Climate Change* **4**(12): 1099.

Sulman BN, Shevliakova E, Brzostek ER, Kivlin SN, Malyshev S, Menge DN, Zhang X. 2019. Diverse mycorrhizal associations enhance terrestrial C storage in a global model. *Global Biogeochemical Cycles* **33**(4): 501-523.

Takriti M, Wild B, Schnecker J, Mooshammer M, Knoltsch A, Lashchinskiy N, Alves RJE, Gentsch N, Gittel A, Mikutta R. 2018. Soil organic matter quality exerts a stronger control than stoichiometry on microbial substrate use efficiency along a latitudinal transect. *Soil Biology and Biochemistry* **121**: 212-220.

Tejera M, Boersma N, Vanloocke A, Archontoulis S, Dixon P, Miguez F, Heaton E. 2019. Multi-year and Multi-site Establishment of the Perennial Biomass Crop Miscanthus× giganteus Using a Staggered Start Design to Elucidate N Response. *BioEnergy Research* **12**(3): 471-483.

Wagner-Riddle C, Congreves KA, Abalos D, Berg AA, Brown SE, Ambadan JT, Gao X, Tenuta M. 2017. Globally important nitrous oxide emissions from croplands induced by freeze–thaw cycles. *Nature Geoscience* **10**(4): 279.

Walker AP, Hanson PJ, De Kauwe MG, Medlyn BE, Zaehle S, Asao S, Dietze M, Hickler T, Huntingford C, Iversen CM. 2014. Comprehensive ecosystem model-data synthesis using multiple data sets at two temperate forest free-air CO2 enrichment

experiments: Model performance at ambient CO2 concentration. *Journal of Geophysical Research: Biogeosciences* **119**(5): 937-964.

Walsh ES, Hudiburg T. 2019. An integration framework for linking avifauna niche and forest landscape models. *Plos One*.

Wang Y, Law R, Pak B. 2010. A global model of carbon, nitrogen and phosphorus cycles for the terrestrial biosphere. *Biogeosciences* **7**(7).

Whitaker J, Field JL, Bernacchi CJ, Cerri CE, Ceulemans R, Davies CA, DeLucia EH, Donnison IS, McCalmont JP, Paustian K. 2018. Consensus, uncertainties and challenges for perennial bioenergy crops and land use. *GCB Bioenergy* **10**(3): 150-164.

Wieder W, Grandy A, Kallenbach C, Bonan G. 2014. Integrating microbial physiology and physio-chemical principles in soils with the MIcrobial-MIneral Carbon Stabilization (MIMICS) model. *Biogeosciences* **11**(14): 3899.

Wieder WR, Bonan GB, Allison SD. 2013. Global soil carbon projections are improved by modelling microbial processes. *Nature Clim. Change* **3**(10): 909-912.

Wu T, Lu Y, Fang Y, Xin X, Li L, Li W, Jie W, Zhang J, Liu Y, Zhang L, et al. 2019. The Beijing Climate Center Climate System Model (BCC-CSM): the main progress from CMIP5 to CMIP6. *Geosci. Model Dev.* **12**(4): 1573-1600.

Ye JS, Bradford MA, Dacal M, Maestre FT, García-Palacios P. 2019. Increasing microbial carbon use efficiency with warming predicts soil heterotrophic respiration globally. *Global Change Biology* **25**(10): 3354-3364.

Zhu Q, Riley WJ, Tang J, Collier N, Hoffman FM, Yang X, Bisht G. 2019. Representing nitrogen, phosphorus, and carbon interactions in the E3SM land model: Development and global benchmarking. *Journal of Advances in Modeling Earth Systems* **11**(7): 2238-2258.

Zhu X, Liang C, Masters MD, Kantola IB, DeLucia EH. 2018. The impacts of four potential bioenergy crops on soil carbon dynamics as shown by biomarker analyses and DRIFT spectroscopy. *Gcb Bioenergy* **10**(7): 489-500.

Chapter 2 : Microbial explicit processes improve modeled soil carbon dynamics.

Abstract

Globally, soils hold approximately half of ecosystem carbon and can serve as a source or sink depending on climate, vegetation, management, and disturbance regimes. Understanding how soil carbon dynamics are influenced by these factors is essential to evaluate proposed natural climate solutions and policy regarding net ecosystem carbon balance. While there is still uncertainty surrounding processes that affect soil carbon dynamics, it is clear that soil microbes play a key role in both carbon fluxes and stabilization. However, biogeochemical models often do not specifically address microbial-explicit processes – a topic of debate in the literature. Here, we incorporated microbial explicit processes into the DayCent biogeochemical model to better represent soil carbon fluxes and stabilization. Specifically, the model now has three major changes: 1) live and dead microbe pools that influence routing of carbon to chemically and physically protected pools, 2) Michaelis-Menten kinetics rather than first-order kinetics in the decomposition function, and 3) feedbacks between decomposition and live microbial pools. We evaluated the performance of microbial and first-order models using observations of net ecosystem production, ecosystem respiration, soil respiration, microbial biomass, and soil carbon from long-term bioenergy research plots in the mid-west United States. Live microbial biomass pools in the new model were validated with measurements taken at the beginning and middle of the growing season. For both measurement dates, modeled microbial biomass was within the standard error of the observed means. The microbial-explicit model had better model-data agreement for ecosystem respiration for switchgrass and miscanthus (switchgrass: $R^2 = 0.86$; miscanthus: $R^2 = 0.70$) compared to the first-order model (switchgrass: $R^2 = 0.81$; miscanthus: $R^2 = 68$). The microbial-explicit model also represented seasonal dynamics of soil carbon fluxes better than the first-order model which consistently overestimated winter soil respiration. Both models simulated total soil carbon within the observed standard error. However, the microbial model allocated less soil carbon to the passive pool (analogous with mineral associated organic matter or MAOM) and more to the slow pool (analogous to particulate

organic matter or POM) than the first-order model. Response to disturbance and management varied between the models. For example, in historic agricultural simulations the microbial model had higher soil carbon loss in response to poor cultivation practices in the era leading up to the Dust Bowl but increased soil carbon at faster rates when agricultural practices improved during the Green Revolution. In simulated soil warming and wetting experiments that also increased plant production, the first-order model showed a linear increase in soil C with the increase in litter inputs, but soil C predictions by the microbial model plateaued after X years. It's clear that adding microbial-explicit mechanisms to ecosystem models will improve model predictions of ecosystem carbon balances, particularly when evaluating management decisions, but more research is necessary to validate disturbance and climate change responses and pool allocation.

Introduction

Understanding the nuances of ecosystem carbon sequestration and storage is critical as governments, researchers, and the private sector grapple with meeting net-zero emission goals outlined by the International Panel on Climate Change (IPCC) and Paris Climate Accord. Among strategies to remove and store atmospheric carbon are 'Natural Climate Solutions' (NCS) which return carbon to the biosphere where it is stored in biomass or soil (Griscom et al., 2017; Osaka et al., 2021). Soil carbon has the potential to make up a quarter (23.8 Gt CO_2 eq yr^{-1}) of the land-based NCS through protection of existing soil carbon stocks as well as increasing soil carbon where stocks have been depleted (Bossio et al., 2020). However, the effectiveness and efficiency of nature-based carbon removal strategies relies on measurements and research to evaluate and predict the amount of carbon being sequestered, how long it will remain in the ecosystem, and how susceptible it is to events that may cause sudden losses of ecosystem carbon (e.g., fire, land use change, etc.).

Perennial bioenergy crops (e.g., miscanthus and switchgrass) have the potential to be used as feedstocks to produce biofuels and bioproducts while also reducing net greenhouse gas emissions and improving water quality relative to other crops (Hudiburg et al., 2015; G. P. Robertson et al., 2017). For example, compared to common annual row crops such as corn and soybeans, these large perennial grasses produce more biomass, require less fertilizer,

may be more drought and flood tolerant, and contribute more plant residue and deeper roots that can increase soil carbon accumulation (He et al., 2022; Heaton et al., 2008).

Soils comprise more than half of terrestrial carbon storage (IPCC, 2018; Scharlemann et al., 2014), yet they are vulnerable to losses from land cover and land use change (IPCC, 2018; G. P. Robertson et al., 2017). Biogeochemical models serve as a way to evaluate how a variety of climate, disturbance, and management scenarios on soil carbon stocks and Net Ecosystem Carbon Balance over long temporal and broad spatial scales. To date, Earth System Models (ESMs) and ecosystem-scale models have largely relied on first-order kinetics and soil pool structures that don't explicitly represent microbial processes or the mechanisms of soil carbon stabilization (Berardi et al., 2020). Parsimonious and data-efficient first-order models have been effective tools to simulate soil organic carbon dynamic trends in decomposition experiments (Bonan et al., 2013; Campbell et al., 2016) as well as large-scale spatial variation and temporal dynamics (Campbell & Paustian, 2015; Wieder, Grandy, Kallenbach, Taylor, & Bonan, 2015; Wieder et al., 2018). However, there remains substantial uncertainty in Earth System Model (ESM) projections of soil carbon under future scenarios due to the lack of crucial biogeochemical processes (Todd-Brown et al., 2018; Wieder et al., 2013).

First-order soil carbon models are commonly built on theories of mean residence times of soil carbon pools to determine decay rates (i.e., k-values) and largely ignore the major role that soil microbes play in the breakdown of plant organic material and soil carbon stabilization. Microbial decomposition disproportionately results in necromass with strong soil particle bonds in the mineral associated organic matter pool (MAOM), where carbon is the most protected from leaching and further decomposition (Cotrufo et al., 2013). Without explicitly addressing microbial biomass pools, biogeochemical models will continue to ignore the feedbacks between microbial biomass and rates of decomposition (Sulman et al., 2017; Wieder et al., 2015).

In the last decade, advances in soil models have allowed more mechanistic, trait-based approaches that include feedbacks between microbial biomass and decomposition as well as plant-microbial interactions (Berardi et al., 2020; Wan & Crowther, 2022). This coincides with empirical studies that have emphasized the importance of soil microbes in

decomposition and soil carbon stabilization. The Microbial Efficiency-Matrix Stabilization (MEMS) v2.0 model was recently developed from the MEMS v1.0 soil model into a full ecosystem scale model that simulates measurable pools of soil organic matter (SOM) and physio-chemical mechanisms of SOC stabilization. MEMS represents complex microbial mechanisms to determine MAOM and POM formation while using first-order kinetics to drive decomposition (A. D. Robertson et al., 2019; Y. Zhang et al., 2021). The Microbial-Mineral Carbon Stabilization (MIMICS) model (Wieder et al., 2014) and the Fixation and Uptake of Nitrogen – Carbon, Organisms, Rhizosphere, and Protection in the Soil Environment (FUN-CORPSE) model (Sulman et al., 2017) use Michaelis-Menten kinetics, rather than first-order, that simulates feedbacks between the size of the microbial biomass pool on decay rates of soil C pools.

Here we seek to understand if current biogeochemical models are limited in their ability to predict soil carbon stocks and net ecosystem carbon balance over long temporal and broad spatial scales by a lack of mechanistic representation of microbial processes. We expect that an ecosystem model may be improved by incorporating these mechanisms, resulting in lower uncertainty and more accurate representation of soil carbon in past data and future projections. In this study, we aim to evaluate how microbial-driven decomposition compares to the first-order model by adapting the decomposition function from a modified version of FUN-CORPSE (Juice et al., 2022) into the DayCent ecosystem model (Parton et al., 1998). However, comparing separate ecosystem models to each other can make it challenging to isolate the effects of recent model improvements on their predictions. To address this issue, we have updated the DayCent model to allow for interchangeable functions and components, including two soil organic matter sub-models (First-Order (FO) and Michaelis-Menten (MM)) and multiple functions that describe soil temperature and moisture effects on decomposition. Doing this creates a form of a model testbed that allows for alternative sub-models to be forced with common inputs in order to quantify how different functions influence the rate of decomposition and SOM formation (Wieder et al., 2018).

Furthermore, realistic inputs to the litter and soil pools from observed or modeled plant biomass are critical to best simulate soil carbon dynamics with both first-order and microbial explicit soil models. Thus, we have continued to develop and validate a new plant

submodel in DayCent to better represent the plant physiology and chemistry of large perennial grasses (Berardi et al., 2020; Moore et al., 2020). Finally, to compare the long-term soil carbon dynamics of each soil carbon model, we simulate perennial bioenergy grasses under potential future climate conditions. By doing so, we aim to determine which model provides more accurate predictions of soil carbon dynamics and assess the potential of these grasses as a bioenergy feedstock.

Methods

Model description and development

The version of DayCent we use for this study, DayCent-CABBI, was developed from DayCent-Photo (Straube et al., 2018). The new version includes a sub-model called 'grasstree', which simulates large annual and perennial bioenergy crops such as sorghum, switchgrass, miscanthus, and sugarcane (Berardi et al 2020, Moore et al 2020). Unlike the original crop sub-model, the grasstree sub-model treats stems and leaves as separate carbon and nitrogen pools, similar to the tree sub-model. Additionally, it includes an additional root pool to represent rhizomes, which accounts for differences in the chemical composition and physiological processes between plant tissues that play important roles in growth, nitrogen demand, decomposition as plant parts enter litter and soil pools, and sensitivity to climate and weather events (e.g. drought, freezing events). The grasstree sub-model also has a gradual senescence over a user-specified period that begins after the autumn equinox and is triggered by user-specified daylength where senescence begins, allowing for variability in the length of senescence by plant species and for better automation of senescence events across broader spatial extents. Additionally, the new model incorporates new parameters and mechanisms for simulating temperature thresholds and the severity of damage caused by frost to above and belowground plant parts. For specific functions and further details describing the new plant sub-model, see Supporting Information (SI).

DayCent-CABBI soil sub-models

The model simulates decomposition and soil organic carbon stabilization by either using the original soil sub-model using first-order kinetics, or using the new microbial

explicit soil sub-model using Michaelis-Menten kinetics. The new sub-model adapts the Michaelis-Menten decomposition functions from the FUN-CORPSE soil model, which has a more representative pool structure and includes a mechanism for roots exudation. The MM model maintains a similar pool structure, pool properties, soil texture effects, and lignin effects on carbon flows from the original DayCent decomposition function but adds surface and soil dead biomass pools and replaces the surface and soil 'active pools' with surface and soil 'microbe biomass pools' (Figure 2.1). In the MM model, most carbon from other pools is now routed through the live microbial and dead microbial pools as material passes through the decomposition process before entering either slow or passive soil pools, though some dead microbe biomass, structural litter, and decomposing dead wood can bypass microbial processing and flow directly to the slow pool.

As an example of the differences between the FO model and the MM model, we consider the amount of C in the soil slow pool (*som2c(SOIL)* that is decomposed daily ($tcflow_{som2c(SOIL)}$, g C m^{-2}). In the FO model $tcflow_{som2c(SOIL)}$ it is computed as:

$$tcflow_{som2c(SOIL)} = som2c(SOIL) \times f(T) \times f(\theta) \times dec5(SOIL) \times cltfac(2) \times pHeff \times dtm$$

where *f(T)* is the temperature effect on decomposition (0– 1) (variable Q_{10}), f(Θ) is the soil moisture effect on decomposition (0– 1) (strictly increasing and plateauing at field capacity), *dec5(SOIL)* is the intrinsic decomposition rate of *som2c(SOIL)* (yr^{-1}), *cltfac(2)* is the cultivation effect for *som2c(SOIL) (it > 1.0 when cultivation has recently occurred and is 1.0 otherwise)*, *pHeff* is the pH effect on decomposition (0 – 1), and *dtm* is the time step (fraction of a year).

In the MM model $tcflow_{som2c(SOIL)}$, is computed as

$$tcflow_{som2c(SOIL)} = V_{maxref,som22} \cdot f_{recalctrnt}(T) \cdot f(\theta) \cdot som2c(SOIL) \cdot \frac{\frac{micc(SOIL)}{som2c(SOIL)}}{\frac{micc(SOIL)}{som2c(SOIL)} + k_{M.som2}} \cdot cltfac(2) \cdot pHeff \cdot dtm$$

where $V_{maxref,som22}$ is the reference Vmax (maximum reaction velocity) for *som2c(SOIL)*(yr^{-1}), *micc(SOIL)* is the amount of live microbial biomass in the soil (g C m^{-2}), $f_{recalcitrant(T)}$ is the temperature effect on decomposition for recalcitrant material (either variable Q_{10} or exponential Q_{10}), f(Θ) is the soil moisture effect on decomposition (either strictly increasing or reaching a maximum at 50% saturation then declining), and $K_{M,som2}$ is the half saturation fraction for the Michaelis-Mention function. The values of *pHeff*, *clteff(2),* and *dtm* are the same as those for the FO model.

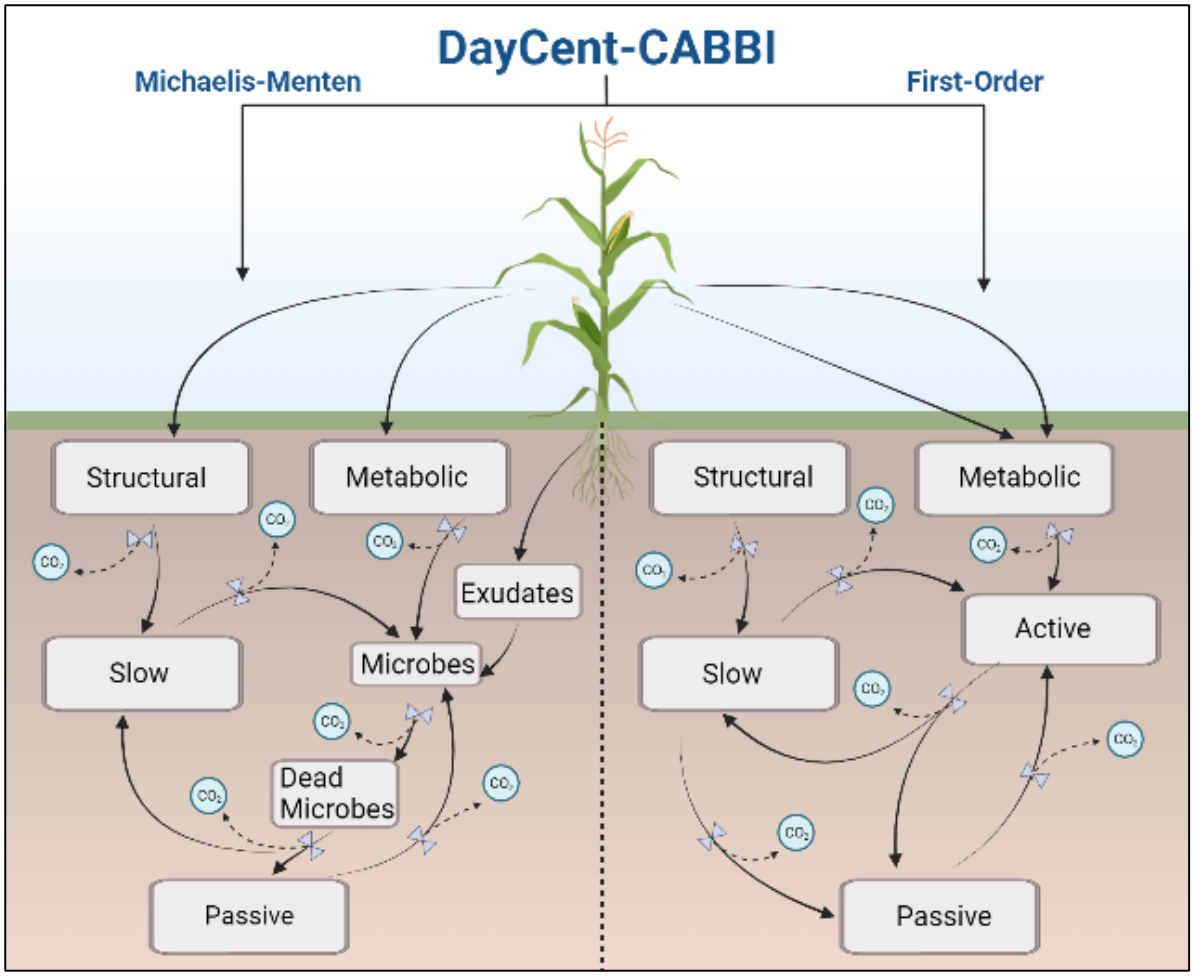

Figure 2.1. Diagram of DayCent-CABBI soil model pool structures and C flows between pools for the MM and FO soil submodels. Solid rounded arrows show the direction of C flow from one pool to another. Bowties indicate decomposition occurring and CO_2 loss as a part of C transfer between pools.

Note that the FO model still protects microbe C (the active pool) as passive C and is not simply decomposition cascade of increasingly recalcitrant material. We consider the passive pool to be analogous with mineral associated organic matter (MAOM) and the slow pool to be analogous with particulate organic matter (POM).

Microbial consumption of organic matter is controlled by abiotic factors as well as Michaelis-Mention dynamics based on the relative amount of live microbial biomass present. DayCent has interchangeable functions that are used to calculate soil temperature and moisture effects on decomposition rates and microbial growth. The first order model uses a

variable Q_{10} temperature effect on decomposition function, and an arc-tangent function to simulate the effect of soil moisture on decomposition using relative soil water content (Del Grosso, Parton, et al., 2005). With the MM model users can select from the following soil temperature and moisture functions: 1a) a variable Q_{10} temperature effect (DayCent) or 1b) an exponential Q_{10} temperature effect (CORPSE, (Sulman et al., 2014)); 2a) an increasing relationship with soil moisture that plateaus when soil water content reaches the field capacity (DayCent) or 2b) a hill relationship where soil moisture effect is highest around 50% saturated water filled pore space (WFPS) and declines as WFPS is greater or less than 50% (CORPSE, (Sulman et al., 2014)). All functions are described in more detail in Model Documentation in the SI.

Observational data and model simulations

The models were calibrated and evaluated with an extensive, long-term dataset from the University of Illinois Champaign-Urbana Energy Farm (UIEF; 40° 3′ 46.209″ N, 88° 11′ 46.0212″ W) located in the Midwest region of the United States. The regional climate is characterized by a hot and humid growing season, no dry season, and severe cold winters. The mean annual temperature is 10.9 C and mean annual precipitation is 1,051 mm (*Illinois State Water Survey*, 2020). The soil is Drummer silty clay loam with poor drainage (Soil Survey Staff, 2015). The switchgrass and miscanthus fields used in this study were established in 2008. Soil samples were collected prior to planting to obtain a baseline of soil C and N. Eddy covariance flux towers were installed in the center of each field with instrumentation measuring C, water, and energy fluxes at high temporal resolution (Zeri et al., 2011). Because this study solely leveraged existing data, measurement of different pools and fluxes aren't consistent for both crops (Table 2.1). Measurements of above- and belowground biogeochemical pools for both crops have been taken annually since the plots were established for long-term evaluation of the crops potential to meet bioenergy GHG mitigation goals (Kantola et al., 2022). Additionally, some observations used for model evaluation were taken as a part of smaller studies to understand specific processes related to one or both crops.

Table 2.1. Calibration and validation periods used for GPP, NEP, ER, NPP, SOC, and microbial biomass C data for Miscanthus and Switchgrass fields.

	Temporal Resolution	Crop	Calibration period	Validation Period
Flux tower (GPP, NEP, ER, AET)	Continuous daily	Switchgrass	2009 – 2011	2012 – 2015
		Miscanthus	2009 - 2013	2014 – 2018
NPP	Annual	Both	2008 - 2011	2012 – 2016
SOC	8 – 9 years	Switchgrass	2008	2018
		Miscanthus	2008	2019
POM & MAOM	Single observation	Miscanthus	NA	2020
Soil Respiration	Continuous daily - biweekly	Switchgrass	NA	2009 – 2011, 2018 – 2019
		Miscanthus	NA	2009 – 2011, 2019
Microbial biomass	Monthly	Switchgrass	NA	2018
		Miscanthus	NA	2018 – 2019

The model was calibrated to an average SOC value for both fields in 2008 through the spinup and historical land use simulations. DayMet weather data (daily max temperature, minimum temperature, and precipitation) for a past 38-year period (1980 – 2017) was used for spinup and historical simulations (Daymet citation). The spinup simulated year 1 – 1847 with a tall grass prairie plant sub-model grown using grasstree. Light grazing occurred annually with a fire every four years. Historic land use was simulated from 1848 to 2007 and consisted primarily of corn and soybean rotations. The same spinup and historic land use simulations were used for both switchgrass and miscanthus fields.

Switchgrass and miscanthus management for 2008-2019 was prescribed following site-specific timing of planting, fertilization, cultivation, and harvest. Both crops were planted early in the 2008 growing season but required a second planting later in the season in patches where establishment failed. Switchgrass was not fertilized throughout the entire field trial whereas miscanthus was fertilized at a rate of 56 kg ha^{-1} 2014 – 2019 after experiencing a decline in productivity. Both the switchgrass and the miscanthus fields were cultivated with a moldboard plow in 2008 when transitioning the fields from corn production to perennial grasses. Both crops were harvested annually between November and January. Detailed descriptions of site management can be found in Moore and others (2020) for switchgrass and for both switchgrass and miscanthus in Kantola and others (2022).

We calibrated DayCent-CABBI to ecosystem carbon fluxes for switchgrass and miscanthus simulations at the Energy Farm. Net primary productivity (NPP) and gross primary productivity (GPP) were calibrated by adjusting parameters that were specific to growth response to temperature (Table 2.2). Ecosystem respiration (ER) was calibrated by adjusting the fraction of GPP applied to maintenance respiration. Net ecosystem productivity (NEP) was calibrated through the combined efforts to calibrate GPP and ER.

Table 2.2. Parameters used to calibrate switchgrass and miscanthus NPP, GPP, ER, and NEP. Photosynthetic parameters were constrained by range values identified by Straube and others (2018).

Parameter	Description	Switchgrass Value	Miscanthus Value
PS2Mrsp	Fraction of GPP applied to maintenance respiration	0.2	0.2
Amax	Maximum net CO_2 assimilation rate	39.0	40.0
AmaxFrac	Average daily max photosynthesis rate as a fraction of Amax	0.75	0.75
AmaxScalar1	Scalar value of Amax during period defined by GrowthDays1	1.0	0.8
AmaxScalar2	Scalar value of Amax during period defined by GrowthDays2	1.2	1.38
AmaxScalar3	Scalar value of Amax during period defined by GrowthDays3	0.8	0.9
AmaxScalar4	Scalar value of Amax during period defined by GrowthDays4	0.2	0.6
GrowthDays1	The first day of growth to apply AmaxScalar1	1	1
GrowthDays2	Number of days after the start of growth to apply AmaxScalar2	150	120
GrowthDays3	Number of days after the start of growth to apply AmaxScalar3	200	210
GrowthDays4	Number of days after the start of growth to apply AmaxScalar4	260	245
PsntMin	Minimum temperature for photosynthesis to occur	1.0	-2.0
PsntOpt	Optimum temperature for photosynthesis to occur	27.0	29.0
PPDF(1)	Optimum temperature for production	27.0	29.0
PPDF(2)	Maximum temperature for production	44.0	44.0
PPDF(3)	Right curve shape for Poisson Density curve function	20.0	20.0
PPDF(4)	Left curve shape for Poisson Density curve function	0.7	0.3
DYLENSEN	Day length after autumn equinox that triggers senescence	11.99	11.95
GSENEDYS	Number of days that senescence occurs	40	50
GSENDETH(1)	Fraction of leaves that dies over senescence	0.96	0.963
GSENDETH(2)	Fraction of stems that dies over senescence	0.96	0.963

We ran the MM model with every combination of soil temperature and soil moisture functions and then evaluated which combination best captured daily observed NEP and ER. We used the MM model with the variable Q_{10} soil temperature effect function and the hill soil moisture effect function, which produced the best match between simulated and

observed daily fluxes relative to the exponential Q_{10} function and the increasing soil moisture function overestimated ER in the winter and the spring.

Total SOC was calibrated to during the spinup and historic land use simulations. The passive pool of both the first order and MM model were calibrated to be equal during the spinup and historical period. The slow and passive pools were slightly different throughout the simulations, but total SOC was equal by year 2008. With the availability of soil particulate organic matter (POM) C and MAOM C in measured in the miscanthus field in 2019 (Ridgeway et al., 2022), we were able to calibrate specific pools to the observed data by adjusting the rate of flow between pools. The slow soil pools in both the first order and MM model were calibrated to observed POM and the passive soil pools were calibrated to observed MAOM while maintaining the total SOC calibration for 2008.

Following model calibration and evaluation, we ran four future climate scenarios from 2020 – 2049 for switchgrass and miscanthus with both soil models. Current management of switchgrass and miscanthus was continued during future simulations. To create the future climate scenarios, the past 30-years of weather were blocked by year and randomized. Using the same set of future weather data, we then constructed the four climate scenarios: 1) Unaltered, but randomized weather (Current); 2) 2°C added to the minimum and maximum temperature (Warming); 3) Increased precipitation during the early growing season (Rain); and 4) 2°C added to the minimum and maximum temperature and increased precipitation during the early growing season (Warming + Rain).

Microbial biomass measurements were taken during the growing season in 2018 for switchgrass and both 2018 and 2019 for miscanthus. There were three measurement dates in 2018 and two in 2019, allowing us to evaluate if the model was capturing the seasonality of microbial biomass growth. Samples were taken in the top 10 cm of the soil profile and frozen until chloroform extractions were performed. Microbial biomass C was measured using a mass spectrometer and then scaled to a square meter. This depth was assumed to account for most of the microbial biomass because the majority of miscanthus and switchgrass root and rhizome biomass is in the top 10 cm of the soil profile (Black et al., 2017) and the distribution of soil microbial biomass mirrors the distribution of roots (Xu et al., 2013).

Microbial biomass data was used to evaluate if DayCent was capturing reasonable values of microbial biomass and growth but was not tuned specifically to microbial biomass data.

Soil respiration data from two different measurement campaigns was used to evaluate modeled soil C flux. We used the daily total soil respiration measurements (R_s) that were taken using automated respiration chambers between 2009 – 2011. The measurement methods and data processing is described by Anderson-Teixeira and others (2013). We also evaluated model performance using soil respiration that had been partitioned into autotrophic (R_a) and heterotrophic (R_h) respiration. These measurements were taken weekly to biweekly during the growing season of 2018 for miscanthus (Moore et al., 2021) and 2017 – 2018 for switchgrass (Moore et al., 2020).

Results

The grasstree model was rigorously tested against flux tower data and other observational datasets at the UIEF. To calibrate GPP we compared model results to observed daily average flux and average daily cumulative flux to ensure that both seasonal variation and annual carbon fluxes were well represented by the model (Figures 2.2, S. 2.1, S. 2.2). There was a tight fit between simulated and observed GPP for both grasses, although annual GPP estimates by the model were slightly underestimated for miscanthus during the calibration years. While switchgrass and miscanthus are both perennial grasses, they have different physiological and phenological traits that provide useful insight for model evaluation. The physiology and phenology of miscanthus in particular presents several modeling challenges. Miscanthus has significantly more biomass (above- and below-ground) compared to switchgrass, ranging from approximately 1,200 to 1,800 g C m^{-2} compared to 700 to 1,300 g C m^{-2} once established at the UIEF (Figure 2.3). Once established, miscanthus has shallow rhizomes that allow it to start photosynthesizing earlier in the growing season than switchgrass. Miscanthus has a longer growing season than switchgrass, and it was difficult to capture early season GPP for miscanthus during most years. Although the GPP calculations in the plant model are not directly affected by the choice of soil models, there were slight differences in simulated GPP between the FO and MM versions of DayCent for both crops caused by slightly higher soil moisture in the MM model as a result of more SOM.

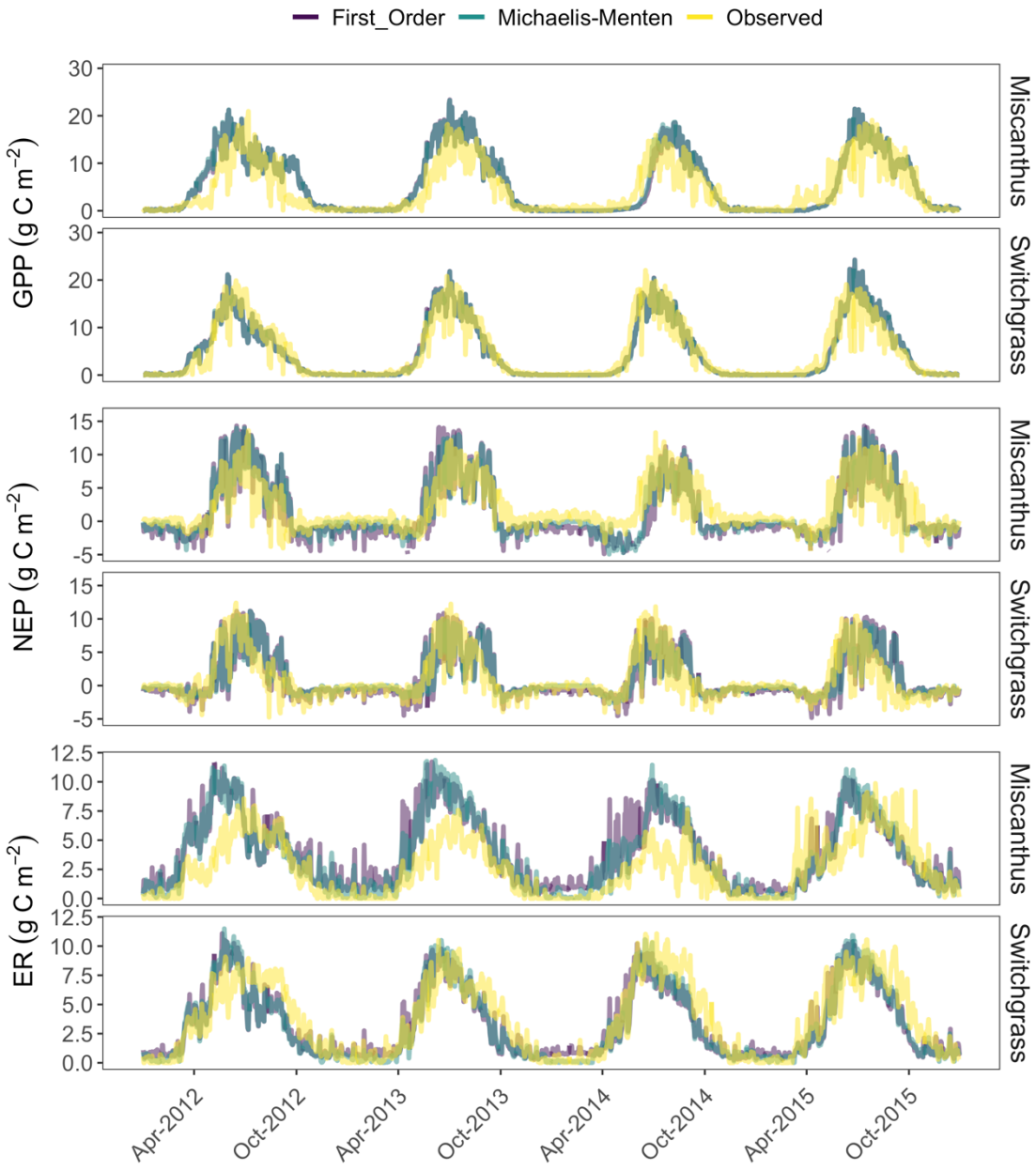

Figure 2.2. Daily observed and modeled GPP, NEP, and ER for switchgrass and miscanthus from 2012 through 2015.

Table 2.3.Statistical evaluation of the FO and MM model compared to daily flux tower data.

Flux	**Crop**	**Model**	**Calibration**		**Validation**	
			R^2	RMSE	R^2	RMSE
GPP	Miscanthus	MM	0.69	3.47	0.80	2.85
	Switchgrass	MM	0.77	2.99	0.82	2.63
ER	Miscanthus	MM	0.49	2.14	0.70	1.84
	Switchgrass	MM	0.83	1.69	0.86	1.42
NEP	Miscanthus	MM	0.64	2.67	0.67	2.60
	Switchgrass	MM	0.56	2.47	0.46	2.55
GPP	Miscanthus	FO	0.67	3.62	0.82	2.77
	Switchgrass	FO	0.79	2.84	0.82	2.61
ER	Miscanthus	FO	0.44	2.30	0.68	1.82
	Switchgrass	FO	0.74	1.77	0.81	1.57
NEP	Miscanthus	FO	0.55	3.13	0.69	2.70
	Switchgrass	FO	0.51	2.61	0.44	2.67

Both crops had the highest observed above-ground peak biomass C in 2011, the fourth year after planting. Above-ground biomass is roughly equivalent to above-ground NPP each year since most above-ground biomass is harvested at the end of the growing season. We were not able to capture this one-year peak in the model for either crop without overestimating NPP in following years. For miscanthus, this discrepancy between simulated and measured above ground biomass in 2011 can at least be partially explained by a "reestablishment" planting in 2010 to fill gaps, reduced harvest in 2010 and 2011 (Moore et al., 2021); these events were not scheduled in the simulations. Switchgrass plots may have received some fertilizer in 2010 that was not scheduled in the simulations. While 2011 above-ground biomass was significantly underestimated by the model, above- and belowground biomass fell within the standard error for both crops most years (Figure 2.3). Modeled biomass directly impacts how much plant biomass C enters the litter, surface, and soil C pools as dead plant material after harvest and subsequently affects rates of decomposition. Modeled plant biomass was nearly identical between the two models, so for simplicity, only modeled NPP in the MM model is shown in Figure 2.3.

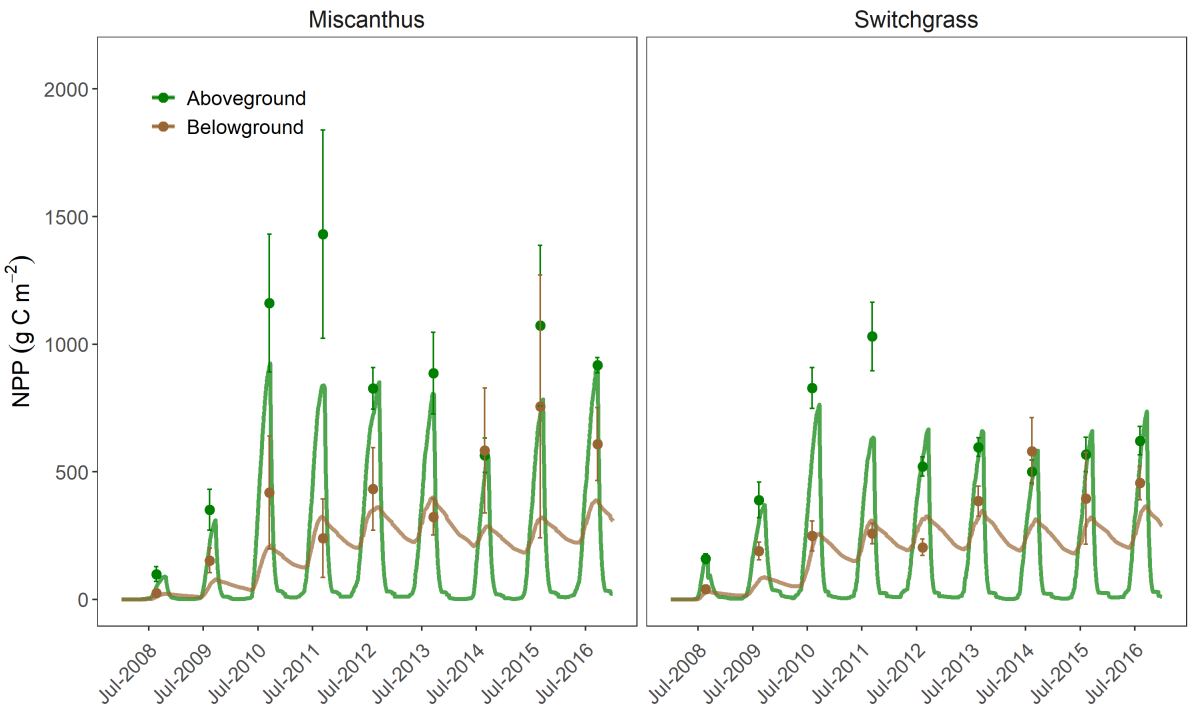

Figure 2.3. Modeled (lines) and observed (points) above- and belowground biomass C for miscanthus and switchgrass.

With GPP and biomass C calibrated, only minor adjustments were required to improve ER and NEP calibration (Figures 2.2, S 2.3, S 2.4, S 2.5, S 2.6). For both crops, the MM model had better model-data agreement of both ER and NEP. In particular, the MM model performed much better at capturing fall, winter, and spring ER whereas the FO model simulated higher than observed ER characterized by spikes in respiration that weren't observed by the eddy covariance tower (Figure 2.2). Both models performed similarly during the summer. For miscanthus, the simulated summer peak ER was shifted sooner in the growing season than was observed (Figure S 2.3) and the cumulative annual ER predicted by the two SOM models was overestimated for both the calibration and validation periods, the MM model was closer to observations (Figure S 2.4). For switchgrass, there was more ER observed than simulated after day 200, and both SOM models underestimated annual ER. For NEP, model estimates were close to observations most of the year, but a discrepancy occurred from days 200 – 300 when NEP was slightly overestimated for miscanthus and underestimated for switchgrass (Figure S. 2.5). Model estimates of cumulative annual NEP for both miscanthus and switchgrass were close to observations although annual NEP was

underestimated for miscanthus during the validation period (Figure S. 2.6). Simulated NEP for miscanthus was underestimated by both SOM models from days 1-150, but the MM-model was closer to observations than the FO model was (Figure S. 2.6).

Soil respiration data was used for validation following calibration to ecosystem carbon fluxes and soil C pools (Figure 2.4). Compared to survey measurements of soil respiration partitioned into autotrophic and heterotrophic respiration (R_a and R_h), both models captured the seasonal variation in R_h when compared to the survey measurements. The FO model simulated large spikes in respiration throughout the year that weren't visible in the survey measurements. The MM model didn't simulate as large of a variation in daily soil respiration and fell closer to the observed values, particularly for miscanthus. There was some variation in R_a between the FO and MM models that would be attributed to the slight variation in GPP between the two models discussed above. Both models have reasonable model-data agreement for R_a, well representing both the magnitude and seasonal variation for switchgrass while capturing the seasonal variation for miscanthus but underestimating the magnitude.

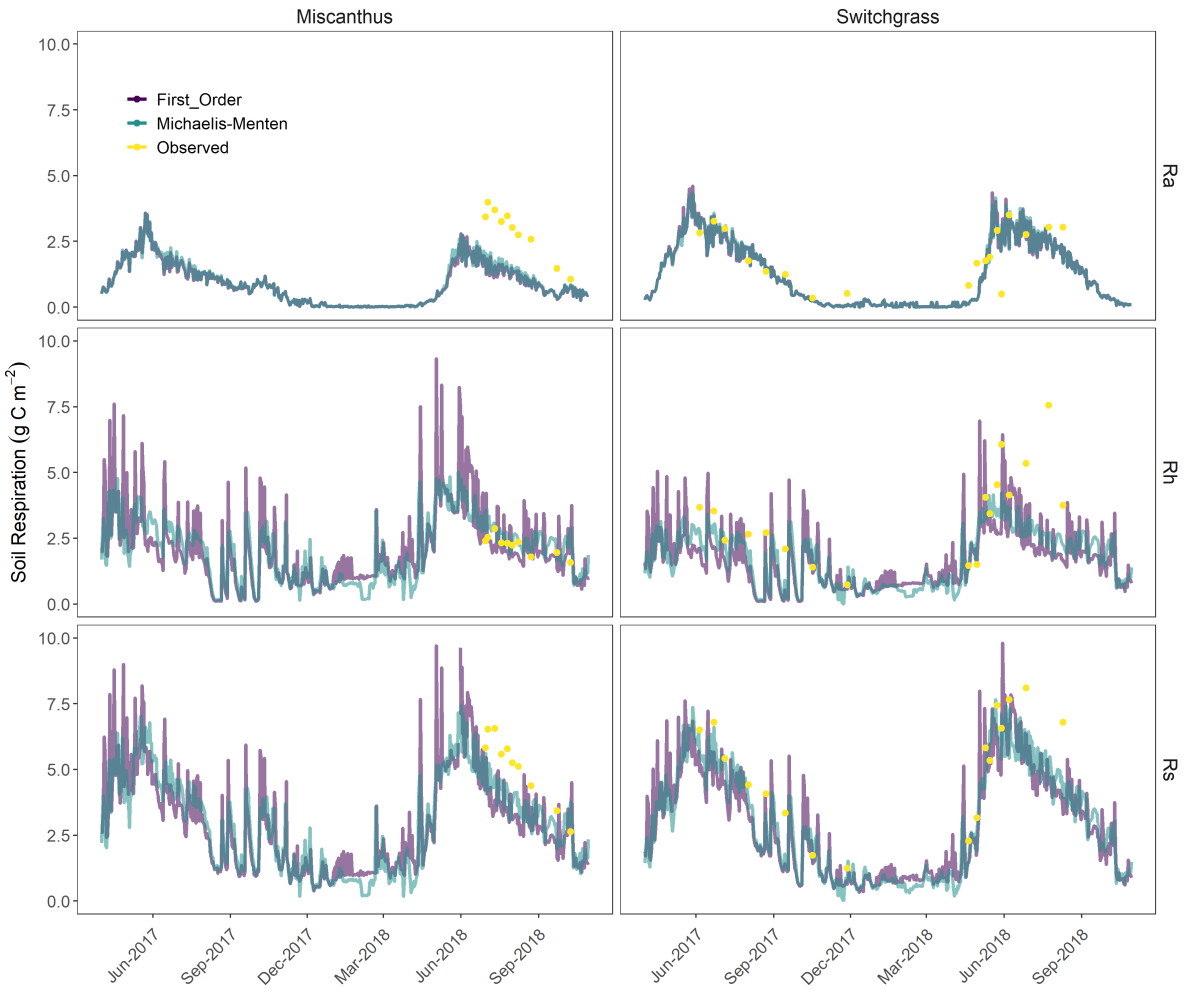

Figure 2.4. Modeled (lines) and observed (points) soil respiration for miscanthus and switchgrass.

The MM model underestimated microbial biomass C but simulated similar increases to the observed values over the growing season (Figure 2.5). However, the estimation of total microbial biomass relies on uncertain factors such as the variation in bulk density in the top 30 cm of soil. There was a decrease in observed microbial biomass C in May 2018 between the first and third measurement period for switchgrass that the model didn't capture. Because of limited data availability, we are unsure what caused this decline and, therefore, unable to determine why the model didn't also simulate a decline in microbial biomass C during that time.

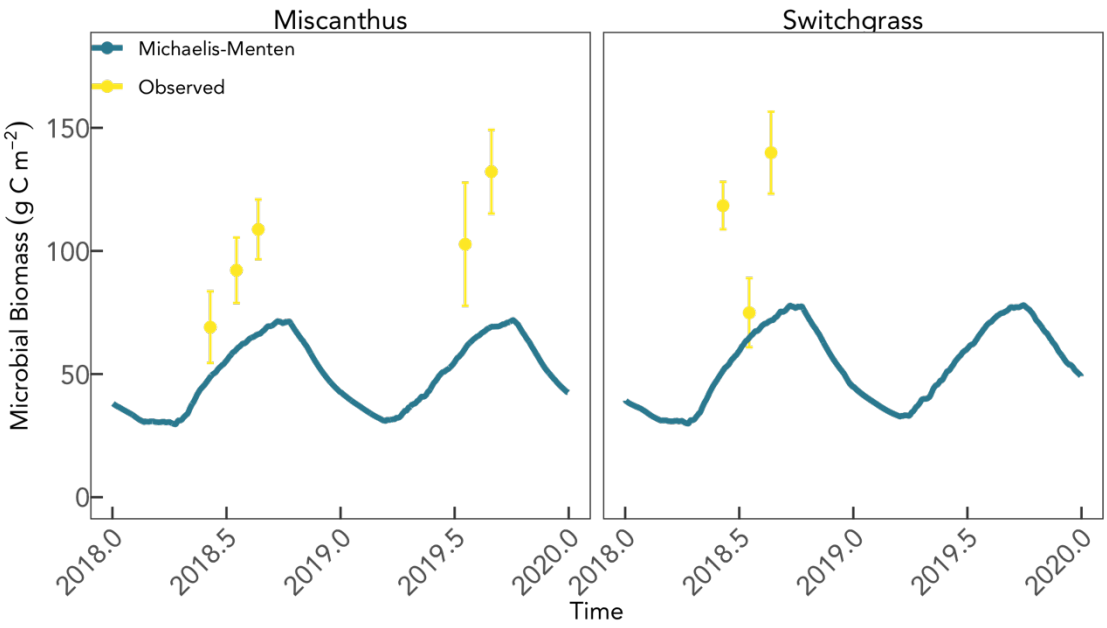

Figure 2.5. Modeled (line) and observed (points) microbial biomass C for switchgrass and miscanthus. Microbial biomass was not measured in 2019 for switchgrass.

Through spinup and historical land use simulations, both models were benchmarked to have approximately the same total soil C (Figure 2.6 and Figure 2.7) and to fall within the standard error of the observed average soil C in 2008 (Figure 2.7). Soil C measurements taken in 2018 and 2019 for switchgrass and miscanthus respectively were used for validation. Both models underestimated soil C during the validation years, falling just shy of the range of the standard error. Additionally, both models were calibrated to have approximately the observed value of protected (MAOM) and unprotected (POM) soil C (Figure 2.7A).

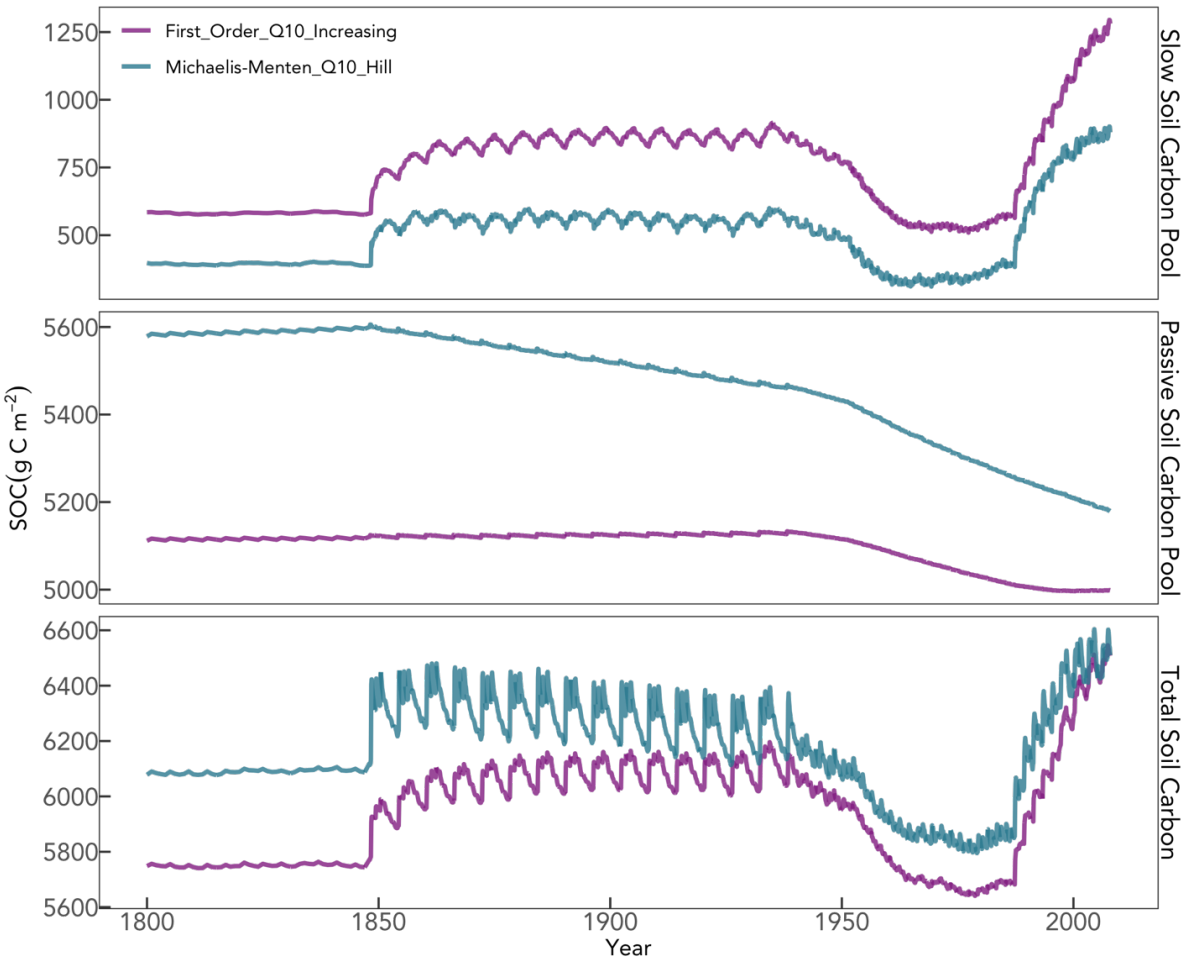

Figure 2.6. The slow and passive soil C pools and the combined total soil C at the end of the spinup period and during the historic land use simulations for both the FO and MM model.

While the FO model started out with nearly the same soil C as the MM model during the period with observed data (2008 -2019) for both crops, it simulated higher soil C by the end of the future simulations (2049) for all climate scenarios. Among the future scenarios with the FO model, the highest simulated soil C accumulation occurred under Warming for miscanthus, followed by the Warming + Rain, Control, and Rain. The MM model also simulated its highest soil C accumulation with Warming, followed by the Control, Warming + Rain, and Rain for miscanthus. The MM model projects a plateau in soil C in the last 5-10 years of the future miscanthus simulations whereas the FO model continues to show increasing trends of soil C through the end of the future simulations. Similar to miscanthus simulations, the FO model projected its highest soil C with the Warming climate scenario for

switchgrass. However, the other three scenarios had very similar soil C by the end of the future simulations. The MM model projected soil C to be very similar in the Control, Rain, and Warming scenarios for switchgrass, but much lower in the Warming + Rain scenario for switchgrass.

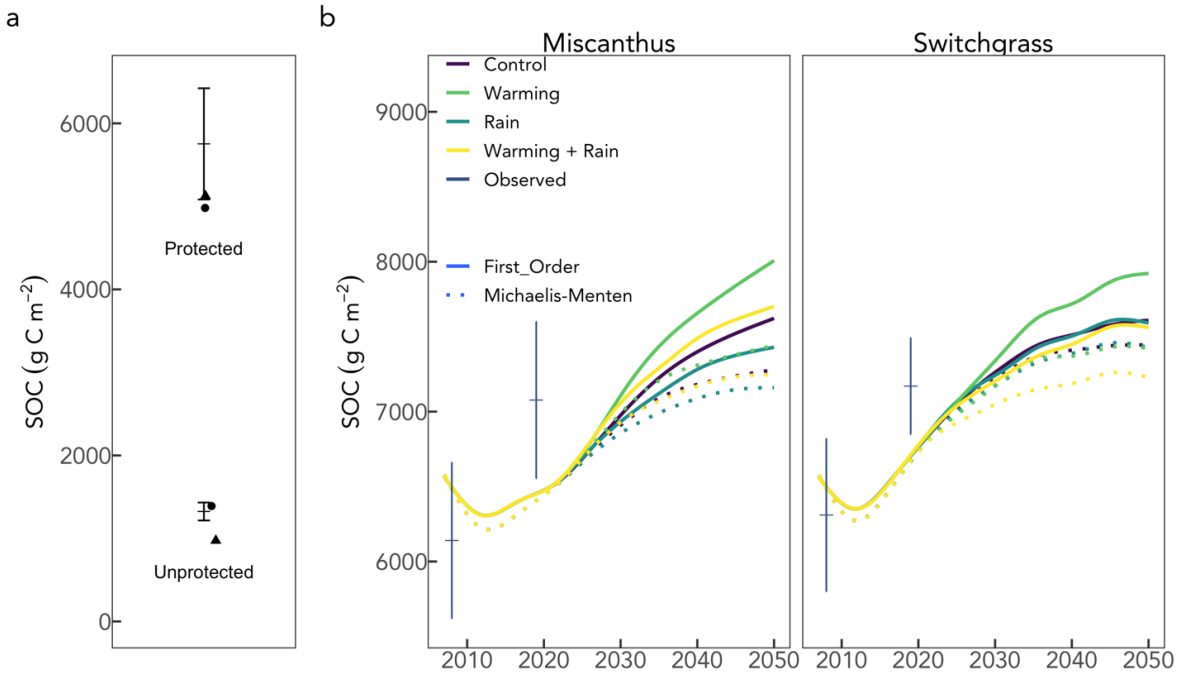

Figure 2.7. Modeled and observed soil carbon. a) The calibration of miscanthus protected and unprotected soil C in 2019 where the MM model is represented by the triangles and the FO model is represent by the circles. b) Soil C projected into the future under four different climate scenarios. Observed soil C is represented by the navy dash with error bars showing standard error of measurements.

Discussion

We developed and used a new plant sub-model that better represents large perennial grasses and a microbial explicit soil organic matter model that can represent measurable soil C pools. We evaluated these two primary advances to the DayCent model that to improve predictions of bioenergy crops and related soil carbon dynamics using an extensive observational dataset of eddy covariance data, above- and belowground biomass C, soil C

(total, MAOM, and POM), microbial biomass C, and partitioned soil respiration (R_s, R_h, and R_a). Selectable features in the DayCent model allowed us to directly compare the predictions of a soil organic matter model with first-order kinetics against one with microbial-explicit controls on decomposition and organic matter formation, and also highlighted the effects of different soil temperature and moisture functions on daily ecosystem respiration fluxes.

The new grasstree sub-model performed well when compared to observed daily C fluxes and peak biomass C for both crops, although better with switchgrass than with miscanthus. While switchgrass is native to the midwestern United States and adapted to harsh winters and more tolerant of drought, miscanthus, native to Eurasia, is not. Miscanthus has shallow rhizomes that are vulnerable to climate extremes. The miscanthus fields in this study had rhizome damage from a harsh winter freeze in 2011 and were further disturbed by a drought in 2012 that substantially lowered productivity during and afterwards (Kantola et al., 2022). The continued lower productivity following disturbance was difficult to capture in the model, even with additional parameters to simulate damage during the disturbance, while still capturing the peak biomass in 2011. Additional miscanthus planting also occurred in 2010 and 2011 to fill in gaps where plants didn't establish (Moore et al., 2021; Zeri et al., 2020), further complicating capturing miscanthus production in model simulations. While this is still not perfect, the new grasstree plant sub-model provided more realistic inputs to the soil system than previously possible with the crop plant sub-model. With more accurate timing of plant C and N inputs through senescence and mortality, as well as more refined representation of litter chemistry, we were better able to evaluate the soil sub-models.

To date, most soil model studies evaluating the inclusion of microbial explicit processes have been stand-alone soil models that require forced litter inputs (Kyker-Snowman et al., 2020; Sulman et al., 2018; Wieder et al., 2013, 2018; H. Zhang et al., 2020). While forced litter inputs, or a model test bed, provide a controlled and useful way to evaluate model performance, there are limits to understanding how the soil model responds to feedbacks between vegetation and environmental conditions. For example, changes in climate will affect plant productivity and chemistry and will have subsequent effects on soil C fluxes and stabilization. DayCent-CABBI is a full ecosystem scale model with interchangeable functions allowing us to understand how the FO and MM model respond to different future climate and vegetation, as well as feedbacks between SOM and vegetation.

Although the increases in model-data agreement in the MM model compared to the FO model are incremental, they are a promising result. Comparing model simulations to observations at the daily scale allows us to evaluate if the model is responding to environmental changes. In other words, if the MM model is capturing daily and seasonal changes better than the FO, it is more likely that it will appropriately simulate future climate effects on decomposition. In particular, the MM-model showed improvements to winter and spring-time respiration fluxes. This was due the extra control that microbial biomass has in the MM-model as well as using the ideal combination of soil temperature and moisture effect functions. Microbial biomass was low in the winter and gradually ramped up as soil temperature increased in the spring (Figure 2.5), creating a lag in the rate of heterotrophic respiration relative to the FO model.

We found that a variable Q_{10} soil temperature effect function and "hill" soil moisture effect function are most appropriate for predicting daily ecosystem respiration fluxes, particularly during the winter and spring (Figure S 2.X). This is consistent with other evaluations of temperature function and soil moisture functions (Del Grosso, Parton, et al., 2005). While this finding isn't a focal point of this study, we do think it is an important consideration for soil biogeochemical models moving forward. Most of the microbial explicit soil models that have been developed use an exponential Q_{10} temperature effect function (A. D. Robertson et al., 2019; Sulman et al., 2014; Wieder et al., 2014) that our results showed to have worse model-data agreement. Earth system models have a variety of combinations these soil temperature and moisture functions in their soil models that contributes to variation in future projections of soil C (Todd-Brown et al., 2018).

Perhaps more interesting than the daily C flux evaluation of the soil models are the differences in simulated soil C during past, present, and future simulations. During the historic land use simulations, there were two key differences between the soil C models: 1) the MM model simulated a greater loss of physically protected C (MAOM, the passive soil C pool) in response to tillage events leading up to the dust bowl compared to the FO model that had a more substantial loss from the POM or slow soil C pool; and 2) the MM model was slower to rebuild soil C in either pool compared to the FO model as cultivation practices improved and crop productivity increased. Both models were calibrated to have approximately the same total soil C in 2008 and the same POM and MAOM in 2019. This

indicates that the models have different responses to disturbance and vegetation yet can be benchmarked to the same data. Without more soil C data, we can't determine which model is more accurately simulating these responses. Observational studies have found that tillage decreases that ratio of protected to unprotected soil C while increasing decomposition of both pools (Jastrow & Miller, 1996; Reicosky et al., 1995) supporting the more substantial loss of MAOM by the MM model.

The increases in soil C during all future simulations are linked to the expected effects of the transition to miscanthus and switchgrass. Both crops are bioenergy feedstock candidates because as perennial grasses that don't require annual tillage, they are expected to rebuild soil C stocks, especially when planted in fields that were previously used for corn production (G. P. Robertson et al., 2017). Differences in how miscanthus and switchgrass soil C respond to climate scenarios demonstrate how differences in vegetation can impact the trajectory of predicted soil C for both of the soil models. For example, there is a much broader range of projected soil C in 2049 in miscanthus for both soil models than there is for switchgrass. The divergence in magnitude of soil C increase by the end of the future simulations between soil models for each climate scenario suggests that the MM model simulates a lower carbon storage capacity for a given plant community and climate. Microbial biomass increases with Warming and Warming+Rain scenarios, mitigating soil C accumulation with litter inputs from miscanthus. There are also differences in the amount of protected (more in MM model) and unprotected C (more in the FO model). Both the FO and MM models used the same pool-specific carbon use efficiencies (CUE). The CUE from the decomposition of the structural litter pools was reduced as a function of lignin content, but otherwise CUE was fixed. Fixed carbon use efficiency in biogeochemical models doesn't allow for carbon acquisition and storage in ecosystems to respond to environmental conditions such as temperature and nitrogen availability (Allison et al., 2010; Bradford & Crowther, 2013). Adding environmental controls on CUE would be a next step in DayCent model development, as CUE is critical in regulating the activity of microbial decomposers (Schimel, 2021).

As biogeochemical models are being adapted for use for land management decisions in the context of climate change by government agencies and the private sector, it is critical that we continue to improve models and understand sources of uncertainty. First-order SOC

models have been criticized for their SOC predictions that linearly increase with litter inputs. The MM model has a built-in priming effect such that increased litter inputs promote increased microbial biomass, preventing a linear increase in SOC with an increase in litter inputs to the soil, producing more conservative and saturating SOC response to increased production. This new MM model for DayCent represents the first step in adding complexity that is appropriate to improve predictions of C stocks and fluxes at the ecosystem level.

Acknowledgements

This research was supported in part by a NIFA-AFRI Predoctoral Fellowship under Award Number 2021-67034-35046 and by the DOE Center for Advanced Bioenergy and Bioproducts Innovation (U.S. Department of Energy, Office of Science, Office of Biological and Environmental Research under Award Number DESC0018420). Any opinions, findings, and conclusions or recommendations expressed in this publication are those of the authors and do not necessarily reflect the views of the U.S. Department of Energy.

References

Abdalla, M., Jones, M., Yeluripati, J., Smith, P., Burke, J., & Williams, M. (2010). Testing DayCent and DNDC model simulations of N2O fluxes and assessing the impacts of climate change on the gas flux and biomass production from a humid pasture. *Atmospheric Environment*, *44*(25), 2961–2970. https://doi.org/10.1016/j.atmosenv.2010.05.018

Adler, P. R., Grosso, S. J. D., & Parton, W. J. (2007). Life-Cycle Assessment of Net Greenhouse-Gas Flux for Bioenergy Cropping Systems. *Ecological Applications*, *17*(3), 675–691. https://doi.org/10.1890/05-2018

Allison, S. D., Wallenstein, M. D., & Bradford, M. A. (2010). Soil-carbon response to warming dependent on microbial physiology. *Nature Geoscience*, *3*(5), 336–340. https://doi.org/10.1038/ngeo846

Anderson-Teixeira, K. J., Masters, M. D., Black, C. K., Zeri, M., Hussain, M. Z., Bernacchi, C. J., & DeLucia, E. H. (2013). Altered Belowground Carbon Cycling Following Land-Use Change to Perennial Bioenergy Crops. *Ecosystems*, *16*(3), 508–520. https://doi.org/10.1007/s10021-012-9628-x

Berardi, D., Brzostek, E., Blanc-Betes, E., Davison, B., DeLucia, E. H., Hartman, M. D., Kent, J., Parton, W. J., Saha, D., & Hudiburg, T. W. (2020). 21st-century biogeochemical modeling: Challenges for Century-based models and where do we go from here? *GCB Bioenergy*, *12*(10), 774–788.

Black, C. K., Masters, M. D., LeBauer, D. S., Anderson-Teixeira, K. J., & DeLucia, E. H. (2017). Root volume distribution of maturing perennial grasses revealed by correcting for minirhizotron surface effects. *Plant and Soil*, *419*(1), 391–404. https://doi.org/10.1007/s11104-017-3333-7

Bonan, G. B., Hartman, M. D., Parton, W. J., & Wieder, W. R. (2013). Evaluating litter decomposition in earth system models with long-term litterbag experiments: An example using the Community Land Model version 4 (CLM4). *Global Change Biology*, *19*(3), 957–974. https://doi.org/10.1111/gcb.12031

Bossio, D. A., Cook-Patton, S. C., Ellis, P. W., Fargione, J., Sanderman, J., Smith, P., Wood, S., Zomer, R. J., von Unger, M., Emmer, I. M., & Griscom, B. W. (2020). The role of

soil carbon in natural climate solutions. *Nature Sustainability*, *3*(5), 391–398. https://doi.org/10.1038/s41893-020-0491-z

Bradford, M. A., & Crowther, T. W. (2013). Carbon use efficiency and storage in terrestrial ecosystems. *The New Phytologist*, *199*(1), 7–9.

Campbell, E. E., Parton, W. J., Soong, J. L., Paustian, K., Hobbs, N. T., & Cotrufo, M. F. (2016). Using litter chemistry controls on microbial processes to partition litter carbon fluxes with the Litter Decomposition and Leaching (LIDEL) model. *Soil Biology and Biochemistry*, *100*, 160–174. https://doi.org/10.1016/j.soilbio.2016.06.007

Cotrufo, M. F., Wallenstein, M. D., Boot, C. M., Denef, K., & Paul, E. (2013). The Microbial Efficiency-Matrix Stabilization (MEMS) framework integrates plant litter decomposition with soil organic matter stabilization: Do labile plant inputs form stable soil organic matter? *Global Change Biology*, *19*(4), 988–995. https://doi.org/10.1111/gcb.12113

Davis, S. C., Parton, W. J., Dohleman, F. G., Smith, C. M., Grosso, S. D., Kent, A. D., & DeLucia, E. H. (2010). Comparative Biogeochemical Cycles of Bioenergy Crops Reveal Nitrogen-Fixation and Low Greenhouse Gas Emissions in a Miscanthus × giganteus Agro-Ecosystem. *Ecosystems*, *13*(1), 144–156. https://doi.org/10.1007/s10021-009-9306-9

Davis, S. C., Parton, W. J., Grosso, S. J. D., Keough, C., Marx, E., Adler, P. R., & DeLucia, E. H. (2012). Impact of second-generation biofuel agriculture on greenhouse-gas emissions in the corn-growing regions of the US. *Frontiers in Ecology and the Environment*, *10*(2), 69–74. https://doi.org/10.1890/110003

Del Grosso, S. J., Mosier, A. R., Parton, W. J., & Ojima, D. S. (2005). DAYCENT model analysis of past and contemporary soil N2O and net greenhouse gas flux for major crops in the USA. *Soil and Tillage Research*, *83*(1), 9–24. https://doi.org/10.1016/j.still.2005.02.007

Del Grosso, S. J., Parton, W. J., Mosier, A. R., Holland, E. A., Pendall, E., Schimel, D. S., & Ojima, D. S. (2005). Modeling soil CO2 emissions from ecosystems. *Biogeochemistry*, *73*(1), 71–91. https://doi.org/10.1007/s10533-004-0898-z

Del Grosso, S. J., Parton, W. J., Mosier, A. R., Ojima, D. S., Kulmala, A. E., & Phongpan, S. (2000). General model for N2O and N2 gas emissions from soils due to dentrification. *Global Biogeochemical Cycles*, *14*(4), 1045–1060. https://doi.org/10.1029/1999GB001225

Del Grosso, S. J., Parton, W. J., Mosier, A. R., Walsh, M. K., Ojima, D. S., & Thornton, P. E. (2006). DAYCENT National-Scale Simulations of Nitrous Oxide Emissions from Cropped Soils in the United States. *Journal of Environmental Quality*, *35*(4), 1451–1460. https://doi.org/10.2134/jeq2005.0160

Del Grosso, S. J., Wirth, T., Ogle, S. M., & Parton, W. J. (2008). Estimating Agricultural Nitrous Oxide Emissions. *Eos, Transactions American Geophysical Union*, *89*(51), 529–529. https://doi.org/10.1029/2008EO510001

Gaillard, R. K., Jones, C. D., Ingraham, P., Collier, S., Izaurralde, R. C., Jokela, W., Osterholz, W., Salas, W., Vadas, P., & Ruark, M. D. (2018). Underestimation of N2O emissions in a comparison of the DayCent, DNDC, and EPIC models. *Ecological Applications*, *28*(3), 694–708. https://doi.org/10.1002/eap.1674

Griscom, B. W., Adams, J., Ellis, P. W., Houghton, R. A., Lomax, G., Miteva, D. A., Schlesinger, W. H., Shoch, D., Siikamäki, J. V., Smith, P., Woodbury, P., Zganjar, C., Blackman, A., Campari, J., Conant, R. T., Delgado, C., Elias, P., Gopalakrishna, T., Hamsik, M. R., … Fargione, J. (2017). Natural climate solutions. *Proceedings of the National Academy of Sciences*, *114*(44), 11645–11650. https://doi.org/10.1073/pnas.1710465114

He, Y., Jaiswal, D., Liang, X.-Z., Sun, C., & Long, S. P. (2022). Perennial biomass crops on marginal land improve both regional climate and agricultural productivity. *GCB Bioenergy*, *14*(5), 558–571. https://doi.org/10.1111/gcbb.12937

Heaton, E. A., Dohleman, F. G., & Long, S. P. (2008). Meeting US biofuel goals with less land: The potential of Miscanthus. *Global Change Biology*, *14*(9), 2000–2014. https://doi.org/10.1111/j.1365-2486.2008.01662.x

Hudiburg, T. W., Davis, S. C., Parton, W., & Delucia, E. H. (2015). Bioenergy crop greenhouse gas mitigation potential under a range of management practices. *GCB Bioenergy*, *7*(2), 366–374. https://doi.org/10.1111/gcbb.12152

Illinois State Water Survey (Water and Atmospheric Resources Program). (2020). Illinois Climate Network. Champaign, IL. http://doi.org/10.13012/J8MW2F2Q

IPCC. (2018). *IPCC, 2018: Global warming of 1.5°C. An IPCC Special Report on the impacts of global warming of 1.5°C above pre-industrial levels and related global greenhouse gas emission pathways, in the context of strengthening the global response to the threat of climate change, sustainable development, and efforts to eradicate poverty*.

Jastrow, J. D., & Miller, R. M. (1996). *Soil aggregate stabilization and carbon sequestration: Feedbacks through organomineral associations* (ANL/ER/CP-88020; CONF-9607182-1). Argonne National Lab. (ANL), Argonne, IL (United States). https://www.osti.gov/biblio/464188

Kantola, I. B., Masters, M. D., Blanc-Betes, E., Gomez-Casanovas, N., & DeLucia, E. H. (2022). Long-term yields in annual and perennial bioenergy crops in the Midwestern United States. *GCB Bioenergy*, *00*, 1–13. https://doi.org/10.1111/gcbb.12940

Kyker-Snowman, E., Wieder, W. R., Frey, S. D., & Grandy, A. S. (2020). Stoichiometrically coupled carbon and nitrogen cycling in the MIcrobial-MIneral Carbon Stabilization model version 1.0 (MIMICS-CN v1.0). *Geoscientific Model Development*, *13*(9), 4413–4434. https://doi.org/10.5194/gmd-13-4413-2020

Moore, C. E., Berardi, D. M., Blanc-Betes, E., Dracup, E. C., Egenriether, S., Gomez-Casanovas, N., Hartman, M. D., Hudiburg, T., Kantola, I., & Masters, M. D. (2020). The carbon and nitrogen cycle impacts of reverting perennial bioenergy switchgrass to an annual maize crop rotation. *GCB Bioenergy*, *12*(11), 941–954.

Moore, C. E., von Haden, A. C., Burnham, M. B., Kantola, I. B., Gibson, C. D., Blakely, B. J., Dracup, E. C., Masters, M. D., Yang, W. H., DeLucia, E. H., & Bernacchi, C. J. (2021). Ecosystem-scale biogeochemical fluxes from three bioenergy crop candidates: How energy sorghum compares to maize and miscanthus. *GCB Bioenergy*, *13*(3), 445–458. https://doi.org/10.1111/gcbb.12788

Osaka, S., Bellamy, R., & Castree, N. (2021). Framing “nature-based” solutions to climate change. *WIREs Climate Change*, *12*(5), e729. https://doi.org/10.1002/wcc.729

Parton, W. J., Hartman, M., Ojima, D., & Schimel, D. (1998). DAYCENT and its land surface submodel: Description and testing. *Global and Planetary Change*, *19*(1), 35–48. https://doi.org/10.1016/S0921-8181(98)00040-X

Parton, W. J., Holland, E. A., Grosso, S. J. D., Hartman, M. D., Martin, R. E., Mosier, A. R., Ojima, D. S., & Schimel, D. S. (2001). Generalized model for NO x and N2O emissions from soils. *Journal of Geophysical Research: Atmospheres*, *106*(D15), 17403–17419. https://doi.org/10.1029/2001JD900101

Parton, W. J., Mosier, A. R., Ojima, D. S., Valentine, D. W., Schimel, D. S., Weier, K., & Kulmala, A. E. (1996). Generalized model for N2 and N2O production from nitrification and denitrification. *Global Biogeochemical Cycles*, *10*(3), 401–412. https://doi.org/10.1029/96GB01455

Reicosky, D. C., Kemper, W. D., Langdale, G. W., Douglas, C. L., & Rasmussen, P. E. (1995). Soil organic matter changes resulting from tillage and biomass production. *Journal of Soil and Water Conservation*, *50*(3), 253–261.

Ridgeway, J. R., Morrissey, E. M., & Brzostek, E. R. (2022). Plant litter traits control microbial decomposition and drive soil carbon stabilization. *Soil Biology and Biochemistry*, *175*, 108857. https://doi.org/10.1016/j.soilbio.2022.108857

Robertson, A. D., Paustian, K., Ogle, S., Wallenstein, M. D., Lugato, E., & Cotrufo, M. F. (2019). Unifying soil organic matter formation and persistence frameworks: The MEMS model. *Biogeosciences*, *16*(6), 1225–1248. https://doi.org/10.5194/bg-16-1225-2019

Robertson, G. P., Hamilton, S. K., Barham, B. L., Dale, B. E., Izaurralde, R. C., Jackson, R. D., Landis, D. A., Swinton, S. M., Thelen, K. D., & Tiedje, J. M. (2017). Cellulosic biofuel contributions to a sustainable energy future: Choices and outcomes. *Science*, *356*(6345), eaal2324. https://doi.org/10.1126/science.aal2324

Scharlemann, J. P., Tanner, E. V., Hiederer, R., & Kapos, V. (2014). Global soil carbon: Understanding and managing the largest terrestrial carbon pool. *Carbon Management*, *5*(1), 81–91. https://doi.org/10.4155/cmt.13.77

Soil Survey Staff. (2015). [Official Soil Series Descriptions]. Natural Resource Conservation Service, United States Department of Agriculture.

https://www.nrcs.usda.gov/wps/portal/nrcs/detail/soils/scientists/?cid=nrcs142p2_053587

Straube, J. R., Chen, M., Parton, W. J., Asso, S., Liu, Y.-A., Ojima, D. S., & Gao, W. (2018). Development of the DayCent-Photo model and integration of variable photosynthetic capacity. *Frontiers of Earth Science*, *12*(4), 765–778. https://doi.org/10.1007/s11707-018-0736-6

Sulman, B. N., Brzostek, E. R., Medici, C., Shevliakova, E., Menge, D. N. L., & Phillips, R. P. (2017). Feedbacks between plant N demand and rhizosphere priming depend on type of mycorrhizal association. *Ecology Letters*, *20*(8), 1043–1053. https://doi.org/10.1111/ele.12802

Sulman, B. N., Moore, J. A. M., Abramoff, R., Averill, C., Kivlin, S., Georgiou, K., Sridhar, B., Hartman, M. D., Wang, G., Wieder, W. R., Bradford, M. A., Luo, Y., Mayes, M. A., Morrison, E., Riley, W. J., Salazar, A., Schimel, J. P., Tang, J., & Classen, A. T. (2018). Multiple models and experiments underscore large uncertainty in soil carbon dynamics. *Biogeochemistry*, *141*(2), 109–123. https://doi.org/10.1007/s10533-018-0509-z

Sulman, B. N., Phillips, R. P., Oishi, A. C., Shevliakova, E., & Pacala, S. W. (2014). Microbe-driven turnover offsets mineral-mediated storage of soil carbon under elevated CO2. *Nature Climate Change*, *4*(12), Article 12. https://doi.org/10.1038/nclimate2436

Todd-Brown, K., Zheng, B., & Crowther, T. W. (2018). Field-warmed soil carbon changes imply high 21st-century modeling uncertainty. *Biogeosciences*, *15*(12), 3659–3671. https://doi.org/10.5194/bg-15-3659-2018

Wan, J., & Crowther, T. W. (2022). Uniting the scales of microbial biogeochemistry with trait-based modelling. *Functional Ecology*, *00*(1–16). https://doi.org/10.1111/1365-2435.14035

Wieder, W. R., Allison, S. D., Davidson, E. A., Georgiou, K., Hararuk, O., He, Y., Hopkins, F., Luo, Y., Smith, M. J., Sulman, B., Todd-Brown, K., Wang, Y.-P., Xia, J., & Xu, X. (2015). Explicitly representing soil microbial processes in Earth system models. *Global Biogeochemical Cycles*, *29*(10), 1782–1800. https://doi.org/10.1002/2015GB005188

Wieder, W. R., Bonan, G. B., & Allison, S. D. (2013). Global soil carbon projections are improved by modelling microbial processes. *Nature Climate Change*, *3*(10), Article 10. https://doi.org/10.1038/nclimate1951

Wieder, W. R., Grandy, A. S., Kallenbach, C. M., & Bonan, G. B. (2014). Integrating microbial physiology and physio-chemical principles in soils with the MIcrobial-MIneral Carbon Stabilization (MIMICS) model. *Biogeosciences*, *11*(14), 3899–3917. https://doi.org/10.5194/bg-11-3899-2014

Wieder, W. R., Hartman, M. D., Sulman, B. N., Wang, Y.-P., Koven, C. D., & Bonan, G. B. (2018). Carbon cycle confidence and uncertainty: Exploring variation among soil biogeochemical models. *Global Change Biology*, *24*(4), 1563–1579. https://doi.org/10.1111/gcb.13979

Xu, X., Thornton, P. E., & Post, W. M. (2013). A global analysis of soil microbial biomass carbon, nitrogen and phosphorus in terrestrial ecosystems. *Global Ecology and Biogeography*, *22*(6), 737–749. https://doi.org/10.1111/geb.12029

Yue, Q., Cheng, K., Ogle, S., Hillier, J., Smith, P., Abdalla, M., Ledo, A., Sun, J., & Pan, G. (2019). Evaluation of four modelling approaches to estimate nitrous oxide emissions in China's cropland. *Science of The Total Environment*, *652*, 1279–1289. https://doi.org/10.1016/j.scitotenv.2018.10.336

Zeri, M., Anderson-Teixeira, K., Hickman, G., Masters, M., DeLucia, E., & Bernacchi, C. J. (2011). Carbon exchange by establishing biofuel crops in Central Illinois. *Agriculture, Ecosystems & Environment*, *144*(1), 319–329. https://doi.org/10.1016/j.agee.2011.09.006

Zeri, M., Yang, W. H., Cunha-Zeri, G., Gibson, C. D., & Bernacchi, C. J. (2020). Nitrous oxide fluxes over establishing biofuel crops: Characterization of temporal variability using the cross-wavelet analysis. *GCB Bioenergy*, *12*(9), 756–770. https://doi.org/10.1111/gcbb.12728

Zhang, H., Goll, D. S., Wang, Y.-P., Ciais, P., Wieder, W. R., Abramoff, R., Huang, Y., Guenet, B., Prescher, A.-K., Viscarra Rossel, R. A., Barré, P., Chenu, C., Zhou, G., & Tang, X. (2020). Microbial dynamics and soil physicochemical properties explain large-scale variations in soil organic carbon. *Global Change Biology*, *26*(4), 2668–2685. https://doi.org/10.1111/gcb.14994

Zhang, Y., Lavallee, J. M., Robertson, A. D., Even, R., Ogle, S. M., Paustian, K., & Cotrufo, M. F. (2021). Simulating measurable ecosystem carbon and nitrogen dynamics with the mechanistically defined MEMS 2.0 model. *Biogeosciences*, *18*(10), 3147–3171. https://doi.org/10.5194/bg-18-3147-2021

Supporting Information

Model documentation

DayCent has interchangeable functions that are used to calculate soil temperature and moisture effects on decomposition rates and microbial growth. The first order model uses a variable Q_{10} temperature effect on decomposition function, and an arc-tangent function to simulate the effect of soil moisture on decomposition using relative soil water content (Del Grosso et al. 2005). With DayCent-MM users can select from the following soilt temperature and moisture functions: 1a) a variable Q_{10} temperature effect (DayCent) or 1b) an exponential Q_{10} temperature effect (CORPSE, Sulman et al. 2014); 2a) an increasing relationship with soil moisture that plateaus when soil water content reaches the saturation point (DayCent) or 2b) a hill relationship where soil moisture effect is highest around 50% saturated water filled pore space (WFPS) and declines as WFPS is greater or less than 50% (CORPSE, Sulman et al. 2014).

1a) a variable Q_{10} temperature effect (DayCent)

The temperature effect on decomposition (*tfunc*) is a variable Q_{10} function (Figure S. 2.1) and is computed as

$$tfunc = \frac{teff_2 + \frac{teff_3}{\pi}\arctan\left(\pi \times teff_4\left(soiltemp - teff_1\right)\right)}{normalizer}$$

$$normalizer = teff_2 + \frac{teff_3}{\pi}\arctan\left(\pi \times teff_4\left(30.0 - teff_1\right)\right)$$

$$tfunc = \max(tfunc, 0.01)$$

where *soiltemp* is the average surface soil temperature for the day, $teff_1 - teff_4$ are *fix.100* parameters, and *normalizer* is the value of the *tfunc* numerator when *soiltemp* = 30 ºC. The function has a low Q_{10} values at high temperatures and high Q_{10} values at low temperatures (Del Grosso et al. 2005).

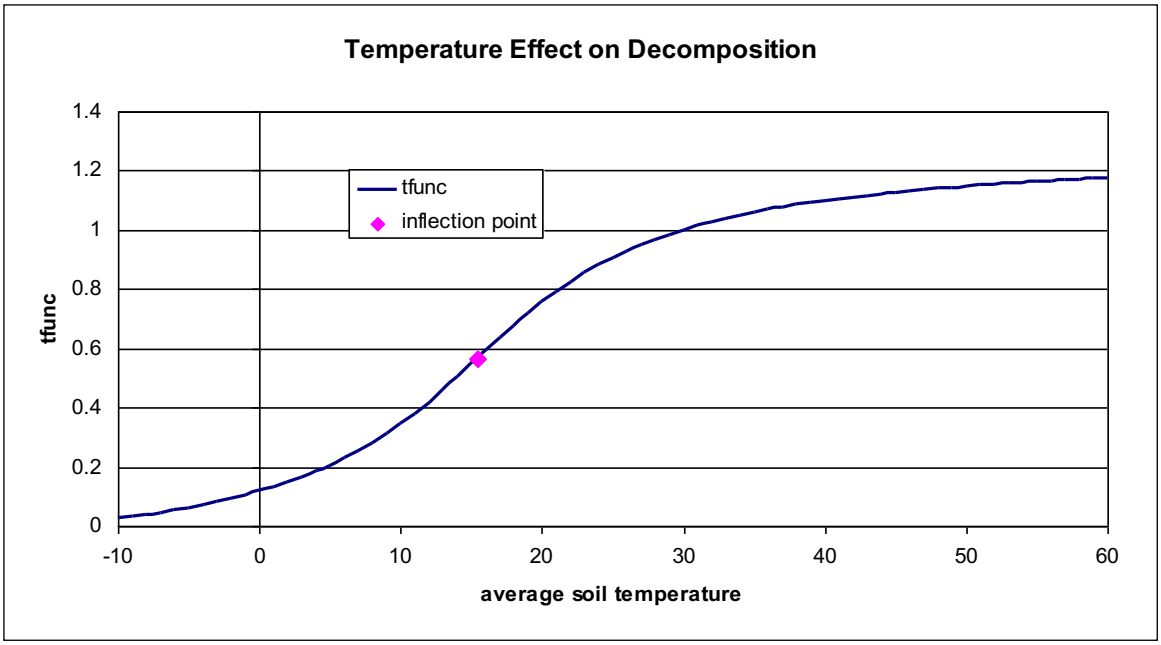

Figure S. 2.1. The variable Q_{10} temperature effect on decomposition (tfunc) with $teff_1$ = 15.4, $teff_2$ = 11.75, $teff_3$ = 29.7, and $teff_4$ = 0.031. The value of tfunc strictly increases with average soil temperature, but has a low Q_{10} values at high temperatures and high Q_{10} values at low temperatures. The $teff_1$ parameter determines the x-location of the inflection point.

1b) an exponential Q_{10} temperature effect (CORPSE) (Sulman et al. 2014)

In the CORPSE model, the decomposition rates of unprotected soil pools are determined by a temperature-dependent maximum enzymatic conversion rate $V_{max,i}(T)$ (yr^{-1}) for the species {i= labile, recalcitrant, and dead microbe pools} (Figure S. 2.2 and S. 2.3), where T is the soil temperature (K), T_{ref} is the reference soil temperature (293.7 K), $V_{maxref,i}$ is the reference *Vmax* for the species (yr^{-1}), Rugas is the ideal gas constant (8.314472 $J\text{-}K^{-1}$ mol^{-1}), $E\alpha_i$ is the activation energy for the species (kJ mol^{-1}). For the new SOM model, we will want a switch that allows us to select between the f(T) function associated with Vmax and DayCent variable Q_{10} f(T) in order to compute the temperature effect on SOM decomposition.

$$\alpha_i = \frac{V_{maxref,i}}{exp\left(\frac{-Ea_i}{Rugas \cdot T_{ref}}\right)}$$

$$V_{max,i}(T) = \alpha_i \cdot exp\left(\frac{-Ea_i}{Rugas \cdot T}\right)$$

$$= V_{maxref,i} \frac{exp\left(\frac{-Ea_i}{Rugas \cdot T}\right)}{exp\left(\frac{-Ea_i}{Rugas \cdot T_{ref}}\right)}$$

$$= V_{maxref,i} * f_i(T)$$

Vmaxref_Fast" = 9.0 (yr^{-1})

Vmaxref_Slow" = 0.25 (yr^{-1})

Vmaxref_Necro"= 4.5 (yr^{-1})

Ea_Fast = 5e3, used 20e3 instead to get a smaller intercept at extremely low temperatures

Ea_Slow = 30e3, used 40e3 instead to get a smaller intercept at extremely low temperatures

Ea_Necro= 3e3, used 30e3 instead to get a smaller intercept at extremely low temperatures

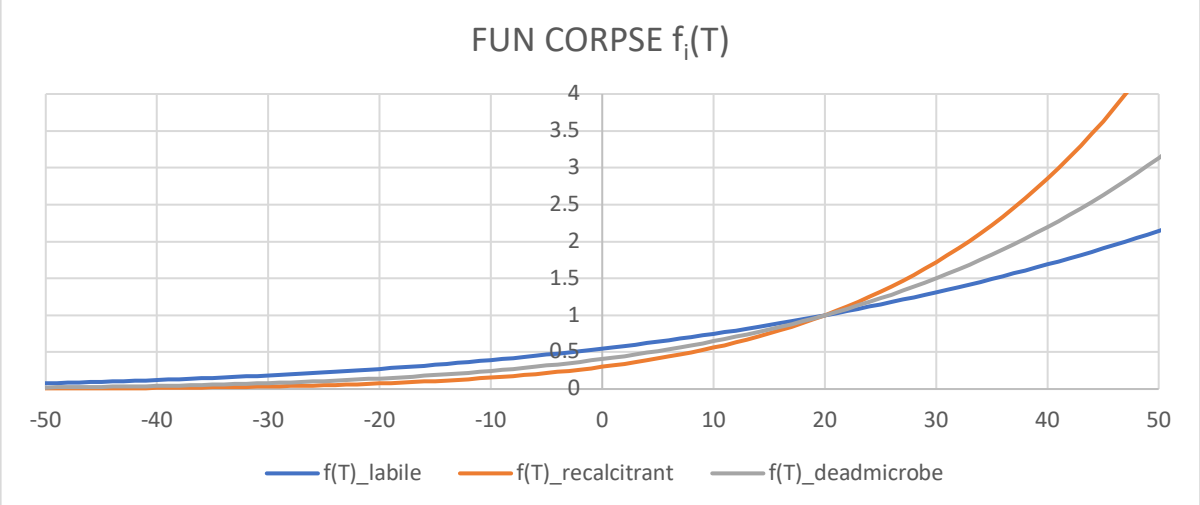

Figure S. 2.2. The species-specific temperature function associate with the maximum enzymatic conversion rate Vmax,i(T) (yr-1) in the FUN CORPSE model. The reference temperature (where f(T) = 1.0) is 20 °C.

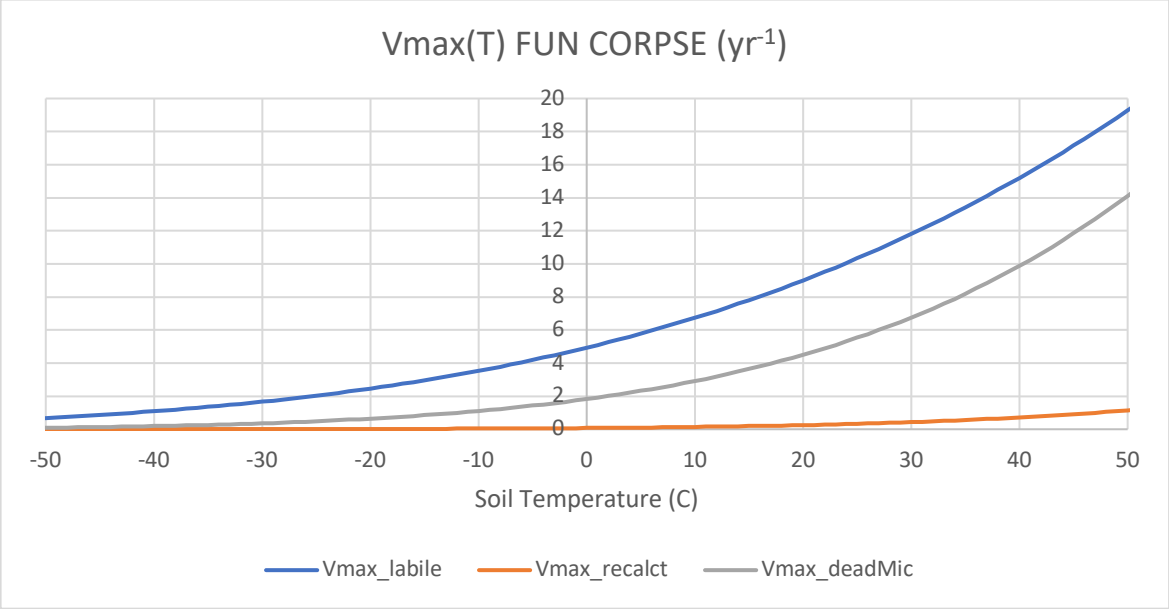

Figure S. 2.3. The species-specific, temperature-dependent maximum enzymatic conversion rate Vmax,i(T) (yr-1) in the FUN CORPSE model. Vmax(T) for a species is a product of Vmaxref for the species and f(T) for the species.

2a) an increasing relationship with soil moisture that plateaus when soil water content reaches the saturation point (DayCent)

The relative water content of soil controls the moisture effect. The relative water content of a soil layer, $relWaterContent_{lyr}$, is computed as

$$relWaterContent_{lyr} = \frac{vswc_{lyr} - swclimit_{lyr}}{fieldc_{lyr} - swclimit_{lyr}}$$

where $vswc_{lyr}$ is the volumetric soil water content of the layer, $fieldc_{lyr}$ is the volumetric soil water content at field capacity, and $swclimit_{lyr}$ is the volumetric fraction that can never be extracted from the soil layer (Figure S. 2.4).

$$wfunc = \frac{1.0}{1.0 + 30 \times \exp\left(-9.0 \times relWaterContent\right)}$$

For aboveground decomposition, *relWaterContent* is the relative water content of the top soil water layer. For belowground decomposition, *relWaterContent* is the weighted average relative soil water content of the second and third soil water layers.

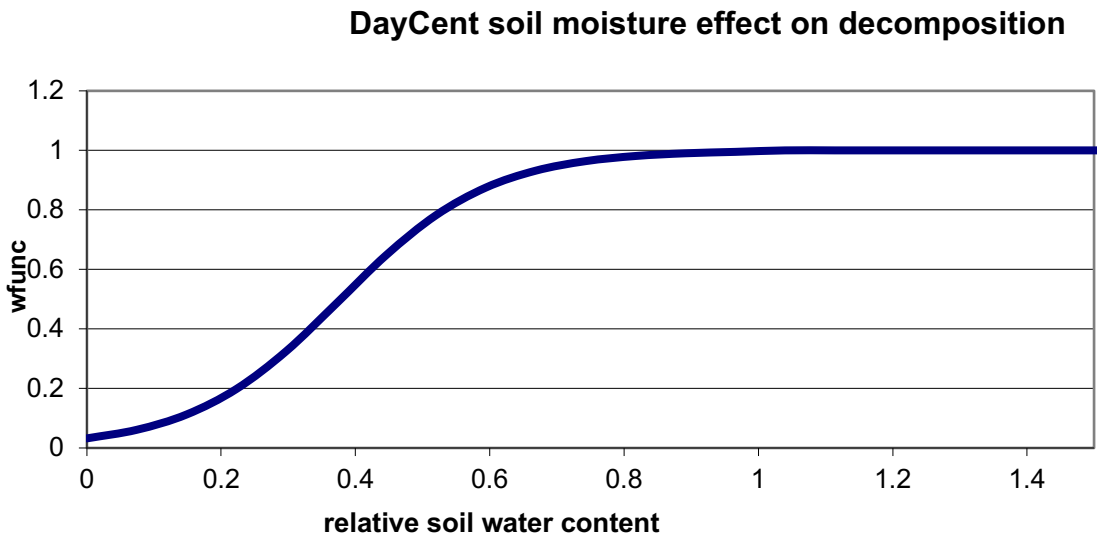

Figure S. 2.4. DayCent's moisture effect on decomposition (wfunc). The value of wfunc strictly increases with available moisture.

2b) a hill relationship where soil moisture effect is highest around 50% saturated water filled pore space (WFPS) and declines as WFPS is greater or less than 50% (CORPSE) (Sulman et al. 2014)

The soil moisture effect on decomposition of soil organic matter in the CORPSE model (Figure S. 2.5) is defined as:

$$f(\theta) = \left(\left(\frac{\theta_l}{\theta_{sat}} \right)^3 + 0.001 \right) \cdot \max\left(\left(1.0 - \frac{\theta_l}{\theta_{sat}} - \frac{\theta_f}{\theta_{sat}} \right)^{2.5}, minAnaerobicRespFactor \right)$$

$$f(\theta) = \max\left(fWmin, f(\theta) \right)$$

where Θ_l is the volumetric liquid soil water content (0.0-1.), Θ_f is the volumetric frozen soil water content (0.0-1.0), and Θ_{sat} is the volumetric soil moisture at saturation (0.0-1.0), *fWmin* is the minimum value of *f(Θ)* (~0.001 as specified in the *corpse_params.nml* file), and *minAnaerobicRespFactor* is 0.003.

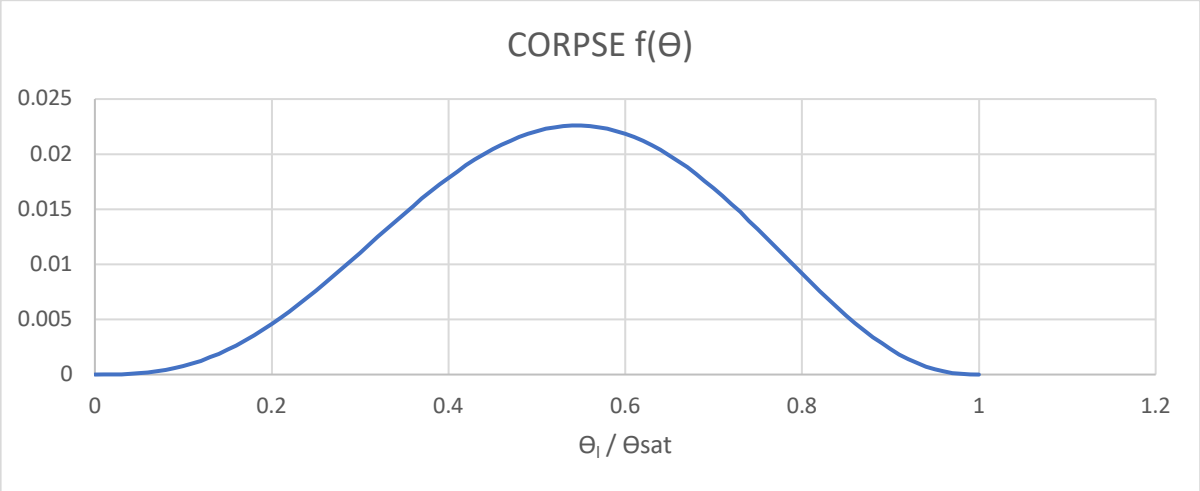

Figure S. 2.5. The soil moisture effect on soil organic matter decomposition in the CORPSE model where Θ_l is the volumetric liquid soil water content, and Θ_{sat} is the volumetric total soil water content at saturation (here the volumetric frozen soil water content, $\Theta_f = 0.0$).

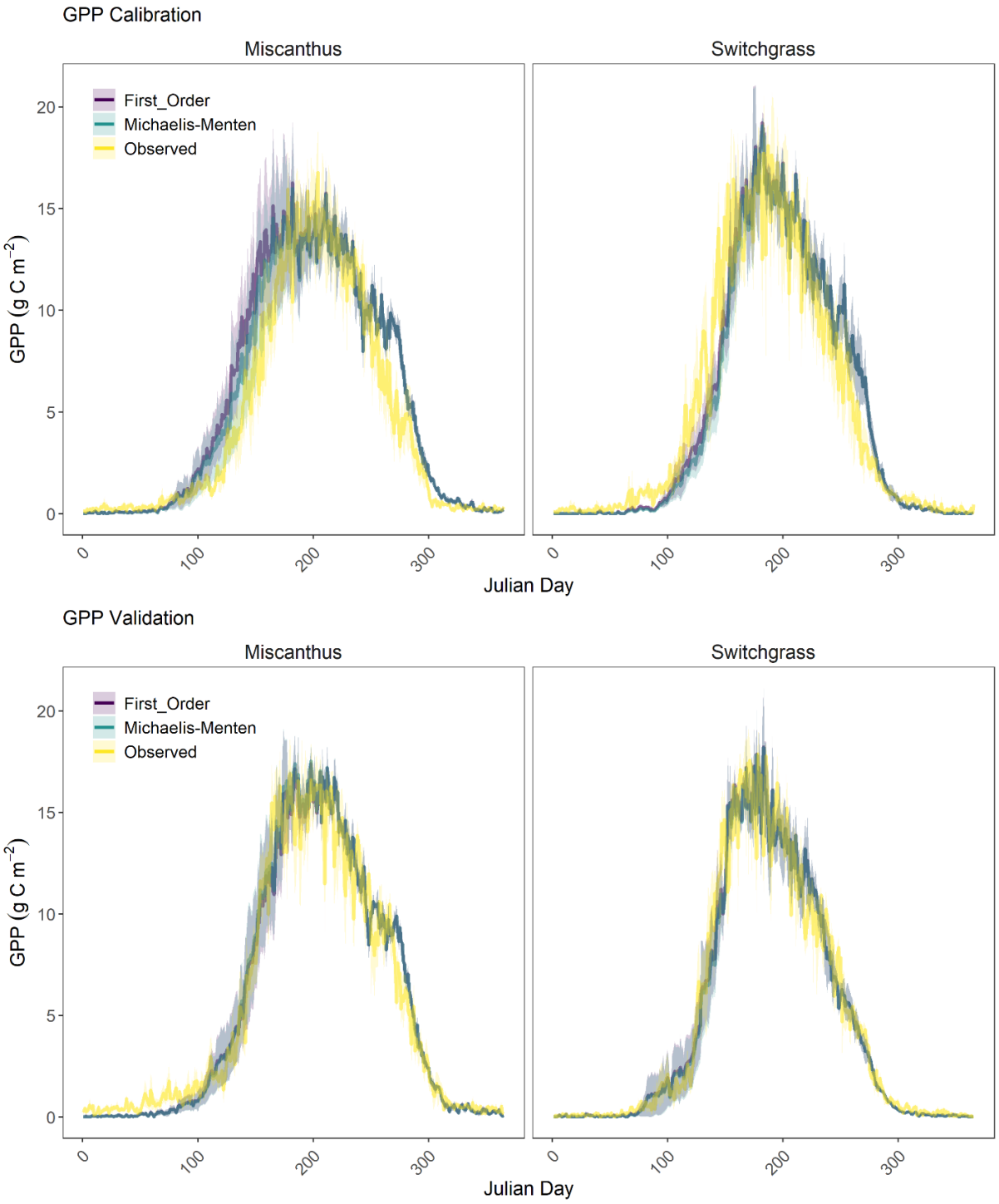

Figure S. 2.6. Mean daily GPP (solid lines) over the calibration and validation periods for miscanthus and switchgrass (Table 2.1). The shaded areas are ±1 standard deviation within the mean.

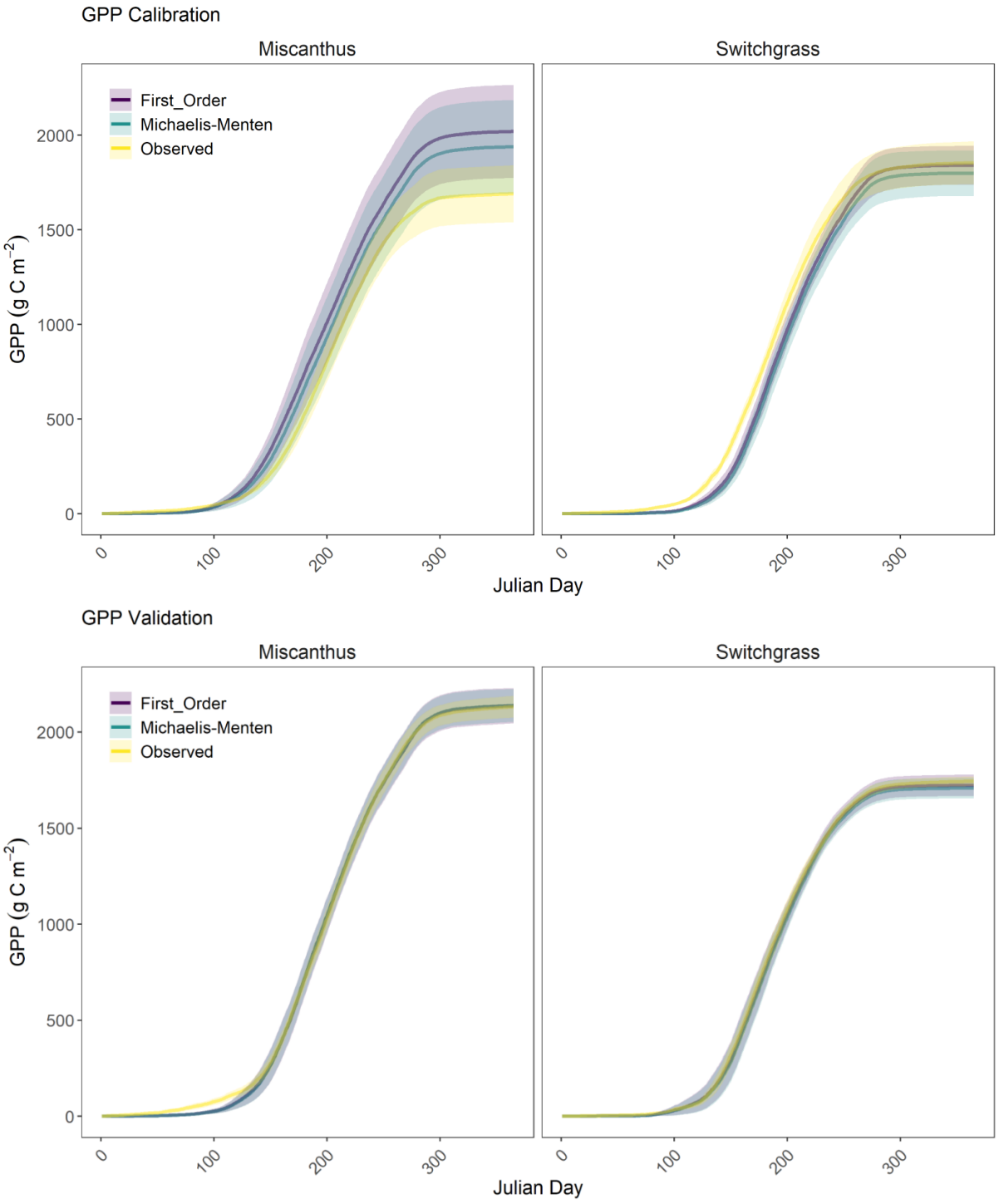

Figure S. 2.7. Mean cumulative GPP (solid lines) over the calibration and validation periods for miscanthus and switchgrass (Table 2.1). The shaded areas are ±1 standard deviation within the mean.

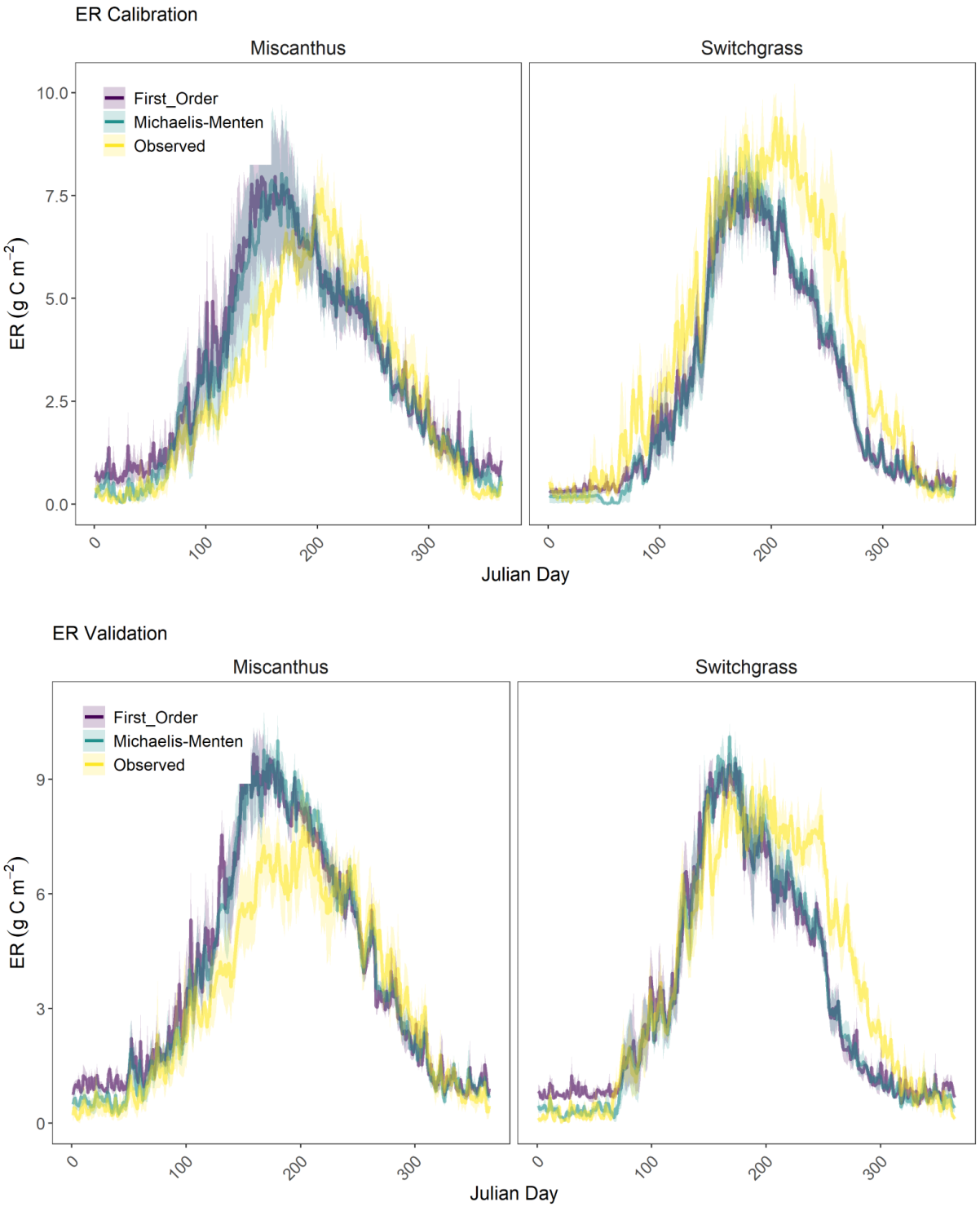

Figure S. 2.8. Mean daily Ecosystem Respiration (ER) (solid lines) over the calibration and validation periods for miscanthus and switchgrass (Table 2.1). The shaded areas are ±1 standard deviation within the mean.

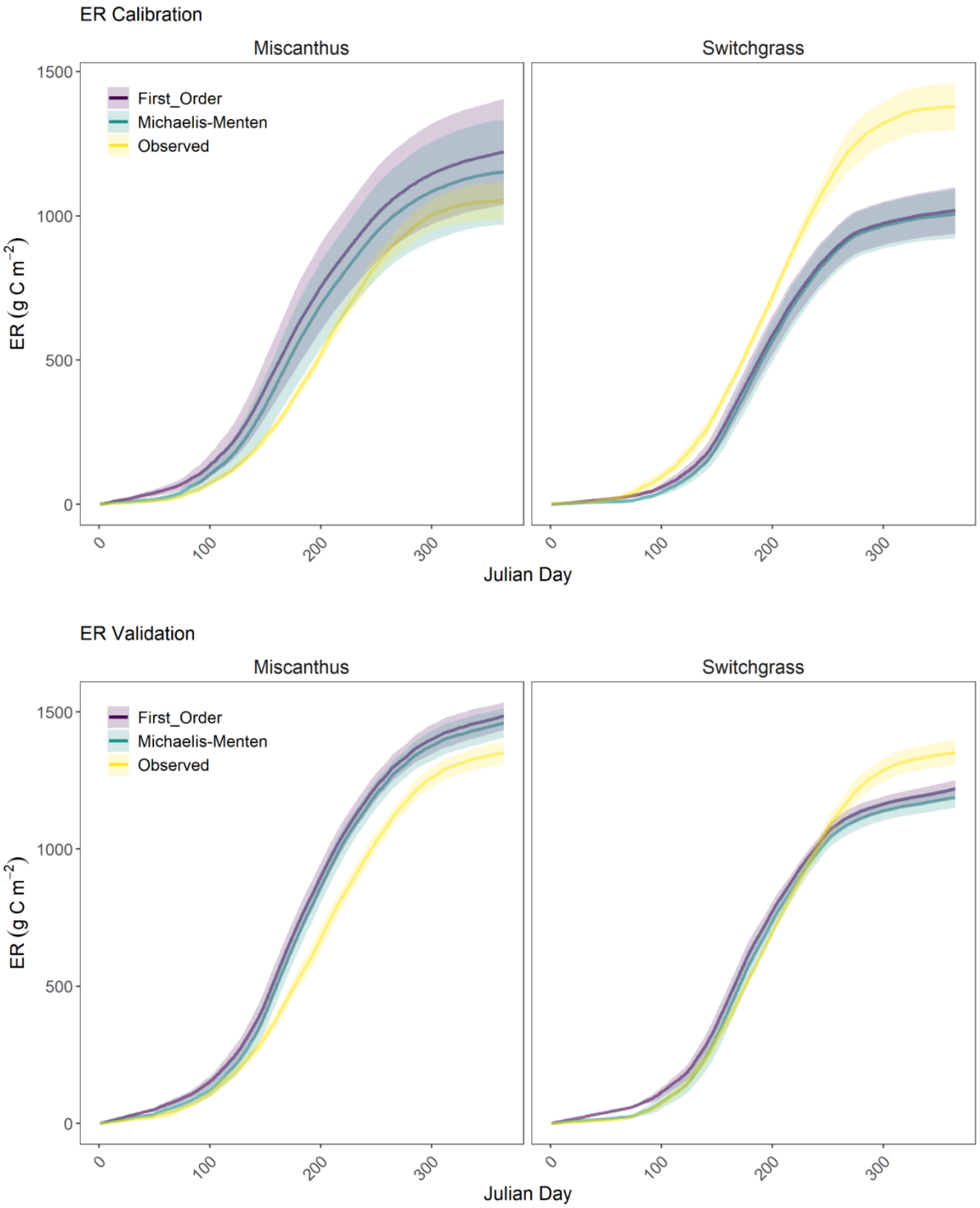

Figure S. 2.9. Mean cumulative Ecosystem Respiration (ER) (solid lines) over the calibration and validation periods for miscanthus and switchgrass (Table 2.1). The shaded areas are ±1 standard deviation within the mean.

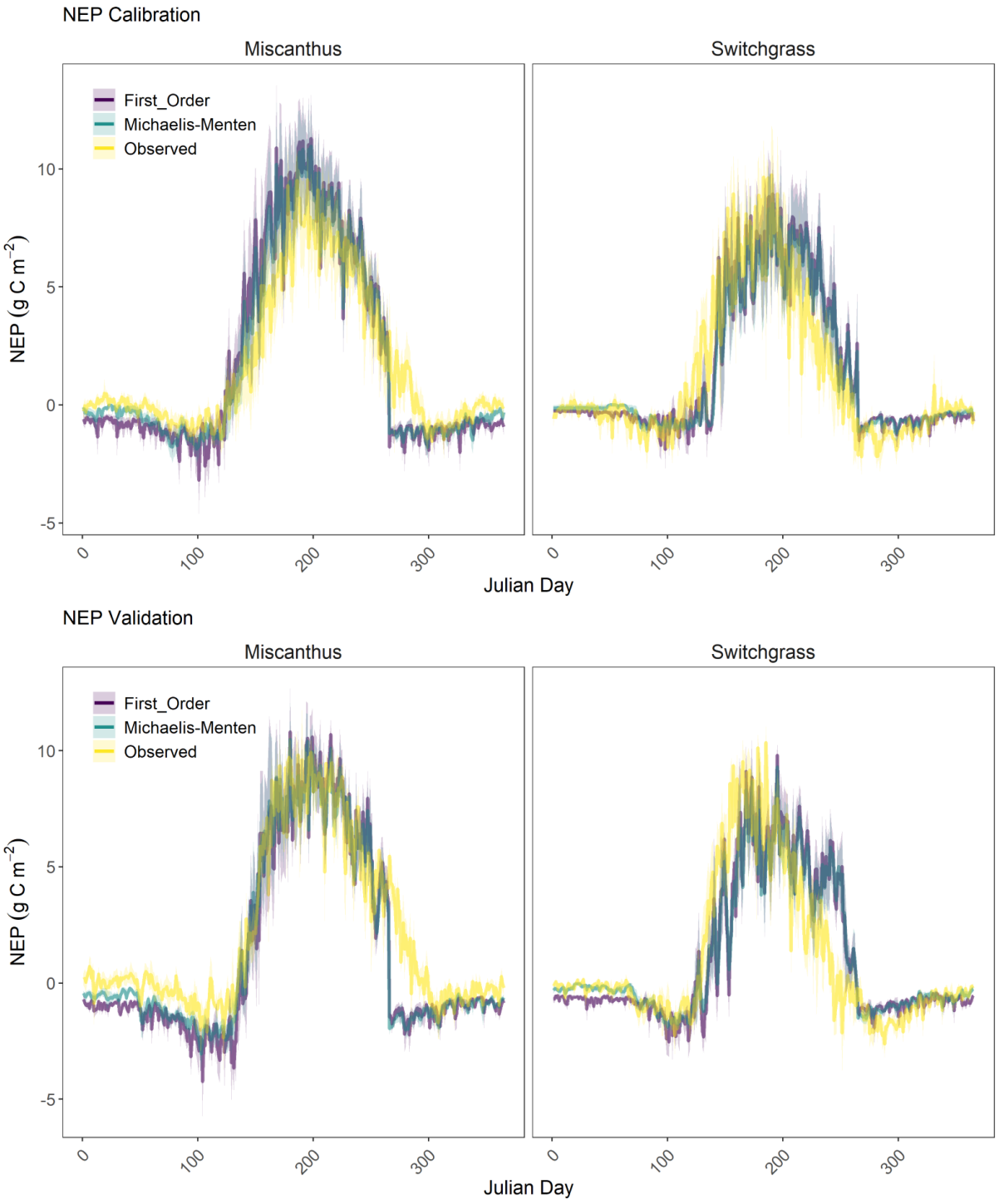

Figure S. 2.10. Mean daily Net Ecosystem Productivity (NEP) (solid lines) over the calibration and validation periods for miscanthus and switchgrass (Table 2.1). The shaded areas are ±1 standard deviation within the mean.

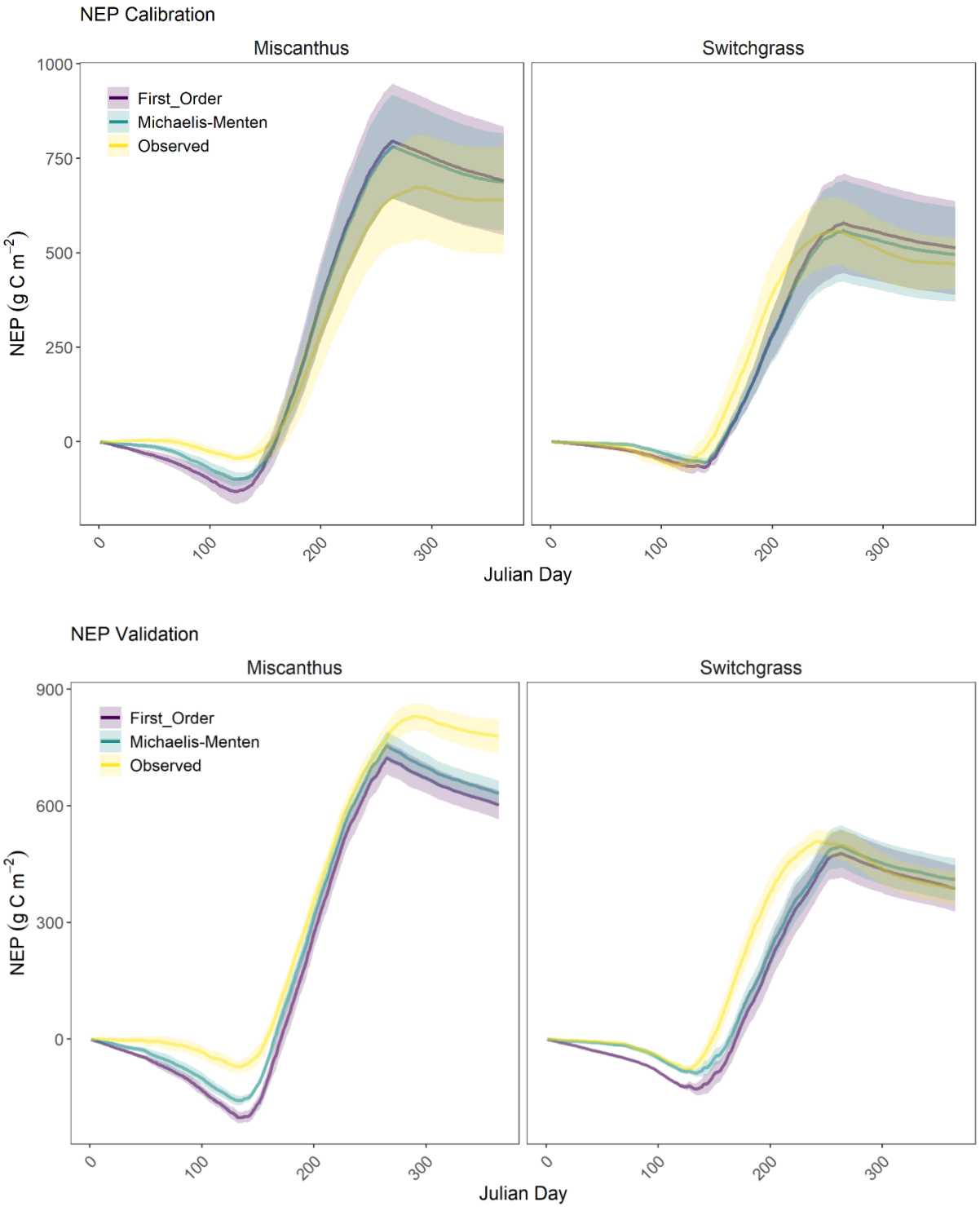

Figure S. 2.11.Mean cumulative Net Ecosystem Productivity (NEP) (solid lines) over the calibration and validation periods for miscanthus and switchgrass (Table 2.1). The shaded areas are ±1 standard deviation within the mean.

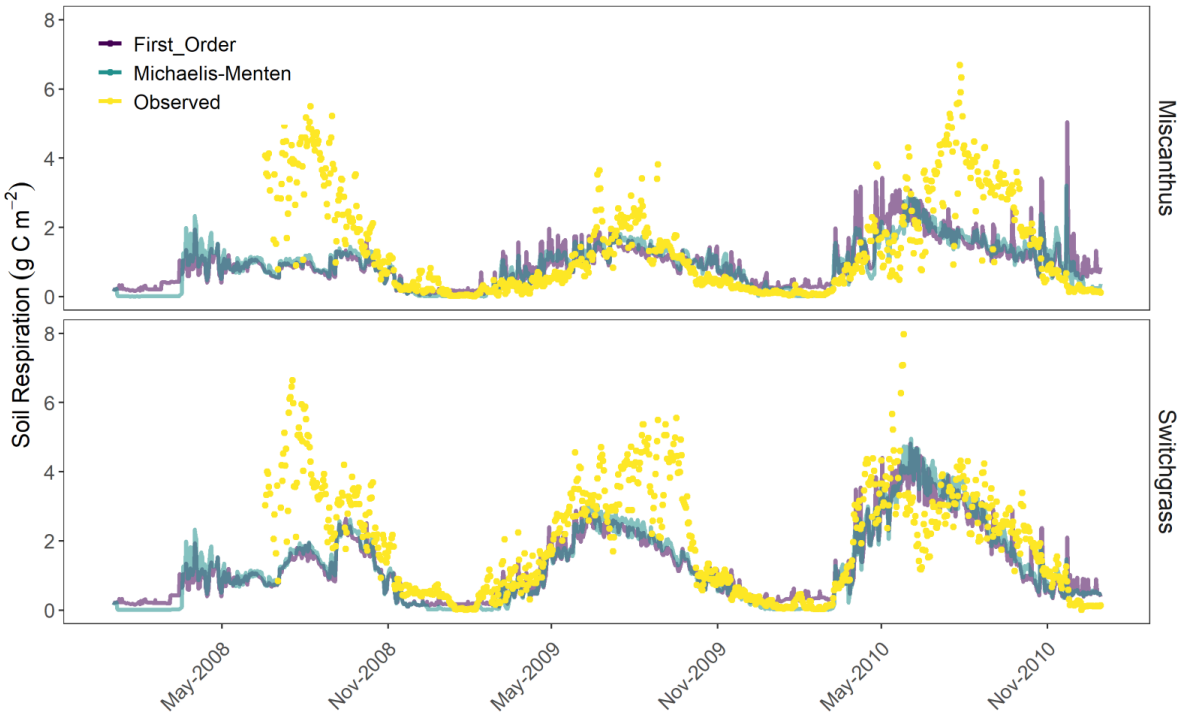

Figure S. 2.12. Simulated and observed soil respiration (sum of heterotrophic and soil autotrophic respiration) for miscanthus (top figure) and switchgrass (bottom figure).

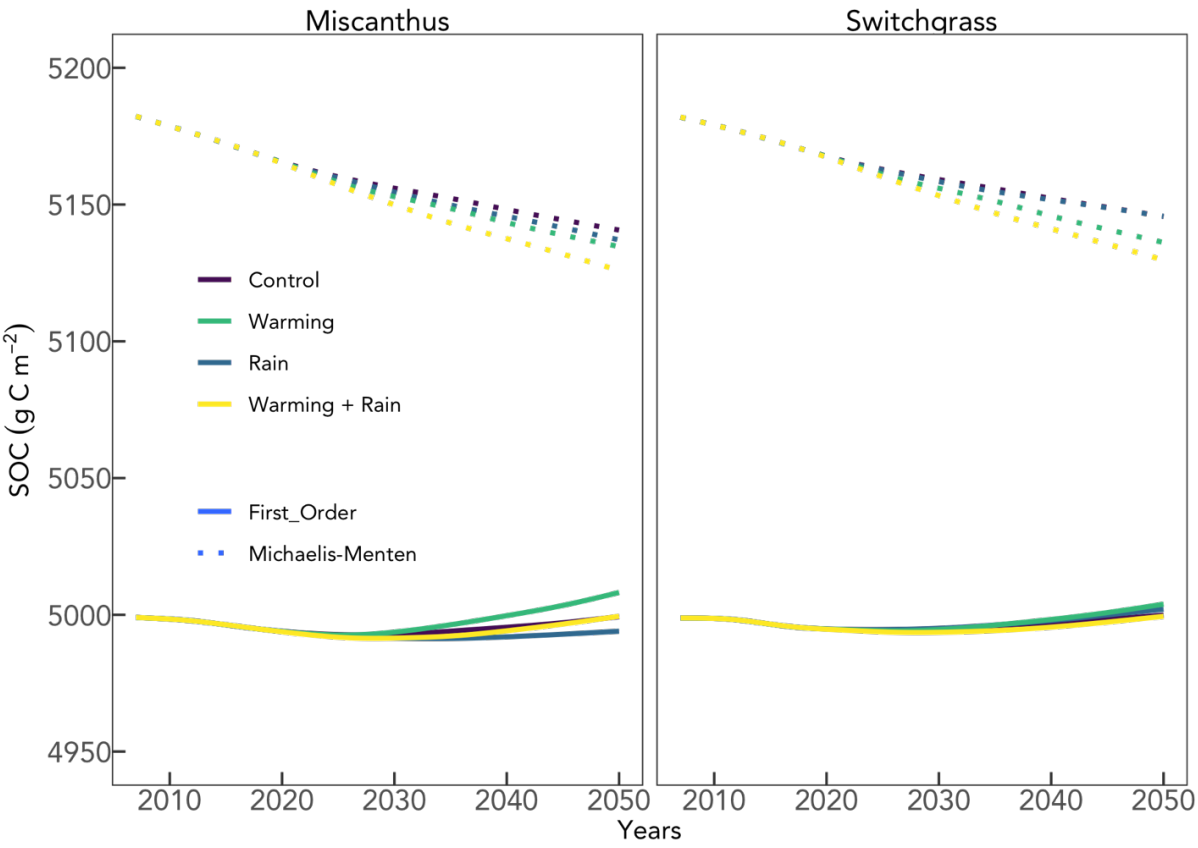

Figure S. 2.13.Simulated physically protected soil C projected into the future under different climate scenarios for switchgrass and miscanthus.

Chapter 3 : Can cellulosic bioenergy crops be used to mitigating corn and soy losses to extreme precipitation events and resulting excessive soil moisture?

Abstract

Transitioning to cellulosic bioenergy crops is a proposed strategy to reduce greenhouse gas emissions in the agriculture and energy sectors and increase soil carbon storage. Switchgrass, a perennial grass native to the United States, has many promising qualities that make it an appealing candidate as a bioenergy feedstock. It requires little to no fertilizer, has a deep perennial root system that encourages soil carbon sequestration, has comparable yield to corn, and is tolerant of drought and flooding, climate extremes that are increasing in frequency and severity with climate change. However, whether the transition to any bioenergy feedstock increases carbon storage depends on where the crop is grown and what was the prior land use. Marginal land that was once used for agriculture but is currently uncultivated has been a target for bioenergy production, but there is not enough marginal land to meet greenhouse gas reduction goals and the carbon deficit created by transitioning currently uncultivated land to bioenergy feedstock production leads to a reduction in carbon storage. Here, I identify current cropland used for corn and soybean production that is frequently flooding leading to crop loss events. Using the DayCent biogeochemical model, I evaluate the transition to flood tolerant switchgrass in flood susceptible cropland. Switchgrass increased soil carbon, reduced nitrogen leaching into waterways, and produced greater yields compared to corn, particularly in years that flooding was simulated.

Introduction

Cellulosic bioenergy crops have potential to meet United States greenhouse gas (GHG) reduction targets and provide energy self-sufficiency. The Renewable Fuel Standard (RFS) calls for increasing the volume of cellulosic biofuel by 16 billion gallons while reducing lifecycle GHG emissions by 60% (Schnepf and Yacobucci, 2013). Consideration of crop selection, location, and management strategies is critical to meet these goals and prevent environmental and economic costs from outweighing benefits. Depending on the productivity

of selected land, 33 to >50 million hectares are required for cellulosic bioenergy production to meet RFS targets (Langholtz et al., 2016; Robertson et al., 2011). This is about 25% of current U.S. agricultural land (USDA-NASS, 2016). Converting this much land into bioenergy production comes with challenges including economic viability, landowner willingness, and potential environmental consequences (e.g. habitat loss, degradation, and carbon debt; (Robertson et al., 2017)).

Identifying appropriate locations for a particular crop is paramount to meeting GHG atmospheric loading reductions, fulfilling socioeconomic needs, and achieving sustainable land use. In comparison to traditional agricultural crops, some bioenergy crops have physiological attributes (e.g., low N requirements, high belowground biomass, no tillage) that will outweigh the potential negatives if grown strategically. However, there is still much uncertainty and controversy surrounding where cellulosic bioenergy crops will be grown. Conversion of land to cellulosic bioenergy crops that is currently used for food production raises concerns about food-scarcity and sequential conversion of uncultivated land converted for food production (indirect land-use change) resulting in catastrophic losses of sequestered carbon and ecosystem services that will not be recouped through annual row crop production. Conversion of land to bioenergy crops that is not currently used for agricultural production also raises environmental concerns including the effects on GHG balances, biodiversity and ecosystem services, increasing reactive nitrogen through fertilizer, and water use. These potential side effects of conversion are thought to be largely avoided if bioenergy crops are produced on land that has been deemed marginal, or unproductive land that was used for agriculture in the recent past. However, because of constraints such as proximity to a potential refinery location (Gelfand et al., 2013), landowner willingness (Skevas et al., 2016), and ecological risks, there is not a path to meet GHG reduction targets with bioenergy production on marginal land alone (Robertson et al., 2017).

Much of the opposition to conversion of current cropland stems from fear of food scarcity (Kline et al., 2017; Woods J et al., 2015). However, there was a large expansion of agricultural land for the purpose of corn grain ethanol production in the late 2000's (Lark et al., 2015). Subsequently, a large portion (approximately 40%) of corn grain is currently being allocated toward ethanol production. This expansion resulted in massive losses of carbon and ecosystem services (Lark et al., 2022, 2020; Spawn et al., 2019). Additionally,

there are substantial and increasing losses of corn and soybean yield in recent years. As much as 75% of these losses are attributed to water inundated fields (USDA-RMA, 2020).

Flooding and extreme precipitation events are projected to increase due to climate variability, leading to a greater loss of corn and soy yield (Hirabayashi et al., 2013; Prein et al., 2017). Crops are susceptible to damage and loss from flooding, ponding, and extreme precipitation, especially in low lying depressions or along floodplains. Corn and soybean losses depend on the time of year and the duration of inundation. Flooding or ponding that occurs prior to planting can delay planting, sometimes to the point that planting corn is no longer a viable option. In this case, sometimes farmers are able to plant soybeans instead since it has a shorter growing season. Ponding or waterlogging that occurs after planting, but prior to emergence, reduces or prevents emergence depending on severity (von Haden et al., 2021). Inundation events that occur following emergence cause root damage, reduce photosynthesis, transpiration, and growth (Zhu et al., 2016) resulting in little to no yield depending on the duration of flooding events. Over the last decade, reported average annual loss of corn and soybean to inundation and extreme precipitation events are 3.2 million ha yr^{-1} and as high as 8.7 million ha yr^{-1} (USDA-RMA, 2020). This data is from crop insurance claims and may not include reduced yields that weren't eligible for coverage, so is likely an underestimate of the damage to corn and soybean crops. With increasing precipitation extremes and flooding events on the horizon, it is essential that we consider strategies to lessen the impact to crop yield while also mitigating GHG emissions.

Perennial bioenergy crops, such as switchgrass and Miscanthus, are tolerant of flooding once they are established (Costello and Ayoub, 2019; Kam et al., 2020), making them a productive alternative in low-lying areas that will otherwise suffer reoccurring losses of corn and soy yield from flooding events. Flooding in agricultural land typically occurs in potholes (i.e., low-lying land that surrounding areas drain into) and floodplains. Targeting low-lying, flood susceptible fields for conversion to flood tolerant bioenergy crops would provide a path to adapt agricultural practices to changing precipitation regimes, mitigate increasing climate variability, and reduce negative environmental impacts of corn production. Documented benefits of perennial grasses in riparian zones include reduced phosphorus and nitrate exports to waterways, decreased nitrous oxide emissions and increased soil carbon sequestration

(Meehan et al., 2013). Lower rates of nitrate leaching and nitrous oxide emissions are expected because Miscanthus requires low fertilization rates and switchgrass does not require fertilization (Wang et al., 2020).

Here, I explore a category of land that is currently in agricultural use, but has compromised production because of frequent losses that are being exacerbated because of climate change. Specifically, I have identified cropland in the rainfed Eastern U.S. that is increasingly experiencing extreme precipitation events that lead to flooding, crop damage, and loss of yield. I then use DayCent, a biogeochemical model, to explore the GHG implications of converting flood susceptible corn and corn – soybean rotating fields to switchgrass.

Methods

Site Selection

Using USDA Indemnity Report data, I identified 337 counties that experienced corn and soybean loss of yield that met the following criteria between 2011 - 2020: 1) average annual loss > 5000 ha, 2) maximum annual loss > 10,000 ha, and 3) frequency of three or more annual loss events > 5000 ha (Figure 3.1; (USDA-RMA, 2020)). I removed counties that were spatially isolated from other counties, and therefore, not likely to be located in close proximity to a biorefinery. I selected only locations that are currently in use for corn or soybean production using the 2017 Cropland Data Layer (USDA-NASS, 2016). Within counties, SSURGO flood and ponding frequency data were used at a 4-km resolution to select sites within counties that experience either category of inundation (Figure 3.2). Of the selected sites, slope ranged from 0-26% gradient, with 97.8% of slopes less than or equal to 5%. The site selection criteria resulted in 10,209 locations on a 4-km grid of the United States, potentially representative of 4.08 million hectares of flood vulnerable cropland or approximately 12.4% of the total land needed for bioenergy production. To reduce the computing requirements, I used R to randomly select a subset of 2,000 of the 10,209 grid points for model simulations.

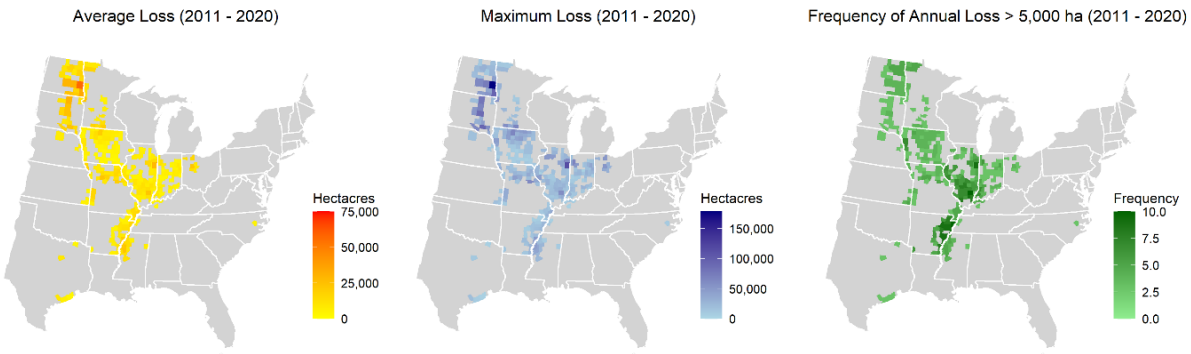

Figure 3.1. County-level average, maximum, and frequency of annual corn and soybean reported losses of at least 5,000 ha over a 10-year period (2011-2020) for counties selected using minimum loss criteria.

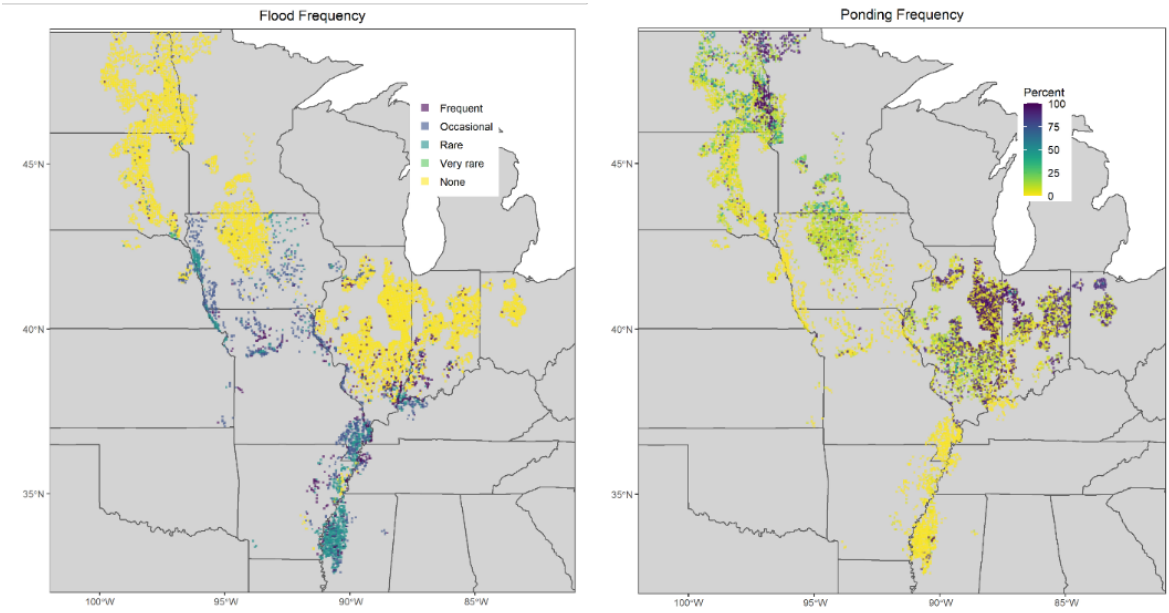

Figure 3.2. Frequency of flooding and ponding from SSURGO data in counties with significant crop loss events (see Figure 3.1).

Model Description and Simulations

To simulate crop yields, soil carbon, GHG emissions, and nitrate leaching for the 2,000 sites, I used DayCent-CABBI that was developed to better represent tall perennial grasses

(Berardi et al., 2020; Moore et al., 2020) and to include a microbial explicit soil sub-model (described in Chapter 2). DayCent is an ecosystem scale biogeochemical model that has been widely used to simulate carbon and nitrogen dynamics in grasslands (S.J. Del Grosso et al., 2005; Grant et al., 2016; Ryals et al., 2015) and agricultural systems (Del Grosso et al., 2009; S. J. Del Grosso et al., 2005; Zhang et al., 2020). To model the effects of flooding on crops, a new parameter that affects the productivity of the plant when the soils are saturated was added to the plant sub-model.

This study leveraged existing DayCent model input files on an established 4 km grid of the United States. Historic weather data from 1980 – 2017, including daily maximum and minimum temperature and precipitation, were obtained for each grid point from the DayMet database (P. Thornton et al., 2018). This weather data sequence was repeated during the spinup and historical land use simulations. Sites were parameterized with SSURGO soil texture, pH, and depth data retrieved from the SoilGrids250 m database.

In order to allow soil carbon and nitrogen to reach equilibrium conditions within each soil pool, pre-cultivation vegetation and disturbance (e.g. fire and grazing) was prescribed at a regional scale for 6,000 years (Melillo et al., 1995). Historic land use (1848 – 1979) was scheduled at a state or sub-divided state scale (Davis et al., 2012; Hudiburg et al., 2016). Recent land use (1980-2019) was prescribed using recent cropping practices of corn-soybean rotations of planting and harvest dates and average nitrogen fertilizer rates at the state level (USDA-NASS, 2018). Only corn was fertilized during these simulations.

Soil carbon was calibrated and validated using the International Soil Carbon Network (ISCN) dataset (Gen 3: Soil Survey Staff, 2020). I selected observation sites that had available measured soil organic carbon within 2 km of a grid point and omitted any observations that weren't on agricultural land. Additionally, soil organic carbon observations greater than 25,000 g C m^{-2} in sites with low Mean Annual Temperature (MAT) and Mean Annual Precipitation (MAP) were excluded because models are unable to capture soil carbon variation in these sites with large spatial scale calibrations (Drewniak et al., 2015). Using these constraints, I was left with 208 sites with observed soil carbon (Figure 3.3). I randomly assigned half of these sites to be used for model training and then used the remainder for model validation.

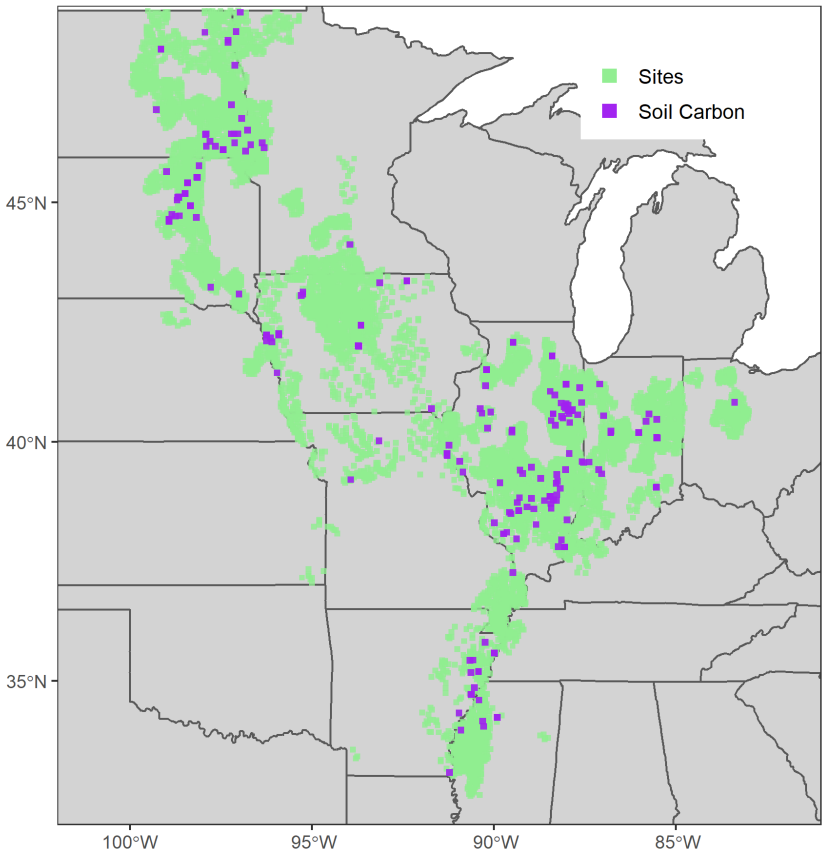

Figure 3.3 Locations of flood prone sites used for modeling (green) and observations of soil carbon on agricultural land used for soil carbon calibration (purple).

During model training and validation, model sites that were paired to sites with SOC observations were modified to match observed soil properties (bulk density, soil texture, soil depth, soil pH). In other words, soil property parameters that were previously informed by SSURGO data were re-parameterized with ISCN site specific parameters. To improve soil carbon calibration, I optimized the non-symbiotic nitrogen fixation value at sites based on mean annual temperature (MAT, Table S. 3.1). The spinup, historic land use, and recent agricultural practices simulations were all run with the new optimal non-symbiotic nitrogen fixation values for all modeling sites.

Since this study was leveraging existing model simulations, corn and soybean parameterizations had already been calibrated and validated using county level yield data (Kent et al., 2020). Because switchgrass isn't grown commercially on large scales, there were

a limited number of sites within the study region with 3-9 years of peak yield data from experimental switchgrass trials (Table S. 3.2). Data from six field sites (n = 28) were used for model training while the remaining three sites (n = 19) were reserved for model validation.

Following model training and validation, I developed future scenarios to evaluate the effects of flooding on corn and soybean rotations and the carbon and nitrogen implications of transitioning flood susceptible agricultural land to switchgrass production. Each of the 2,000 sites was simulated from 2017 – 2045 using the following scenarios: 1) Current corn and soybean rotations with current climate (Corn Control); 2) current corn and soybean rotations with increased precipitation and warmer temperatures (Corn Flooding); 3) transition to switchgrass with increased precipitation and warmer temperatures (Switchgrass Flooding). To create future weather files, weather data files from 1980 – 2016 from all sites from were randomized by year using the same randomization scheme for each site. This created the weather input files for the Corn Control scenario. To create the flooding scenario weather files, 20% of the years from the randomized future Corn Control weather files were selected to have warmer and wetter weather. During the warmer and wetter years, the daily maximum and minimum temperatures were increased by 2°C, daily precipitation was multiplied by 1.5, and 1-week rainstorm event of 3.5 cm of precipitation was added to each day during the second week of June, when a flooding event would cause damage to corn and soybean plants and prevent or greatly reduce grain yield (Mukhtar et al., 1990). While not directly used, monthly flood and ponding frequency and duration data from SSURGO for April – July (Figures S. 3.2, S. 3.3, S. 3.4, and S.3.5) were considered to justify the flooding climate scenarios.

Flooding was simulated by parameterizing site drainage in DayCent using SSURGO drainage class (Table 3.1, Figure S. 3.1) and allowing the model to use waterfilled pore space at saturation to simulate flooding events. In DayCent, when the drainage parameter is less than one, water flow out of the bottom of the soil profile is restricted allowing water to accumulate from the bottom of the soil profile. Because of this, flooding may have occurred during years that were not designated as “flood years” during all future scenarios. To simulate the effects of flooding on plant productivity, corn and soybean productivity was

lowered during flooding and didn't recover following flooding. Switchgrass productivity was lowered during flooding events but recovered after flooding.

Table 3.1 DayCent drainage parameters used based on SSURGO drainage class category (Figure S. 3.1).

SSURGO Drainage Class	DayCent Drainage Parameter
Excessively drained	1
Somewhat excessively drained	0.86
Well drained	0.71
Moderately well drained	0.57
Somewhat poorly drained	0.43
Poorly drained	0.29
Very poorly drained	0.14

Results

Observed SOC values ranged from < 2,000 g C m^{-2} to more than 40,000 g C m^{-2} in the Great Plains region of the modeled area. Prior to model training, there was very little model-data agreements. Soil carbon was largely underestimated in the Great Plains region (North Dakota, South Dakota, and Minnesota) and overestimated in the southern portion of the study region. Following model training, soil carbon model-data agreement was improved with R^2 values of 0.32 for the calibration dataset and 0.37 for the validation dataset (Figure 3.4). Similarly to other modeling studies that have used the ISCN database for SOC calibration and validation, DayCent tended to underestimate SOC in sites with observed SOC over 15,000 g C m^2 (Drewniak et al., 2015). While the model was benchmarked to SOC with observations from land under current corn and soybean cultivation, there was insufficient data to calibrate to changes in SOC under switchgrass cultivation.

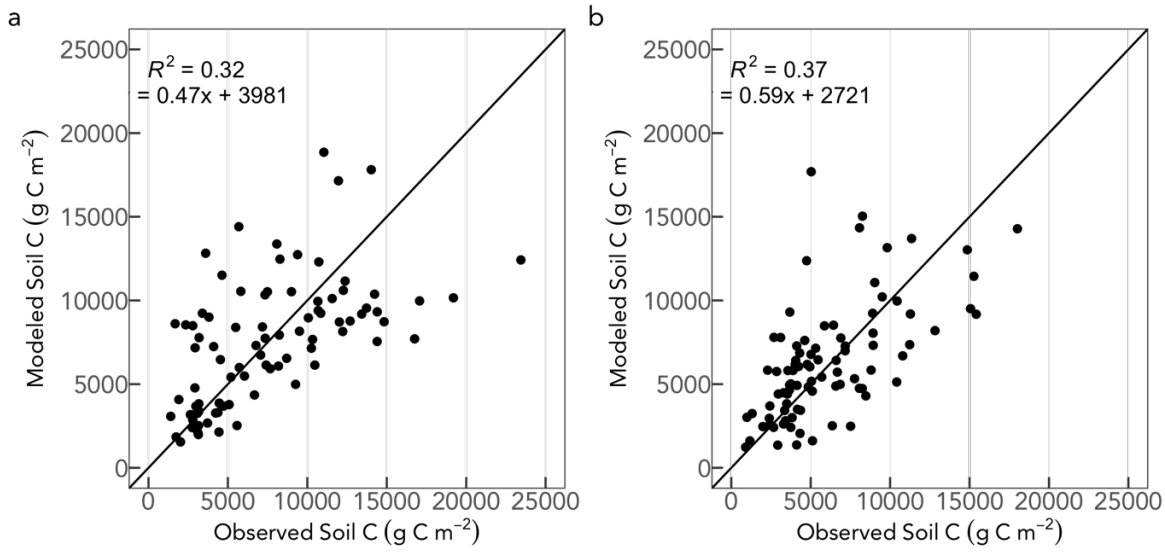

Figure 3.4 Comparison of modeled versus observed soil carbon used for (a) calibration and (b) validation. The solid lines represent the 1:1 ratio of modeled to observed data.

Switchgrass was calibrated to annual yield measured in dry weight (Mg ha^{-1}). Prior to model training, switchgrass biomass carbon was mostly underestimated. During model training, parameters determining plant response to drought and nitrogen limitation were adjusted, as well as a parameter that determines the soil depth that plants can access water and nitrogen from. Following model training, the model achieved an R^2 of 0.26 with the training dataset and an R^2 of 0.20 with the validation dataset (Figure 3.5).

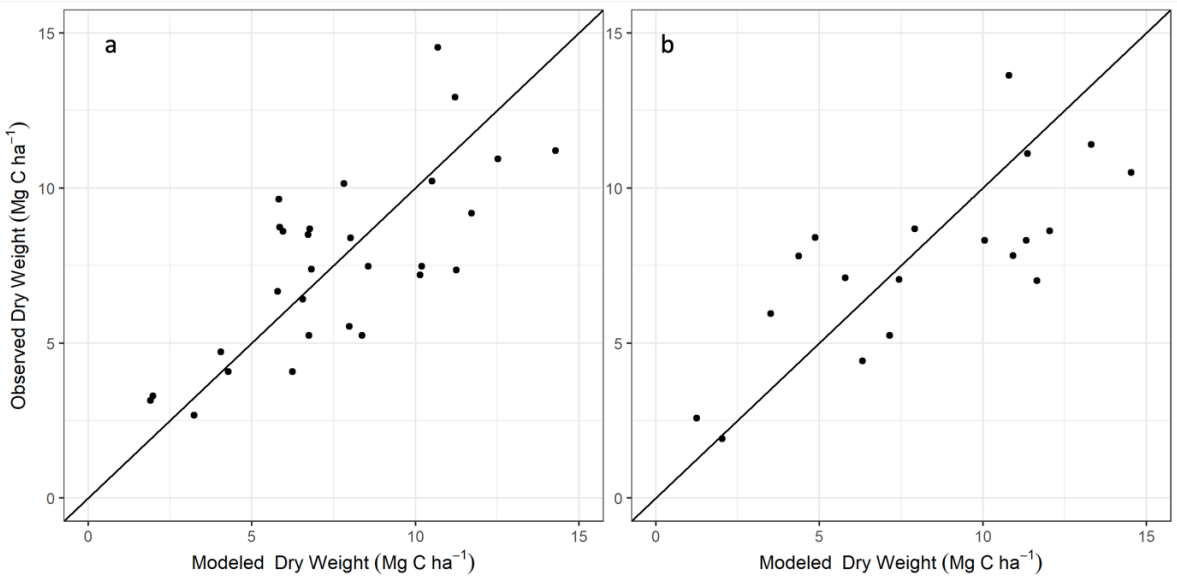

Figure 3.5 Comparison of modeled vs observed switchgrass yield used for (a) model training and (b) model validation using independent data from seventeen field sites located throughout the study region. The solid lines represent the 1:1 ratio of modeled to observed data.

Simulated switchgrass yields under flooding conditions (Figure 3.6d) were similar or greater than corn yield predicted under control climate conditions (Figure 3.6a). As expected, corn yield was lower in the Corn Flooding simulations (Figure 3.6b) compared to the Corn Control simulations. However, surprisingly, corn yield was also lower in years that didn't flood (Figure 3.6c) compared to Corn Control yield (Figure 3.6a). This is likely linked to greater nitrogen leaching in Corn Flooding simulations affecting productivity in all years.

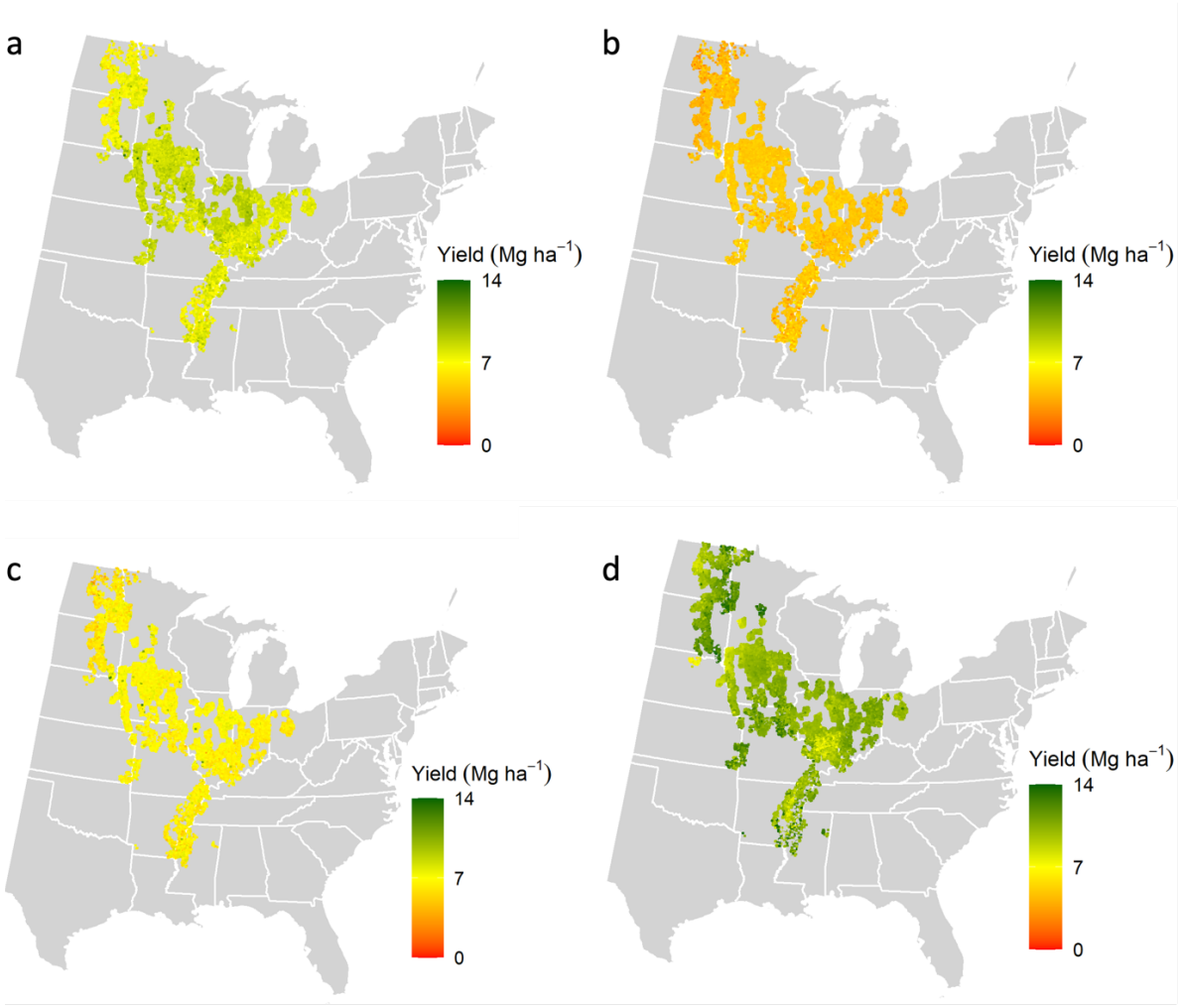

Figure 3.6 Simulated average annual yield for (a) Corn Control for all years of future simulations, (b) Corn Flooding for all years of future simulations, (c) Corn Flooding in non-flood years of future simulations, and (d) Switchgrass Flooding of all years of future simulations.

Simulated nitrogen leaching was highest in Corn Flooding followed by Corn Control (Figure 3.7a and c). There was very little nitrogen leaching associated with future switchgrass production (Figure 3.7e), which was not fertilized in these simulations. Nitrogen leaching in corn simulations was generally higher in areas that receive higher mean annual precipitation. Nitrogen leaching in corn ranged from 9 kg N ha^{-1} to 87 kg N ha^{-1}.

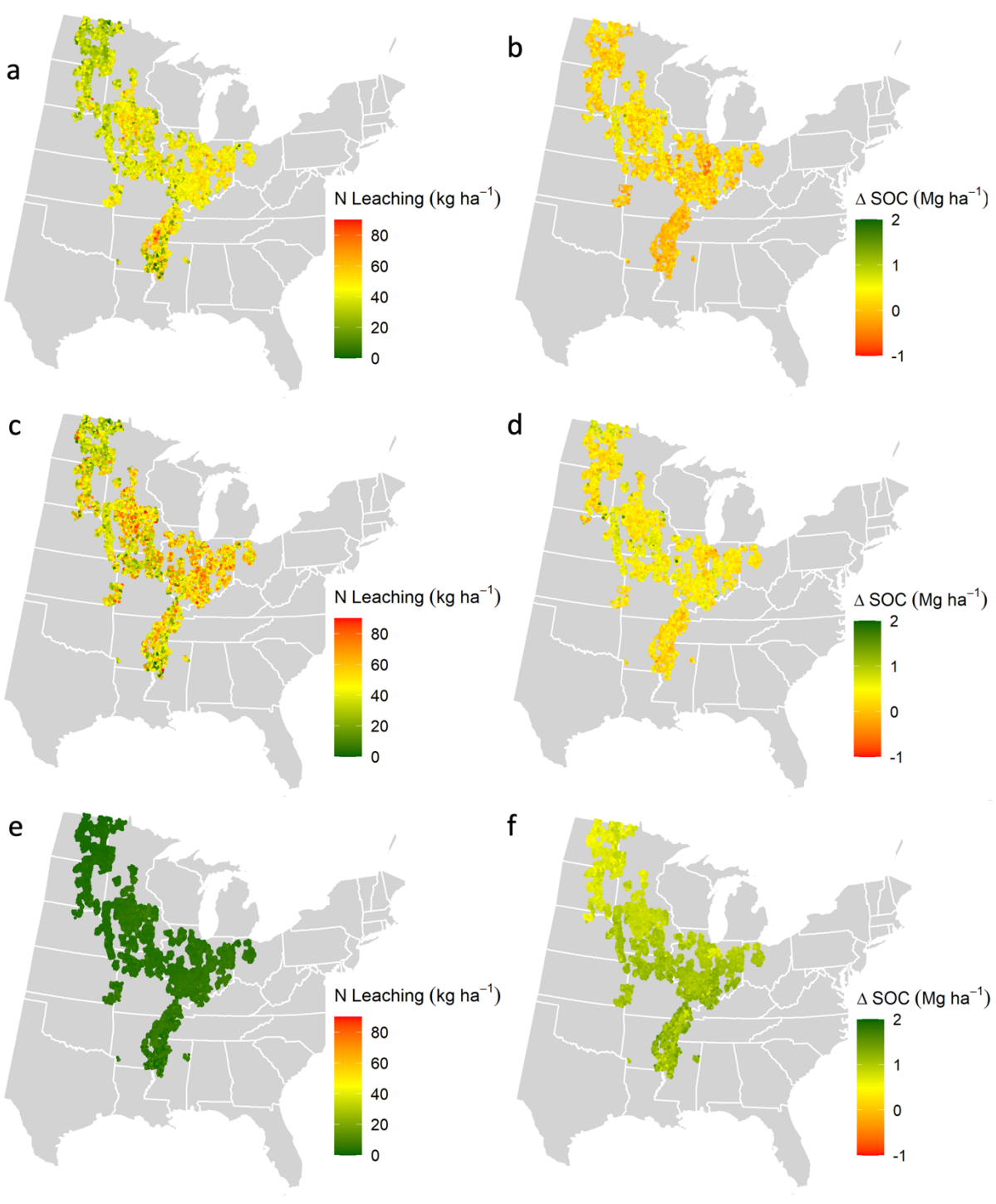

Figure 3.7. Modeled average annual leaching (a, c, and e) and change in SOC from 2017 - 2048 (b, d, and f) over future simulations under Corn Control (a and b), Corn Flooding (c and d), and Switchgrass Flooding (e and f).

Change in simulated soil organic carbon was the most favorable in the Switchgrass Flooding simulations with all sites resulting in a net increase in soil organic carbon ranging from 0.47 Mg C ha^{-1} to 1.67 Mg C ha^{-1} (Figure 3.7f). Surprisingly, soil organic carbon increases were generally higher in the Corn Flooding scenario (Figure 3.7d) compared to the Corn Control scenario (Figure 3.7b). This is because corn was not harvest after flooding occurred leading to higher plant biomass carbon inputs to the soil system during flood years. Most Corn Control sites experienced very little change in soil organic carbon, ranging from -0.96 Mg C ha^{-1} to 1.4 Mg C ha^{-1}.

Discussion

Our results suggest that growing switchgrass in flood susceptible areas will produce higher and likely more reliable yield, greatly reduce nitrogen leaching, and lead to greater soil carbon sequestration compared to corn under current climate and increased flooding and warming scenarios. Producing switchgrass in flood susceptible areas could increase crop diversity, which has declined in the last century, providing economic and environmental resilience (Crossley et al., 2021). Additionally, switchgrass is native to the United States and tolerant of drought (Liu et al., 2015), as well as flooding. This, along with low fertilizer requirements make it a beneficial crop for production on frequently waterlogged soil.

While it was expected, and prescribed, that corn biomass yield would be lower under flooding conditions, it was also lower in years that flooding didn't occur. Soil nitrogen was lower during all years as a result of flooding, likely due to a combination of leaching and nitrous oxide emissions caused by saturated soil conditions during flood years. Although leaching and nitrous oxide emissions were not calibrated for this study because a lack of available data, DayCent has been extensively calibrated and validated to both (Del Grosso et al., 2008; S. J. Del Grosso et al., 2005). The range of nitrate loss from leaching simulated for corn fell within the observational ranges (Andraski et al., 2000; Jemison Jr. and Fox, 1994). The sites selected for this study are in low-lying areas with poor drainage and have some flooding or ponding during parts of the year. Whether or not these sites experience flooding events that cause crop loss events, they do likely have higher nitrous oxide emissions from

denitrification in waterlogged soils and will experience increasing nitrogen leaching with increasing extreme precipitation events and are becoming less suitable and sustainable for crops that require high amounts of fertilizer, like corn.

To determine an effective path for the U.S. transition to cellulosic bioenergy, understanding of how each crop may integrate in a landscape from field to fuel is essential. In the absence of observational and experimental studies exploring the transition to bioenergy crops on flood susceptible land, biogeochemical modeling can provide insight to potential yield and ecosystem services, GHG mitigation, and water quality, that are incorporated into lifecycle analyses. There are limitations to how these modeling results can be used, but they do suggest that transitioning fields with diminishing corn yields to switchgrass would lead to reduced GHG emissions, improved soil health, and better water quality.

Acknowledgements

This research was supported in part by a NIFA-AFRI Predoctoral Fellowship under Award Number 2021-67034-35046 and by the DOE Center for Advanced Bioenergy and Bioproducts Innovation (U.S. Department of Energy, Office of Science, Office of Biological and Environmental Research under Award Number DESC0018420). Any opinions, findings, and conclusions or recommendations expressed in this publication are those of the authors and do not necessarily reflect the views of the U.S. Department of Energy. This work was facilitated by the International Soil Carbon Network. This work benefited from extensive data contributions to the International Soil Carbon Network from the (i) USDA Natural Resources Conservation Service, National Cooperative Soil Survey, and (ii) the U.S. Geological Survey.

References

Andraski, T.W., Bundy, L.G., Brye, K.R., 2000. Crop Management and Corn Nitrogen Rate Effects on Nitrate Leaching. Journal of Environmental Quality 29, 1095–1103. https://doi.org/10.2134/jeq2000.00472425002900040009x

Berardi, D., Brzostek, E., Blanc-Betes, E., Davison, B., DeLucia, E.H., Hartman, M.D., Kent, J., Parton, W.J., Saha, D., Hudiburg, T.W., 2020. 21st-century biogeochemical modeling: challenges for Century-based models and where do we go from here? GCB Bioenergy 12, 774–788.

Costello, C., Ayoub, N., 2019. Chapter 6 - Exploring the potential for riparian marginal lands to enhance ecosystem services and bioenergy production, in: Debnath, D., Babu, S.C. (Eds.), Biofuels, Bioenergy and Food Security. Academic Press, pp. 101–123. https://doi.org/10.1016/B978-0-12-803954-0.00006-1

Crossley, M.S., Burke, K.D., Schoville, S.D., Radeloff, V.C., 2021. Recent collapse of crop belts and declining diversity of US agriculture since 1840. Global Change Biology 27, 151–164. https://doi.org/10.1111/gcb.15396

Davis, S.C., Parton, W.J., Grosso, S.J.D., Keough, C., Marx, E., Adler, P.R., DeLucia, E.H., 2012. Impact of second-generation biofuel agriculture on greenhouse-gas emissions in the corn-growing regions of the US. Frontiers in Ecology and the Environment 10, 69–74. https://doi.org/10.1890/110003

Del Grosso, S. J., Mosier, A.R., Parton, W.J., Ojima, D.S., 2005. DAYCENT model analysis of past and contemporary soil N2O and net greenhouse gas flux for major crops in the USA. Soil and Tillage Research, Greenhouse Gas Contributions and Mitigation Potential in Agricultural Regions of North America 83, 9–24. https://doi.org/10.1016/j.still.2005.02.007

Del Grosso, S.J., Ojima, D.S., Parton, W.J., Stehfest, E., Heistemann, M., DeAngelo, B., Rose, S., 2009. Global scale DAYCENT model analysis of greenhouse gas emissions and mitigation strategies for cropped soils. Global and Planetary Change, Changes in land use and water use and their consequences on climate, including biogeochemical cycles 67, 44–50. https://doi.org/10.1016/j.gloplacha.2008.12.006

Del Grosso, S.J., Parton, W.J., Mosier, A.R., Holland, E.A., Pendall, E., Schimel, D.S., Ojima, D.S., 2005. Modeling soil CO2 emissions from ecosystems. Biogeochemistry 73, 71–91. https://doi.org/10.1007/s10533-004-0898-z

Del Grosso, S.J., Parton, W.J., Ojima, D.S., Keough, C.A., Riley, T.H., Mosier, A.R., 2008. Chapter 18 - DAYCENT Simulated Effects of Land Use and Climate on County Level N Loss Vectors in the USA, in: Hatfield, J.L., Follett, R.F. (Eds.), Nitrogen in the Environment (Second Edition). Academic Press, San Diego, pp. 571–595. https://doi.org/10.1016/B978-0-12-374347-3.00018-4

Drewniak, B.A., Mishra, U., Song, J., Prell, J., Kotamarthi, V.R., 2015. Modeling the impact of agricultural land use and management on US carbon budgets. Biogeosciences 12, 2119–2129. https://doi.org/10.5194/bg-12-2119-2015

Fike, J.H., Parrish, D.J., Wolf, D.D., Balasko, J.A., Green, J.T., Rasnake, M., Reynolds, J.H., 2006. Switchgrass production for the upper southeastern USA: Influence of cultivar and cutting frequency on biomass yields. Biomass and Bioenergy 30, 207–213. https://doi.org/10.1016/j.biombioe.2005.10.008

Fike, J.H., Pease, J.W., Owens, V.N., Farris, R.L., Hansen, J.L., Heaton, E.A., Hong, C.O., Mayton, H.S., Mitchell, R.B., Viands, D.R., 2017. Switchgrass nitrogen response and estimated production costs on diverse sites. GCB Bioenergy 9, 1526–1542. https://doi.org/10.1111/gcbb.12444

Garten, C.T., Smith, J.L., Tyler, D.D., Amonette, J.E., Bailey, V.L., Brice, D.J., Castro, H.F., Graham, R.L., Gunderson, C.A., Izaurralde, R.C., Jardine, P.M., Jastrow, J.D., Kerley, M.K., Matamala, R., Mayes, M.A., Metting, F.B., Miller, R.M., Moran, K.K., Post, W.M., Sands, R.D., Schadt, C.W., Phillips, J.R., Thomson, A.M., Vugteveen, T., West, T.O., Wullschleger, S.D., 2010. Intra-annual changes in biomass, carbon, and nitrogen dynamics at 4-year old switchgrass field trials in west Tennessee, USA. Agriculture, Ecosystems & Environment 136, 177–184. https://doi.org/10.1016/j.agee.2009.12.019

Gelfand, I., Sahajpal, R., Zhang, X., Izaurralde, R.C., Gross, K.L., Robertson, G.P., 2013. Sustainable bioenergy production from marginal lands in the US Midwest. Nature 493, 514–517. https://doi.org/10.1038/nature11811

Generation 3: Soil Survey Staff, 2020. National Cooperative Soil Characterization Data. Soil Survey Laboratory, National Soil Survey Center, USDA-Natural Resources Conservation Service, Lincoln, NE. . Accessed 9 August 2020.

Grant, B.B., Smith, W.N., Campbell, C.A., Desjardins, R.L., Lemke, R.L., Kröbel, R., McConkey, B.G., Smith, E.G., Lafond, G.P., 2016. Comparison of DayCent and DNDC Models: Case Studies Using Data from Long-Term Experiments on the Canadian Prairies, in: Synthesis and Modeling of Greenhouse Gas Emissions and Carbon Storage in Agricultural and Forest Systems to Guide Mitigation and Adaptation. John Wiley & Sons, Ltd, pp. 21–57. https://doi.org/10.2134/advagricsystmodel6.2013.0035

Heaton, E.A., Dohleman, F.G., Long, S.P., 2009. Seasonal nitrogen dynamics of Miscanthus×giganteus and Panicum virgatum. GCB Bioenergy 1, 297–307. https://doi.org/10.1111/j.1757-1707.2009.01022.x

Heaton, E.A., Dohleman, F.G., Long, S.P., 2008. Meeting US biofuel goals with less land: the potential of Miscanthus. Global Change Biology 14, 2000–2014. https://doi.org/10.1111/j.1365-2486.2008.01662.x

Heggenstaller, A.H., Moore, K.J., Liebman, M., Anex, R.P., 2009. Nitrogen Influences Biomass and Nutrient Partitioning by Perennial, Warm-Season Grasses. Agronomy Journal 101, 1363–1371. https://doi.org/10.2134/agronj2008.0225x

Hirabayashi, Y., Mahendran, R., Koirala, S., Konoshima, L., Yamazaki, D., Watanabe, S., Kim, H., Kanae, S., 2013. Global flood risk under climate change. Nature Clim Change 3, 816–821. https://doi.org/10.1038/nclimate1911

Hudiburg, T.W., Wang, W., Khanna, M., Long, S.P., Dwivedi, P., Parton, W.J., Hartman, M., DeLucia, E.H., 2016. Impacts of a 32-billion-gallon bioenergy landscape on land and fossil fuel use in the US. Nat Energy 1, 1–7. https://doi.org/10.1038/nenergy.2015.5

Jemison Jr., J.M., Fox, R.H., 1994. Nitrate Leaching from Nitrogen-Fertilized and Manured Corn Measured with Zero-Tension Pan Lysimeters. Journal of Environmental Quality 23, 337–343. https://doi.org/10.2134/jeq1994.00472425002300020018x

Kam, J., Traynor, D., Clifton-Brown, J.C., Purdy, S.J., McCalmont, J.P., 2020. Miscanthus as Energy Crop and Means of Mitigating Flood, in: Naddeo, V., Balakrishnan, M., Choo, K.-H. (Eds.), Frontiers in Water-Energy-Nexus—Nature-Based Solutions, Advanced Technologies and Best Practices for Environmental Sustainability, Advances in Science, Technology & Innovation. Springer International Publishing, Cham, pp. 461–462. https://doi.org/10.1007/978-3-030-13068-8_115

Kantola, I.B., Masters, M.D., Blanc-Betes, E., Gomez-Casanovas, N., DeLucia, E.H., 2022. Long-term yields in annual and perennial bioenergy crops in the Midwestern United States. GCB Bioenergy 00, 1–13. https://doi.org/10.1111/gcbb.12940

Kent, J., Hartman, M.D., Lee, D.K., Hudiburg, T., 2020. Simulated Biomass Sorghum GHG Reduction Potential is Similar to Maize. Environ. Sci. Technol. 11.

Kline, K.L., Msangi, S., Dale, V.H., Woods, J., Souza, G.M., Osseweijer, P., Clancy, J.S., Hilbert, J.A., Johnson, F.X., McDonnell, P.C., Mugera, H.K., 2017. Reconciling food security and bioenergy: priorities for action. GCB Bioenergy 9, 557–576. https://doi.org/10.1111/gcbb.12366

Langholtz, M., Stokes, B., Eaton, L., 2016. 2016 Billion-Ton Report: Advancing Domestic Resources for a Thriving Bioeconomy (Executive Summary). Industrial Biotechnology 12, 282–289. https://doi.org/10.1089/ind.2016.29051.doe

Lark, T.J., Hendricks, N.P., Smith, A., Pates, N., Spawn-Lee, S.A., Bougie, M., Booth, E.G., Kucharik, C.J., Gibbs, H.K., 2022. Environmental outcomes of the US Renewable Fuel Standard. Proc. Natl. Acad. Sci. U.S.A. 119, e2101084119. https://doi.org/10.1073/pnas.2101084119

Lark, T.J., Salmon, J.M., Gibbs, H.K., 2015. Cropland expansion outpaces agricultural and biofuel policies in the United States. Environ. Res. Lett. 10, 044003. https://doi.org/10.1088/1748-9326/10/4/044003

Lark, T.J., Spawn, S.A., Bougie, M., Gibbs, H.K., 2020. Cropland expansion in the United States produces marginal yields at high costs to wildlife. Nat Commun 11, 4295. https://doi.org/10.1038/s41467-020-18045-z

Liu, Y., Zhang, X., Tran, H., Shan, L., Kim, J., Childs, K., Ervin, E.H., Frazier, T., Zhao, B., 2015. Assessment of drought tolerance of 49 switchgrass (Panicum virgatum)

genotypes using physiological and morphological parameters. Biotechnol Biofuels 8, 152. https://doi.org/10.1186/s13068-015-0342-8

Meehan, T.D., Gratton, C., Diehl, E., Hunt, N.D., Mooney, D.F., Ventura, S.J., Barham, B.L., Jackson, R.D., 2013. Ecosystem-Service Tradeoffs Associated with Switching from Annual to Perennial Energy Crops in Riparian Zones of the US Midwest. PLOS ONE 8, e80093. https://doi.org/10.1371/journal.pone.0080093

Melillo, J.M., Borchers, J., Chaney, J., Fisher, H., Fox, S., Haxeltine, A., Janetos, A., Kicklighter, D.W., Kittel, T.G.F., McGuire, A.D., McKeown, R., Neilson, R., Nemani, R., Ojima, D.S., Painter, T., 1995. Vegetation/ecosystem modeling and analysis project: Comparing biogeography and biogeochemistry models in a continental-scale study of terrestrial ecosystem responses to climate change and CO2 doubling. Global Biogeochemical Cycles 9, 407–438. https://doi.org/10.1029/95GB02746

Mooney, D.F., Roberts, R.K., English, B.C., Tyler, D.D., Larson, J.A., 2009. Yield and Breakeven Price of 'Alamo' Switchgrass for Biofuels in Tennessee. Agronomy Journal 101, 1234–1242. https://doi.org/10.2134/agronj2009.0090

Moore, C.E., Berardi, D.M., Blanc-Betes, E., Dracup, E.C., Egenriether, S., Gomez-Casanovas, N., Hartman, M.D., Hudiburg, T., Kantola, I., Masters, M.D., 2020. The carbon and nitrogen cycle impacts of reverting perennial bioenergy switchgrass to an annual maize crop rotation. GCB Bioenergy 12, 941–954.

Mukhtar, S., J. L. Baker, and R. S. Kanwar. Corn growth as affected by excess soil water. *Transactions of the ASAE* 33.2 (1990): 437-0442.

Owens, V.N., Viands, D.R., Mayton, H.S., Fike, J.H., Farris, R., Heaton, E., Bransby, D.I., Hong, C.O., 2013. Nitrogen use in switchgrass grown for bioenergy across the USA. Biomass and Bioenergy 58, 286–293. https://doi.org/10.1016/j.biombioe.2013.07.016

P. Thornton, Thornton, M., Mayer, B., Wei, Y., Devarakonda, R., Vose, R., Cook, R., 2018. Daymet: Daily Surface Weather Data on a 1-km Grid for North America, Version 3.

Prein, A.F., Rasmussen, R.M., Ikeda, K., Liu, C., Clark, M.P., Holland, G.J., 2017. The future intensification of hourly precipitation extremes. Nature Clim Change 7, 48–52. https://doi.org/10.1038/nclimate3168

Robertson, G.P., Hamilton, S.K., Barham, B.L., Dale, B.E., Izaurralde, R.C., Jackson, R.D., Landis, D.A., Swinton, S.M., Thelen, K.D., Tiedje, J.M., 2017. Cellulosic biofuel contributions to a sustainable energy future: Choices and outcomes. Science 356, eaal2324. https://doi.org/10.1126/science.aal2324

Robertson, G.P., Hamilton, S.K., Del Grosso, S.J., Parton, W.J., 2011. The biogeochemistry of bioenergy landscapes: carbon, nitrogen, and water considerations. Ecological Applications 21, 1055–1067. https://doi.org/10.1890/09-0456.1

Ryals, R., Hartman, M.D., Parton, W.J., DeLonge, M.S., Silver, W.L., 2015. Long-term climate change mitigation potential with organic matter management on grasslands. Ecological Applications 25, 531–545. https://doi.org/10.1890/13-2126.1

Schnepf, R., Yacobucci, B.D., 2013. Renewable Fuel Standard (RFS): Overview and Issues.

Skevas, T., Hayden, N.J., Swinton, S.M., Lupi, F., 2016. Landowner willingness to supply marginal land for bioenergy production. Land Use Policy 50, 507–517. https://doi.org/10.1016/j.landusepol.2015.09.027

Spawn, S.A., Lark, T.J., Gibbs, H.K., 2019. Carbon emissions from cropland expansion in the United States. Environ. Res. Lett. 14, 045009. https://doi.org/10.1088/1748-9326/ab0399

Springer, T.L., 2017. Effect of Nitrogen Fertilization and Residual Nitrogen on Biomass Yield of Switchgrass. Bioenerg. Res. 10, 648–656. https://doi.org/10.1007/s12155-017-9827-6

USDA-NASS, 2018. USDA National Agricultural Statistics Service Cropland Data Layer.

USDA-NASS, 2016. Crop Production Summary 2015.

USDA-RMA, 2020. 2020 Cause of Loss Historical Data Files. United States Department of Agriculture: Risk Management Agency.

von Haden, A.C., Burnham, M.B., Yang, W.H., DeLucia, E.H., 2021. Comparative establishment and yield of bioenergy sorghum and maize following pre-emergence waterlogging. Agronomy Journal 113, 5602–5611. https://doi.org/10.1002/agj2.20832

Wang, S., Sanford, G.R., Robertson, G.P., Jackson, R.D., Thelen, K.D., 2020. Perennial Bioenergy Crop Yield and Quality Response to Nitrogen Fertilization. Bioenerg. Res. 13, 157–166. https://doi.org/10.1007/s12155-019-10072-z

Woods J, L.L., Laser, M., Kline, K.L., Faaij, A., 2015. Chapter 9, Land and Bioenergy in Scientific Committee on Problems of the Environment (SCOPE), Bioenergy & Sustainability: bridging the gaps. SCOPE Bioenergy & Sustainability, Sao Paulo, Brazil.

Zhang, Y., Gurung, R., Marx, E., Williams, S., Ogle, S.M., Paustian, K., 2020. DayCent Model Predictions of NPP and Grain Yields for Agricultural Lands in the Contiguous U.S. Journal of Geophysical Research: Biogeosciences 125, e2020JG005750. https://doi.org/10.1029/2020JG005750

Zhu, M., Li, F.H., Shi, Z.S., 2016. Morphological and photosynthetic response of waxy corn inbred line to waterlogging. Photosynthetica 54, 636–640. https://doi.org/10.1007/s11099-016-0203-0

Supporting Information

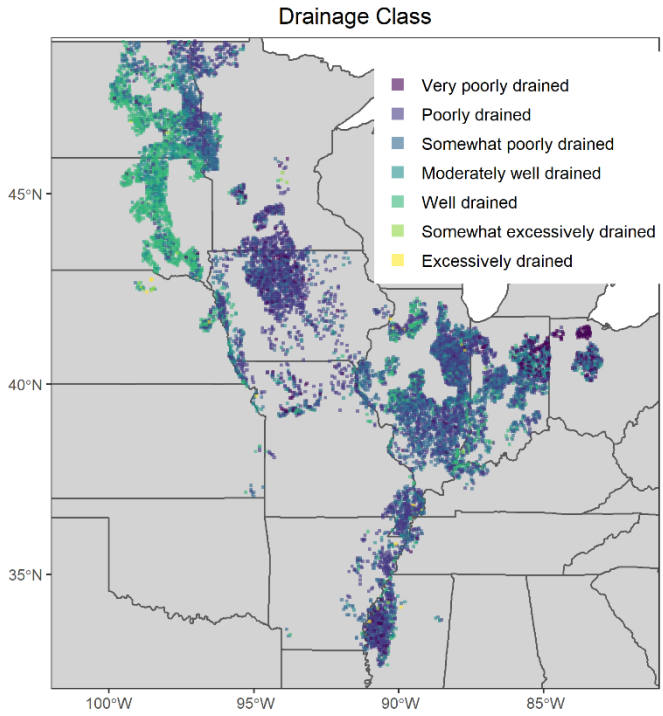

Figure S. 3.1 Drainage class assigned from SSURGO data.

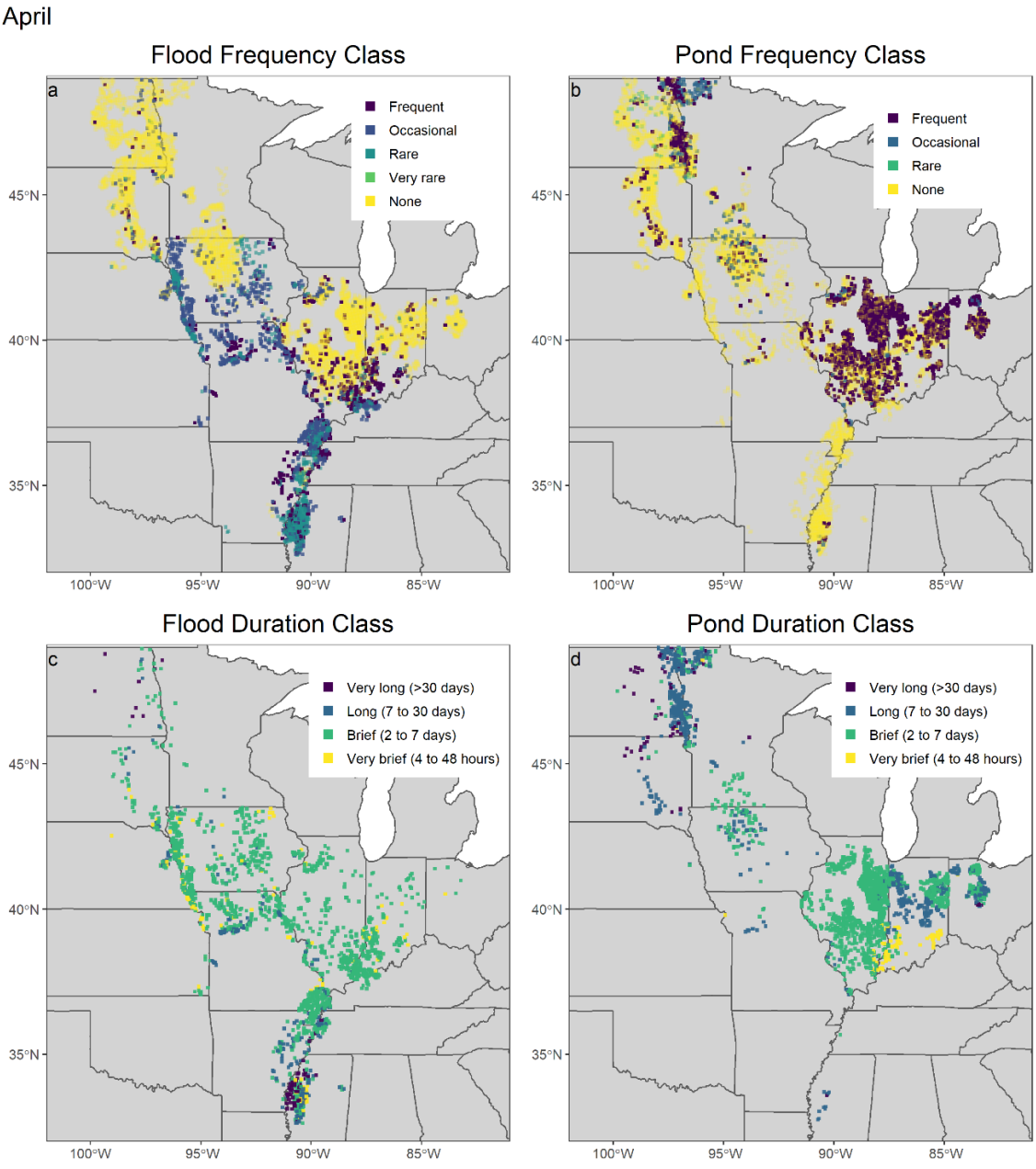

Figure S. 3.2. April flooding and ponding frequency and duration from SSURGO data.

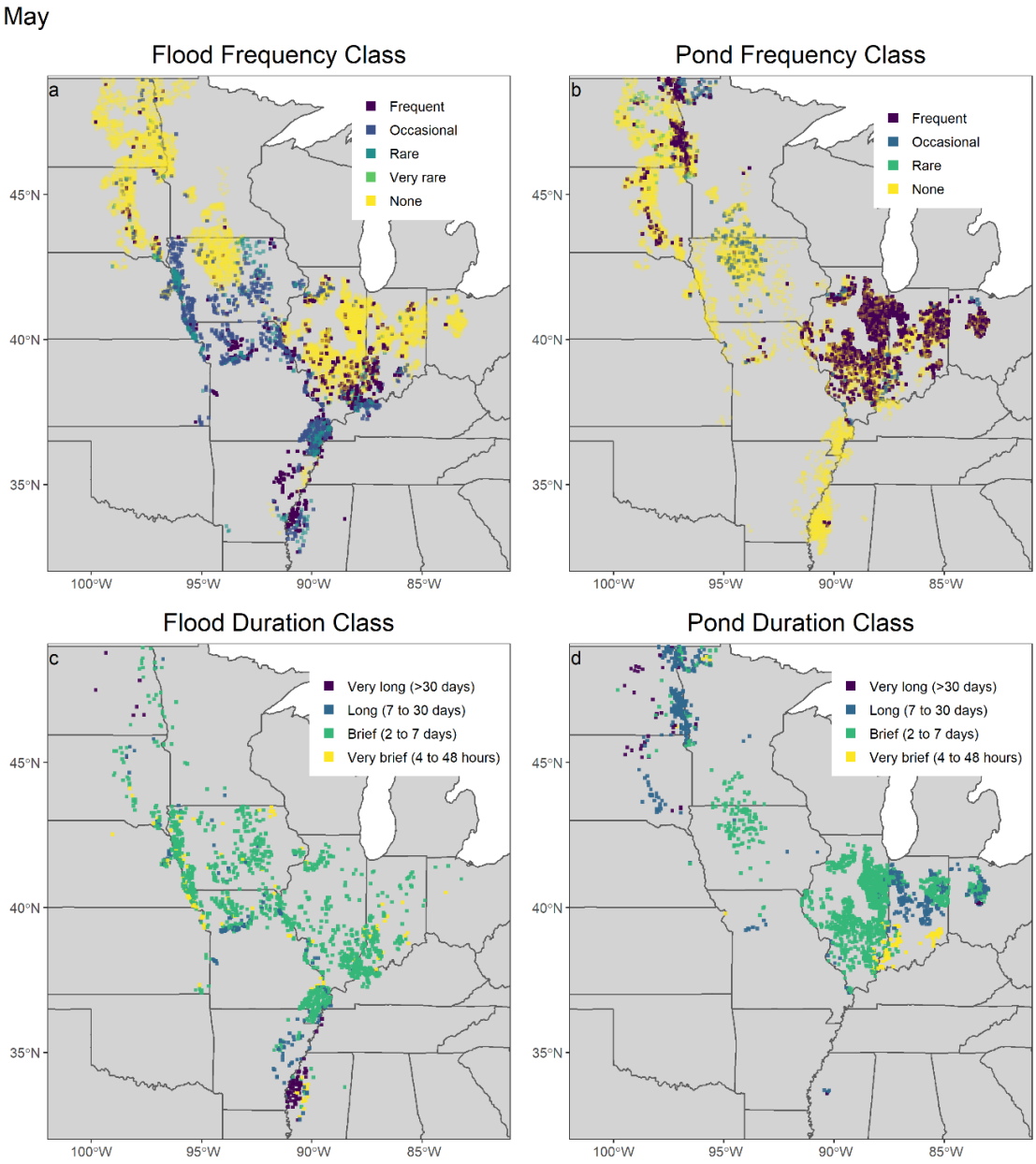

Figure S. 3.3. May flooding and ponding frequency and duration from SSURGO data.

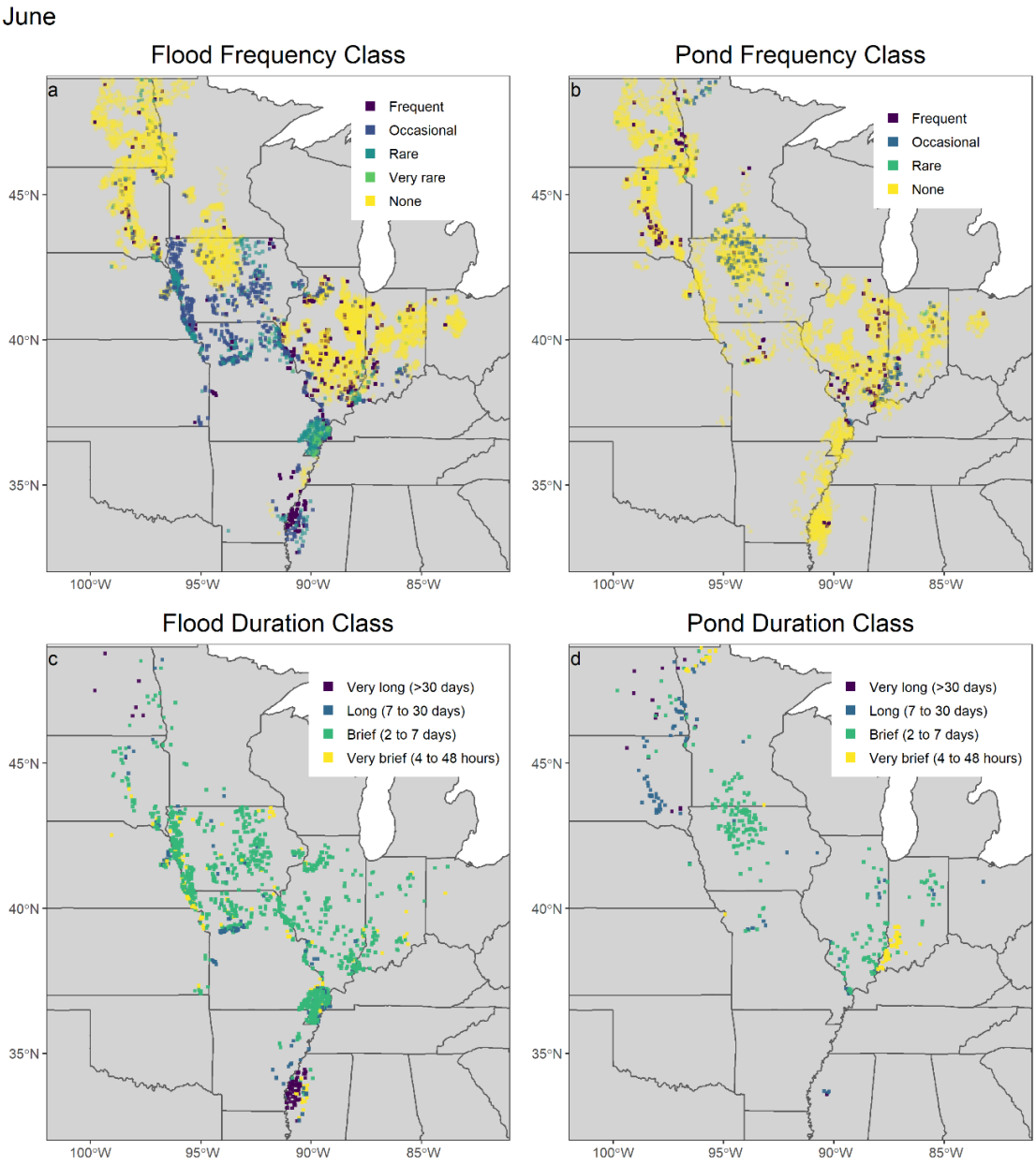

Figure S. 3.4. June flooding and ponding frequency and duration from SSURGO data.

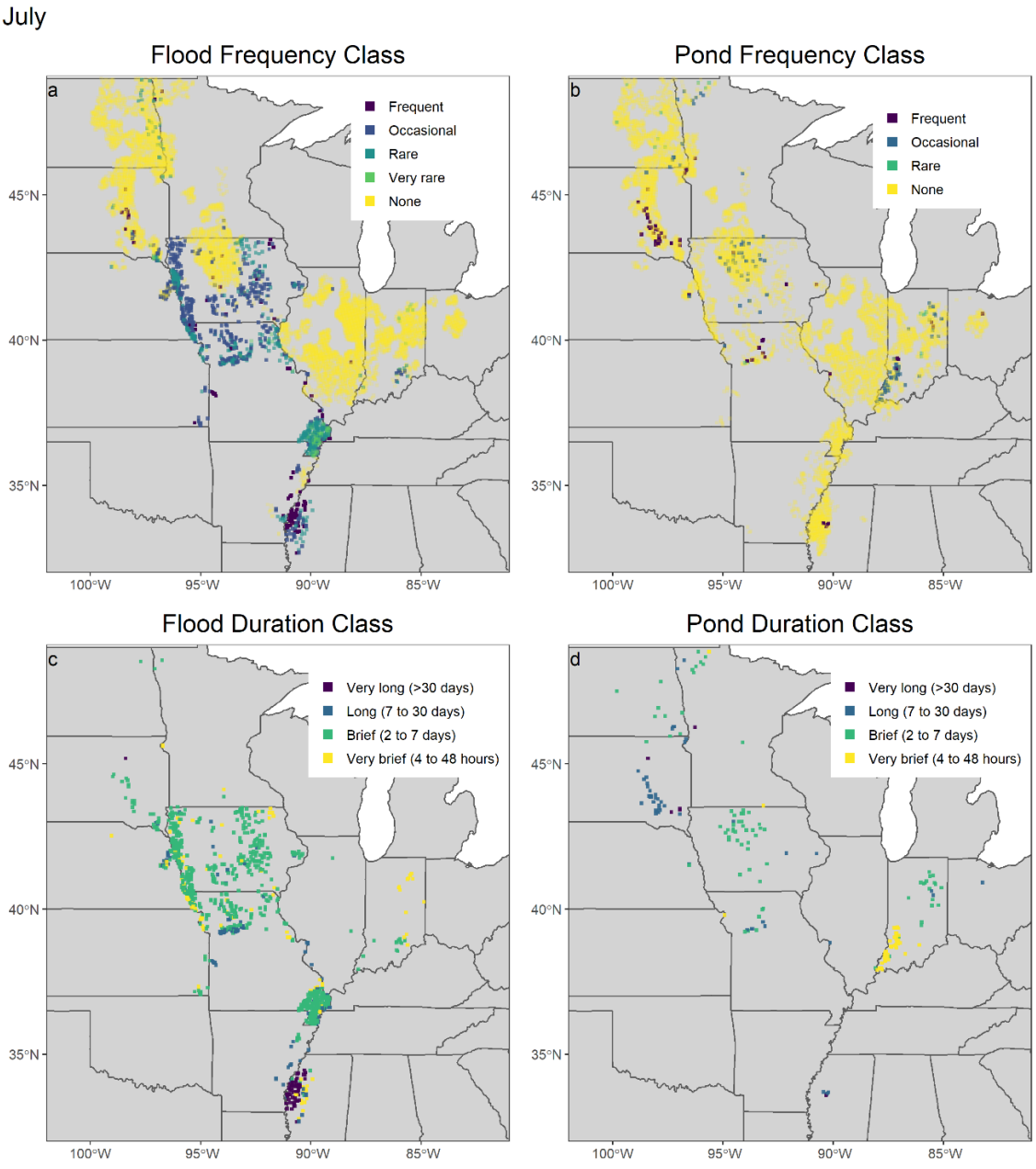

Figure S. 3.5. July flooding and ponding frequency and duration from SSURGO data.

Table S 3.1 Values used for the intercept (EPNFS(1)) and the slope (EPNFS(2)) parameters determining the effect of annual precipitation on non-symbiotic soil nitrogen fixation determined by MAT.

MAT	EPNFS(1) - Intercept	EPNFS(2) - Slope
< 10°C	30*(MAT/10)	0.025
10°C - 16°C	30	0.020
> 16°C	35	0.015

Table S 3.2 Studies used for switchgrass calibration and validation with approximate location of study sites.

Citation	Location	Latitude and Longitude	Calibration/ Validation
(Fike et al., 2006)	Princeton, KY	37.06 N, 87.49 W	Calibration
(Fike et al., 2006)	Jackson, TN	35.37 N, 88.50 W	Calibration
(Fike et al., 2017)	Story County, IA	41.98 N, 93.70 W	Validation
(Fike et al., 2017)	Day County, SD	45.27 N, 97.84 W	Calibration
(Heaton et al., 2009, 2008; Kantola et al., 2022)	Urban, IL	40.08 N, 88.23 W	Calibration
(Heaton et al., 2009, 2008)	Shabbona, IL	41.85 N, 88.85 W	Validation
(Heaton et al., 2009, 2008)	Simpson, IL	37.45 N, 88.67 W	Validation
(Heggenstaller et al., 2009)	Boone County, IA	42.06 N, 93.88 W	Validation
(Owens et al., 2013)	Bristol, SD	45.16 N, 97.50 W	Calibration
(Owens et al., 2013)	Ames, IA	41.58 N, 93.41 W	Validation
(Wang et al., 2020)	Kellogg Biological Station, MI	42.23 N, 85.22 W	Validation